Hypothesis-free discovery from epidemiological data by automatic detection and local inference for tree-based nonlinearities and interactions

Giorgio Spadaccini (Vrije Universiteit Amsterdam, Leiden University)

Marjolein Fokkema (Leiden University)

Mark van de Wiel (Vrije Universiteit Amsterdam)

Abstract

In epidemiological settings, Machine Learning (ML) is gaining popularity for hypothesis-free discovery of risk (or protective) factors. Although ML is strong at discovering non-linearities and interactions, this power is currently compromised by a lack of reliable inference. Although local measures of feature effect can be combined with tree ensembles, uncertainty quantifications for these measures remain only partially available and oftentimes unsatisfactory. We propose RuleSHAP, a framework for using rule-based, hypothesis-free discovery that combines sparse Bayesian regression, tree ensembles and Shapley values in a one-step procedure that both detects and tests complex patterns at the individual level. To ease computation, we derive a formula that computes marginal Shapley values more efficiently for our setting. We demonstrate the validity of our framework on simulated data. To illustrate, we apply our machinery to data from an epidemiological cohort to detect and infer several effects for high cholesterol and blood pressure, such as nonlinear interaction effects between features like age, sex, ethnicity, BMI and glucose level.

KEYWORDS: Bayesian uncertainty quantification, Tree ensembles, Shapley values, Interactions, Nonlinearity

1 Introduction

Risk and protective factors are at the center of many studies in epidemiology. These studies aim to understand how policies, behaviors and treatments are associated to negative and positive health outcomes. In most cases, (generalized) linear regression is employed, for which inference is readily available. This approach, however, is very rigid: unless prior knowledge enables explicit specification of interaction terms, the association between a feature and the outcome is either statistically relevant for all or none of the observations, depending on whether the coefficient of the linear term is significantly non-zero. In practice, the strict assumptions of a linear model can be far from the truth: the shapes of effects are often nonlinear and (treatment) effects, for example, may be heterogeneous across different population groups. For contexts in which linearity is too restrictive, the

expression "hypothesis-free discovery" is often used to refer to scientific investigation made through least restrictive Machine Learning (ML) models [1] [2]. Unlike parametric models such as linear regression, ML models typically capture more complex patterns in the data, as they do not require any prior specification of the shape of the association between the features and the outcome. This gives researchers an edge over the standard approach, as methods such as a tree ensemble can, for instance, automatically capture trends like saturations, exponential growths and interactions, which a linear model would miss.

To obtain both the flexibility of ML and the inferential power of traditional methods, many researchers rely on a two-step procedure [2] [3] [4]: first, an ML model (typically a tree ensemble such as XGBoost) is fitted on the data and feature importance measures are computed. Second, the most influential features according to this importance ranking are used for inference through means of a simpler generalized linear regression model. However, this approach is suboptimal: type I error is inflated when using the same data for both screening of features and inference. This is due to the fact that the noise features that pass the filtering stage are precisely the ones that, by chance, fit the current sample best, and the regression stage does not take this into account (see Example 3 in the Supplementary material). The obvious solution of using separate portions of the dataset for screening and testing is unfortunately often not an option for settings where the sample size is not extremely large or high power is needed. Either way, the inferential results are not truly hypothesis-free, since the inferential step remains a simple regression. For example, while the ML model could select a feature due to its interacting or nonlinear effects, the regression model would ignore these effects due to its excessive simplicity. Careful semi-parametric modeling, e.g. through Generalized Additive Models (GAMs [5][6]) may capture some of the nonlinearities, but may not suffice for discovering general interaction terms. Bayesian Additive Regression Trees (BART) provide the full flexibility of tree ensembles, while aiming to naturally account for the uncertainty in the model fit. They have also been used in combination with local feature importance measures to produce local inference of feature effects [7]. However, this approach may present suboptimal coverage [8] [9], and consequentially high false discovery rates, as we later show with simulations.

We aim to obtain both flexibility and inference. We employ a strategy inspired by RuleFit [10] and Horserule [11], directly incorporating the knowledge of the first ML-based step into the second regression-based step. More specifically, the trees in the ensemble are disaggregated into 0-1 encoded dummy variables and included alongside the original predictor variables in the linear fit. The complex patterns in the data detected by the tree ensemble are thereby "transferred" to the linear model, so that they can also be used for inference. The aim is to build a regression model that is augmented with ML, where the extra rule terms offer a supportive role to an otherwise linear model. With the incorporation of such patterns into the model, the prediction mechanism goes beyond simple additivity and the effect of one feature can now depend on unique combinations of all other features. For these reasons, an observation-specific interpretation of the effect of features on the outcome becomes more and more relevant, and testing feature effects on a local level becomes much more informative and desirable. With this in mind, local feature importance measures have already been introduced for these two models [10] but we will show them to be misleading. Further, while HorseRule allows for uncertainty quantifications of the model, we will show that these cannot be used for statistical testing on the importance measures. More generally, the problem is that RuleFit and HorseRule optimize predictive performance, rather than scientific discovery, and we show them to be unsuitable for detecting and testing complex relationships between the features

and the outcome.

We propose RuleSHAP, a framework for using rule-based, hypothesis-free discovery that combines Bayesian regression, tree ensembles and Shapley values and carries out a one-step procedure that both detects and tests complex patterns. While it builds on the principles of RuleFit and HorseRule, it is designed to rely on a linear model as much as possible, while also incorporating rules to specifically model the nonlinearities and interactions. Moreover, it is designed to more accurately account for uncertainty in the estimation so that type I error is not inflated. First, it generates rules in a manner that prevents them from overfitting or overpowering the linear terms. Second, it relies on the good coverage properties of Bayesian horseshoe regression [12] to produce credible intervals which can asymptotically be interpreted in the frequentist sense. A final contribution of RuleSHAP is the use of the widely used marginal Shapley values [13][14] as a more accurate decomposition of prediction into its feature-specific effects than the local importance measures introduced in RuleFit. To ease computation, it relies on a direct formula that we derive in order to write marginal Shapley values of the model as a linear combination of the coefficients. In doing so, the valid uncertainty quantification of RuleSHAP can be propagated to the level of Shapley values, allowing for inference through credible intervals. Lastly, we show RuleSHAP to be competitive and often superior in terms of predictive performance thanks to its ability to rely on the strengths of both tree ensembles and linear regression according to the context.

The work is structured as follows: in Section 2, we discuss the target dataset that this method may be used for. In Section 3 we introduce RuleFit and HorseRule, together with how feature effects are currently quantified for these methods. In Section 4, we introduce RuleSHAP and Shapley values. In Section 5 we produce an explicit formula to compute the Shapley values associated to an individual rule and discuss how it can be easily generalized for many rule-based settings. In Section 6 we use simulations to confirm that RuleSHAP correctly reconstructs the effects of each feature and that it does not flag noise features as significant. In Section 7 we apply our method to the data collected in the HELIUS cohort study [15] to explore the protective and risk factors for high cholesterol level and high systolic blood pressure, uncovering nonlinear interaction effects of covariates such as age, sex, ethnicity, BMI and glucose level. Conclusions on the results of the analyses, together with the strengths and limitations of this approach and possible future steps, are described in Section 8.

2 Targeted study design

The methodology discussed in this paper is designed for tabular observational data with continuous or binary outcomes. Extensions to any type of generalized linear regression are feasible if a horseshoe prior regression can be implemented and working residuals can be computed. The focus is inspired by many epidemiological settings in which the effect of features on the outcome goes beyond linearity: age, for example, is a feature whose effect is hardly ever linear and instead often tends to saturate. Confounding and heterogeneity of treatments, on the other hand, require the need to include joint effects which may be represented by complex interactions between features. Many epidemiological studies contain several thousands of observations on, say, tens of covariates. To establish reliable reconstruction and inference of the effects our methodology targets n/p ratios which go beyond the ten-to-one rule. Less ideal ratios are marginally explored in our simulations and discussed in the Discussion section.

This paper tackles the challenge of making tree-based ML models applicable to this context: while ML models are already successfully used for prediction, they are not designed for etiological purposes. In epidemiology, by contrast, the nature of the relationship between features and response is often of major interest. Furthermore, uncertainty quantifications remain necessary, as the number of observations in many epidemiological studies is typically not large enough for the ML model variance to be negligible in the inferential phase.

3 Tree-based models

3.1 RuleFit

3.1.1 Model

A RuleFit model (also known as Prediction Rule Ensemble [16]), is a linear regression model that is enhanced with complementary dichotomous features defined as rules on the features themselves [10]. These decision rules are typically generated by through one or more tree ensemble methods, such as Random Forests, Gradient Boosting or XGboost. The resulting model then takes the form:

$$F(x) = \hat{a}_0 + \sum_{k=1}^{q} \hat{a}_j r_j(x) + \sum_{j=1}^{p} \hat{b}_j x_j, \tag{1}$$

where r_1, \ldots, r_q are the decision rules and x_1, \ldots, x_p are the linear terms which may also undergo Winsorization to enforce stability, as perscribed in [10] (with the standard of truncating to the 2.5-th and the 97.5-th percentiles).

Because the rules are generated from decision trees, they may be seen as products of rules that involve a single feature: let us consider the exemplary tree in Figure 1. This tree would contribute to the RuleFit model with seven rules:

$$\begin{split} r_1(x) &:= I(x_1 < 3), \\ r_2(x) &:= I(x_1 \ge 3) \cdot I(x_3 < 2), \\ r_3(x) &:= I(x_1 \ge 3) \cdot I(x_3 \ge 2), \\ r_4(x) &:= I(x_1 \ge 3) \cdot I(x_3 < 2) \cdot I(x_2 < 4), \\ r_5(x) &:= I(x_1 \ge 3) \cdot I(x_3 < 2) \cdot I(x_2 \ge 4), \\ r_6(x) &:= I(x_1 \ge 3) \cdot I(x_3 \ge 2) \cdot I(x_4 < 1), \\ r_7(x) &:= I(x_1 \ge 3) \cdot I(x_3 \ge 2) \cdot I(x_4 > 1), \end{split}$$

The enhanced linear model F(x) shown in Equation 1 is obtained by fitting a sparse linear regression (such as a LASSO fit) on the terms $x_1, \ldots, x_p, r_1, \ldots, r_q$.

The idea behind this model is that since all rules that define a tree ensemble are carried over to the linear model, RuleFit should retain (most of) the accuracy of the original black-box model

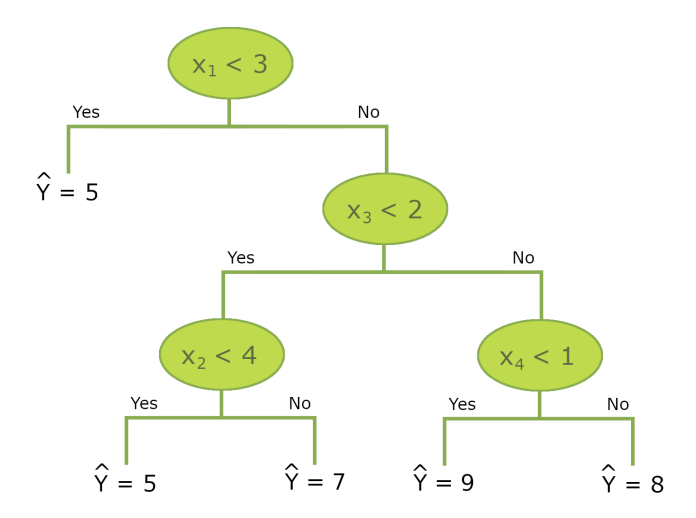


Figure 1: Example of one of the many trees generated from a tree ensemble. Seven decision rules are extracted from this tree, according to the RuleFit rule extraction scheme: $I(x_1 < 3)$, $I(x_1 \geq 3, x_3 < 2)$, $I(x_1 \geq 3, x_3 \geq 2)$, $I(x_1 \geq 3, x_3 < 2, x_2 < 4)$, $I(x_1 \geq 3, x_3 < 2, x_2 \geq 4)$, $I(x_1 \geq 3, x_3 \geq 2, x_4 < 1)$, and $I(x_1 \geq 3, x_3 \geq 2, x_4 \geq 1)$

that generated the rules while also simplifying it, since the final tool is still a sparse linear model. Furthermore, RuleFit allows for a combination of multiple types of tree ensembles: one can, for instance, combine rules taken from Random Forests and Gradient Boosting.

3.1.2 Feature effect measures

RuleFit's definition of feature importance is based on the fact that RuleFit is a linear model. More specifically, the local importance of the j-th feature for the prediction of the datapoint x is defined as:

$$I_j(x) := |\hat{b}_j| \cdot |x_j - \overline{x}_j| + \sum_{\substack{k \text{ s.t.} \\ x_j \in r_k}} \frac{|\hat{a}_k| \cdot |r_k(x) - \overline{r}_k|}{m_k}, \tag{2}$$

where \overline{x}_j and \overline{r}_k are the observed means of x_j and r_k respectively, m_k denotes the number of features involved in the k-th rule and, with an abuse of notation, $x_j \in r_k$ is meant as "the j-th feature is involved in the rule r_k ". Concretely, this means that the local effect of the linear term is added to the local effects of all rules that involve the j-th feature, and the effect of a rule is divided equally across all features it involves.

An analogous construction is also defined for a global importance measure, across all points:

$$I_j := |\hat{b}_j| \cdot sd(x_j) + \sum_{\substack{k \text{ s.t.} \\ x_j \in r_k}} \frac{|\hat{a}_k| \cdot \sqrt{\overline{r}_k \cdot (1 - \overline{r}_k)}}{m_k}.$$
 (3)

The same rationale is used here.

While their definition comes naturally and allows for an easy computation, these measures are based on the intuition that the effects of the rules should be equally split across the features involved, which does not necessarily have to be the case. Furthermore, in Equation 3, the importances of the different terms are added up, even though they could possibly correspond to conflicting or complementary effects that therefore partially compensate each other. We expand these considerations further in Example 2 in the Supplementary material.

3.2 HorseRule

HorseRule [11] is a Bayesian variation of RuleFit where, instead of a LASSO fit, a Bayesian regression is used to obtain a model of the form described in Equation 1. This is performed through means of a Horseshoe prior [17]. HorseRule also introduces a structured penalization: stronger shrinkage is applied to rules with higher depth (i.e. many features involved in its definition) or very extreme support (i.e. almost all or almost no points follow the rule). This is achieved with the following prior distribution on the coefficients:

$$y|X, \beta, \sigma^{2} \sim \mathcal{N}(X\beta, \sigma^{2}I_{n}),$$
$$\beta_{j}|\lambda, \tau, \sigma^{2} \sim \mathcal{N}(0, \lambda_{j}^{2}\tau^{2}\sigma^{2}),$$
$$\lambda_{j} \sim \mathcal{C}^{+}(0, A_{j}),$$
$$\tau \sim \mathcal{C}^{+}(0, 1),$$
$$\sigma^{2} \sim \sigma^{-2}d\sigma^{2}.$$

In this prior, Nalenz and Villani [11] set $A_j = 1$ for the coefficients of linear terms, while for the coefficient of a rule r_j the prior is defined with:

$$A_j = \frac{\left(2 \cdot \min(1 - \overline{r}_j, \overline{r}_j)\right)^{\mu}}{(m_j)^{\eta}},\tag{4}$$

where \bar{r}_j is the observed frequency/mean of the rule and m_j denotes the number of features involved in the definition of the j-th rule. The hyperparameters $\mu, \eta > 0$ determine the level of shrinkage applied to rules with extreme support and high depth, respectively. While cross-validation may be used to determine them, the authors report the default values of $\mu = 1, \eta = 2$ to work well. This prior favors the use of linear terms by construction, since linear terms are never shrunken more than a rule and are shrunken as much as a rule of support $\bar{r}_j = 0.5$ and depth $m_j = 1$.

Nalenz and Villani suggest using the same feature effect measures as RuleFit to determine the effect of each feature. They also mention the possibility of inference, but they only test the significance of individual coefficients, which is not strongly meaningful in a context where the effect of a feature is distributed over multiple terms. It is not straightforward to use the uncertainty of the coefficients to test on the importance measures defined for RuleFit, since the natural null for this measure, which would be $I_j(x) = 0$, is at the edge of the space in which the measure is defined, i.e. $I_j(x) \in \mathbb{R}^+$. This means that even for a noise feature, the confidence interval of $I_j(x)$ would almost always exclude the zero and thus would almost always reject the null hypothesis.

4 RuleSHAP

While the model above is designed to contain both linear terms and rules, the presence of linear terms does not seem to make a large difference in predictive performance [11]. This is understandable, since rule generation and model fitting happen on the same data and therefore the rules that are being fed to the HorseRule/RuleFit model have already been tailored around the training dataset. This overlooking of linear terms should be avoided if possible, since the advantages of using linear terms when they adequately approximate the feature-outcome relationship are twofold: on the one hand, this gives the model more simplicity. On the other hand, linear terms induce an effect across all observations, and thus allow the local effect estimates to better borrow information from each other. As using two separate datasets for rule generation and model fitting might be quite costly and might not solve the problem entirely (an ensemble of very many rules can still fit the data better than few linear terms), we devised several tweaks in the rule generation and model fitting that aim at counteracting this phenomenon. Our tweaks also address other goals, such as a better quantification of uncertainty and interaction effects.

4.1 Rule generation

Altering rule generation to accommodate linear terms has already been done before. For instance, in [18],[19] and [20] trees are generated based on some residualized version of the outcome, so that the rules are generated to only account for the part of the outcome that a linear regression cannot already model. We follow the same approach: more specifically, we fitted the tree ensembles on the residuals of a Bayesian linear regression fit with a horseshoe prior. For logistic regression, where residuals are not as straightforwardly defined as in the linear case, we used the working residuals $\frac{y-\hat{y}}{\hat{y}(1-\hat{y})}$. This is because these estimated residuals are on the scale of the features, which is the same scale that the rules are added to.

Another concern raised about rule generation was the fact that rules are generated on the same dataset that is later used for the linear fit: more specifically, in a Random Forest, each tree uses a bootstrapped sample which, up to multiple copies of the same observations, contains around 66% of the total number of osbervations. These observations, when recycled into the linear fit, will likely fit the rules better than the linear term. To prevent this from happening, we applied the following three-step strategy to generate the rules:

- 1. Fit a Random Forest where the residuals r_1, \ldots, r_n are the outcome.
- 2. Make the distributional assumption:

$$r_i \sim \mathcal{N}(\hat{r}_i, \hat{\sigma}^2) \qquad \forall i = 1, \dots, n,$$

where \hat{r}_i is the Random Forest's out-of-bag prediction of r_i and $\hat{\sigma}^2 = \frac{1}{n} \sum_{i=1}^n (r_i - \hat{r}_i)^2$.

3. Fit a new Random Forest in which the k-th tree is fitted on a tweaked random bootstrap sample: if the sample for the k-th tree uses observations indexed as $i_{k,1}, \ldots, i_{k,n}$, the outcomes in this bootstrap sample are:

$$\hat{r}_{i_{k,1}} + \epsilon_1^{(k)}, \dots, \hat{r}_{i_{k,n}} + \epsilon_n^{(k)}, \qquad \epsilon_i^{(k)} \sim \mathcal{N}(0, \hat{\sigma}^2) \quad \forall i = 1, \dots, n \quad \forall k = 1, \dots, \text{Ntree}$$

This approach allows rule generation to incorporate the outcome's irreducible error, since every time an observation is bootstrapped it uses a different synthetic error term $\epsilon_i^{(k)}$. This makes rule generation more stable and less likely to overfit the data, as it is not fitted on the actual observed outcomes but rather on synthetic duplicates of them. More importantly, this procedure naturally accounts for the uncertainty in the rule generation, which needs to be taken into account for inferential purposes. We will refer to this rule generation strategy as Parametric Random Forest. Although other tree ensembling methods can additionally be employed for rule generation as in [11], our experiments in Section 6 indicate that sole use of the Parametric Random Forest yields optimal type I error rate, while a maximum rule depth of three provides optimal interpretability.

Further measures were taken to counter the overfitting of rules. Firstly, we took winsorization further and enforced that the end nodes of the trees also contain at least 2.5% of the observations, and in any case at least 10 observations, since the ten-to-one rule would recommend using at least ten observations to estimate the coefficient of the generated rule. Furthermore, to avoid unnecessary interactions that specifically target some of the training observations, RuleSHAP fully disaggregates the rules. This means that, given any leaf node in a tree, all individual subrules that lead to the node are merged in all possible combinations. Going back to the example in Figure 1, the rules that are generated from the end node $I(x_1 < 3, x_3 < 2, x_2 \ge 4)$ are:

```
\begin{split} &I(x_1<3),\\ &I(x_3<2),\\ &I(x_2\geq 4),\\ &I(x_1<3,x_3<2),\\ &I(x_3<2,x_2\geq 4),\\ &I(x_1<3,x_2\geq 4),\\ &I(x_1<3,x_3<2,x_2\geq 4). \end{split}
```

This expands the set of conditions produced by RuleFit for this specific end node, which would only be:

```
I(x_1 < 3),

I(x_1 < 3, x_3 < 2),

I(x_1 < 3, x_3 < 2, x_2 \ge 4).
```

Thanks to this disaggregation, combined with a choice of prior that discourages longer rules, interactions are freely generated but will only be used if actually necessary to the model. Without disaggregation, the model could include a complex rule such as $I(x_1 < 3, x_3 < 2)$ only because there was no other way to express a simpler condition contained in it such as $I(x_3 < 2)$.

4.2 Linear fit

A favoring of linear terms over rules may also be enforced by tuning how the linear fit is performed. For instance, while HorseRule standardizes the rules generated from the tree ensembles and then applies structured shrinkage to enforce simplicity, RuleFit avoids standardization of rules so that rules involving very few or very many observations are naturally shrunken more.

The two approaches are connected, since rescaling a feature before fitting a horseshoe model is equivalent to leaving the feature unchanged and re-scaling the local parameter A_j instead. The explicit computations that show this equivalent is found in the Supplementary material as Remark 1. For HorseRule this means that standardization may be avoided by replacing A_j with:

$$A'_{j} = \frac{A_{j}}{\sqrt{\overline{r}_{j}(1 - \overline{r}_{j})}}$$

$$= \frac{(2\min(\overline{r}_{j}, 1 - \overline{r}_{j}))^{\mu - 0.5}}{m_{j}^{\eta}} \cdot \sqrt{\frac{2}{\max(\overline{r}_{j}, 1 - \overline{r}_{j})}}$$

In particular, standardization is equivalent to reducing the penalization parameter μ by 0.5 and introducing a (much more stable) multiplicative factor of $\sqrt{\frac{2}{\max(\overline{r}_j,1-\overline{r}_j)}}$. This rescaling prevents instability in the standardization process while having the same effect on shrinkage. In RuleSHAP, rules are thus not standardized but the standardization is accounted for by defining the following local shrinkage scale:

$$\begin{split} A_j &= \frac{1}{2} \cdot \frac{(2\min(\overline{r}_j, 1 - \overline{r}_j))^{\mu - 0.5}}{m_j^{\eta}} \cdot \sqrt{\frac{2}{\max(\overline{r}_j, 1 - \overline{r}_j)}} \\ &= \frac{(2\min(\overline{r}_j, 1 - \overline{r}_j))^{\mu - 0.5}}{m_j^{\eta} \sqrt{2\max(\overline{r}_j, 1 - \overline{r}_j)}}. \end{split}$$

The extra multiplicative factor of $\frac{1}{2}$ is applied to ensure that the scale parameter A_j for a rule is never higher than that of a linear term.

A second feature of RuleSHAP is that it relies on a tweaked horseshoe prior which allows for separate global shrinkages τ_0 and τ_1 for rules and linear terms respectively:

$$y|X, \beta, \sigma^2 \sim \mathcal{N}(X\beta, \sigma^2 I_n),$$

$$\beta_j|\lambda, \tau, \tau_0, \tau_1, \sigma^2 \sim \mathcal{N}(0, \lambda_j^2 \tau_{\delta(j)}^2 \tau^2 \sigma^2),$$

$$\lambda_j \sim \mathcal{C}^+(0, A_j),$$

$$\tau, \tau_0, \tau_1 \sim \mathcal{C}^+(0, 1),$$

$$\sigma^2 \sim \sigma^{-2} d\sigma^2.$$

where $\delta(j)$ is an indicator of whether the j-th term is a rule $(\delta(j) = 0)$ or a linear term $(\delta(j) = 1)$. This tweak prevents overshrinkage: uninformative rules do not induce higher shrinkage of linear terms, and vice versa. We employ a Gibbs sampling scheme for Horseshoe regression to estimate the model, as described in [21] and implemented in [22] [23].

4.3 Feature effect measures

To mitigate the problems of the RuleFit importances discussed above, we propose the use of marginal Shapley values to retrieve the local effect of each feature in the model. Shapley values [13] are an increasingly popular tool for deconstructing the predictions of a (black-box) model into the sum of effects of individual features [14] [24]. To illustrate the reasoning behind the definition of Shapley values, let us consider a fitted model F(x). For any datapoint x^* and any feature index j, Shapley values are a local measure that estimates how much the j-th feature contributes to a specific prediction $F(x^*)$. Partial dependence plots (PDPs), which aim at doing the same, would quantify this effect as:

$$\mathcal{PDP}_j(x^*) := \mathbb{E}[F(x_1, \dots, x_p) | x_j = x_j^*] - \mathbb{E}[F(x_1, \dots, x_p)]. \tag{5}$$

This contrast, however, does not take into account cooperation between features, as we show in Example 1, in the Supplementary material. Shapley values, on the other hand, acknowledge the fact that the importance of a feature x_j depends on which features x_j is cooperating with. Therefore, PDP-like contrasts are computed for any combination of all remaining features. More specifically, the Shapley value of the j-th feature for a datapoint x^* is computed as:

$$\phi_j(x^*) = \sum_{S \subseteq \{1, \dots, p\} \setminus \{j\}} \frac{1}{p\binom{p-1}{|S|}} \Big(\mathbb{E}[F(x)|x_S = x_S^*, x_j = x_j^*] - \mathbb{E}[F(x)|x_S = x_S^*] \Big), \tag{6}$$

where the notation $x_S = x_S^*$ means $x_k = x_k^* \, \forall k \in S$. In this formula, the weights $\frac{1}{p\binom{p-1}{|S|}}$ take into account the fact that there are fewer subsets S where |S| is very small or very large.

Shapley values have also been proposed as a way to quantify the predictive effect of interactions [25]. Their definition is analogous to that of Formula 6, but contrasts are replaced with ANOVA-like interaction effects:

$$\phi_{j,k}(x^*) = \sum_{S \subseteq \{1,\dots,p\} \setminus \{j,k\}} \frac{1}{(p-1)\binom{p-2}{|S|}} \left(\mathbb{E}[F(x)|x_S = x_S^*, x_j = x_j^*, x_k = x_k^*] - \mathbb{E}[F(x)|x_S = x_S^*, x_j = x_j^*] - \mathbb{E}[F(x)|x_S = x_S^*, x_k = x_k^*] + \mathbb{E}[F(x)|x_S = x_S^*] \right).$$

$$(7)$$

What is left after subtracting all the interaction Shapley values may then be viewed as main effects.

The additivity property of Shapley values, combined with the additive nature of RuleFit, allows us to focus on Shapley values of individual terms. The overall model effects are then obtained by summing up the effects across all terms. An alternative to Shapley values as computed in Equation 6 are marginal Shapley values, also called Random Baseline Shapley values or interventional Shapley values, where the conditional expectations $\mathbb{E}[F(x)|x_S=x_S^*]$ are replaced by their interventional counterparts $\mathbb{E}[F(x)|do(x_S=x_S^*)]$. This eases computation greatly, and produces Shapley values that are more representative of the model's prediction mechanisms, rather than taking correlations between features into account to reconstruct the underlying truth [26]. Furthermore, as also discussed in [26], the marginal Shapley values are not far from their exact, non-interventional counterparts in a model like ours, since the effect of correlated terms is naturally spread out by the Bayesian linear regression in our model. This is not the case for RuleFit, in which the frequentist

LASSO regression will tend to penalize correlated duplicates out of the model and assign all of the predictive effect to one term only.

Aside from the many model-agnostic approaches that approximate Shapley values [27], there are also tree-specific computations for the models described in Section 3. More specifically, upon viewing an individual rule as a specific 0-1-valued tree, TreeSHAP [28][29] may be used to compute the Shapley values of a dichotomous rule. In the next section, we introduce an explicit formula for computing it in a more direct manner.

5 Direct computation of Shapley values

In this section we produce an explicit formula for a computation of marginal Shapley values of a single dichotomous condition. The formula estimates each $\mathbb{E}[f(x)|do(x_S = x_S^*)]$ with its respective sample mean and is thus an "exact" computation in this sense.

In the context of a dichotomous condition as it appears in RuleSHAP, by additivity of Shapley values, this formula may be used to efficiently compute Shapley values for any of the models described in Section 3. The result, whose proof is found in the Supplementary material for a more general setting, is the following:

Theorem 1. Assume to have a dataset \mathcal{T} of size n. Consider a 0-1 coded rule decomposed as the product of single conditions and thus of the form $r(x_1, \ldots, x_p) = \prod_{l=1}^p R_l(x_l)$, with $R_l : \mathbb{R} \to \{0, 1\}$. Given $j \in \{1, \ldots, p\}$, an unbiased estimator of the marginal Shapley value of the term $\hat{a} \cdot r(x)$ for the j-th feature and datapoint x^* is:

$$\widehat{\phi}_{j}(x^{*}) = \widehat{a} \cdot \left(\frac{1}{n(p - q(x^{*}) + R_{j}(x_{j}^{*}))} \sum_{\substack{t \in \mathcal{T}s.t. \\ R_{k}(t) = 1 \lor R_{k}(x^{*}) = 1 \ \forall k}} \frac{R_{j}(x_{j}^{*}) - R_{j}(t_{j})}{\binom{2p - q(x^{*}) - q(t) - 1 + R_{j}(x_{j}^{*}) + R_{j}(t_{j})}{p - q(x^{*}) + R_{j}(x_{j}^{*})}} \right),$$

where $q: \mathbb{R}^p \to \mathbb{N}$ is defined as $q(x) = \sum_{j=1}^p R_l(x_l)$.

This formula suggests computing Shapley values with an algorithm such as Algorithm 1. For rules that involve only some of the features, one may restrict the computation to those features and ignore the remaining ones (see Lemma 4 in the Supplementary Material). For a regular tree, which may be decomposed as the sum of its end nodes, the computational cost is thus the same as path-independent TreeSHAP [29], which also coincides with Algorithm 1 in terms of estimates. However, Algorithm 1 allows us to look at individual rules rather than whole trees for the same computational cost. Computing Shapley values for an individual rule with TreeSHAP would require converting a rule back into a full 0-1-valued tree of depth D, with D+1 terminal nodes. Because of this, TreeSHAP is D+1 times slower than Algorithm 1 when the purpose is to obtain the Shapley values of each rule separately, as in our setting. However, as both algorithms are quite fast and D is typically capped at a very low value for RuleSHAP, this difference might not be large. Our algorithm remains more advantageous in contexts where trees have high depth but few covariates per tree, since in these settings the inner for loop in Algorithm 1 only needs to be run for the features involved in the rule. An example of such a setting is Planted Trees or Planted Tree Forests [30].

As shown in the Supplementary material, the same argument can be applied to compute interaction Shapley values and thus implement Algorithm 2:

Theorem 2. Assume to have a dataset \mathcal{T} of size n. Consider a 0-1 coded rule decomposed as the product of single conditions and thus of the form $r(x_1, \ldots, x_p) = \prod_{k=1}^p R_l(x_l)$, with $R_l : \mathbb{R} \to \{0, 1\}$. Given two different indices $j, k \in \{1, \ldots, p\}$, an unbiased estimator of the marginal interaction Shapley value of the term $\hat{a} \cdot r(x)$ for the j-th and k-th features and the datapoint x^* is:

$$\widehat{\phi}_{j,k}(x^*) = \widehat{a} \cdot \left(\frac{1}{n(p-1-q(x^*)+R_j(x_j^*)+R_k(x_k^*))} \right) \\ \cdot \sum_{\substack{t \in \mathcal{T}s.t. \\ R_k(t)=1 \lor R_k(x^*)=1 \lor k}} \frac{R_j(x_j^*)R_k(x_k^*)+R_j(t_j)R_k(t_k)-R_j(x_j^*)R_k(t_k)-R_j(t_j)R_k(x_k^*)}{\binom{2p-q(x^*)-q(t)-3+R_j(x_j^*)+R_k(x_k^*)+R_j(t_j)+R_k(t_k)}{p-q(x^*)+R_j(x_j^*)+R_k(x_k^*)}} \right),$$

where $q: \mathbb{R}^p \to \mathbb{N}$ is defined as $q(x) = \sum_{i=1}^p R_l(x_l)$.

In the Supplementary material, we show how the same argument may be taken further. For instance, it may be used to also estimate (interaction) Shapley values for interaction terms that combine rules and linear terms, i.e. of the form $x_i \cdot r(x)$, where r(x) is a 0-1-encoded rule. This means that RuleSHAP could potentially be extended to include terms that appear in a GLM tree (i.e. a tree that presents linear models at its leaf nodes, [31]). This presents an alternative, direct computation to the work of [32], where the TreeSHAP algorithm is adjusted in order to obtain such estimates. Lastly, all such formulas write Shapley values as sample means over the dataset, which allows us to asses the instability of the Shapley estimatation itself. As this uncertainty quickly vanishes as sample size grows, we considered it to be negligible for our setting. However, this uncertainty might be taken into account when computing Shapley values for extremely small sample sizes. Furthermore, this formulation might be convenient for contexts such as stratified sampling where re-weighting of the observations may be needed.

6 Empirical evaluation

In this section we describe the experiments on simulated datasets. Our aims were twofold: first, we compared RuleSHAP to the analogous approaches RuleFit, HorseRule and Random Forest. This part focused on signal reconstruction and shows the limitations motivating us to develop RuleSHAP. Second, we compared RuleSHAP with BART and HorseRule, since they may also be combined with Shapley values to provide uncertainty estimates for local importance measures. This part focused on the task of distinguishing signal from noise, as this is a typical use of uncertainty quantification in research.

6.1 Evaluation of feature effect reconstruction

6.1.1 Method

We first set up a simulation study to compare RuleSHAP with other methods typically used for prediction and interpretation purposes: OLS regression, Lasso regression (from *glmnet* R package [33]), RuleFit (from *pre* R package, [16]), HorseRule (from *horserule* R package, [34]) and Random Forest (from *randomForest* R package, [35]). HorseRule was fitted in two ways: as the authors prescribe in [11] (a mix of boosted trees and Random Forest trees, with no favoritism to linear terms)

```
Algorithm 1 Estimating Shapley values \phi_1(x^*), \ldots, \phi_p(x^*) for F(x) = \prod_{l=1}^p R_l(x_l)
Require:
   R_1(x_1^{(1)}), \dots, R_p(x_p^{(1)}), \dots, R_1(x_1^{(n)}), \dots, R_p(x_p^{(n)}) \in \{0, 1\}

R_1(x_1^*), \dots, R_p(x_p^*) \in \{0, 1\}
Ensure:
   q^* \leftarrow \sum_{l=1}^p R_l(x_l^*)
   phiSum_1 \leftarrow \cdots \leftarrow phiSum_p \leftarrow 0
                                                                                                  ▶ Preallocate summations as in formula
   for i = 1, \ldots, n do
                                                                                                      ▶ Loop over points used for estimates
         if \sum_{l=1}^{p} (1 - R_l(x_l^{(i)}))(1 - R_l(x_l^*)) = 0 then
                                                                                                > Check if point contributes to estimates
              q \leftarrow \sum_{l=1}^{p} R_l(x_l^{(i)}) for j = 1, \dots, p do
                    phiSum_{j} \leftarrow phiSum_{j} + \frac{R_{j}(x_{j}^{*}) - R_{j}(x_{j})}{\binom{2p - q^{*} - q - 1 + R_{j}(x_{j}^{*}) + R_{j}(x_{j}^{(i)})}{p - q^{*} + R_{i}(x_{j}^{*})}}
                                                                                                                                ▶ Update summations
               end for
         end if
   end for
   for j = 1, \dots, p \operatorname{do}

\phi_j \leftarrow \frac{phiSum_j}{n(p-q^* + R_j(x_i^*))}
                                                                                     ▶ Rescale summations to obtain Shapley values
```

and with a combination of hyperparameters more similar to our approach (only using Random Forest, with a relaxation on the shrinkage of linear terms by a factor $A_j = 100$). The comparison was carried out in terms of predictive performance, recovery of individual effects and ability to prioritize linear terms over (many) rules. The methods were tested on the following benchmark data-generating procedure, initially proposed by Friedman [36]:

end for

$$x_1, \dots, x_5 \sim \mathcal{U}(0, 1),$$

 $\epsilon \sim \mathcal{N}(0, \sigma^2),$
 $y = 10\sin(\pi x_1 x_2) + 20(x_3 - 0.5)^2 + 10x_4 + 5x_5 + \epsilon.$ (8)

The feature set was extended with noise features also drawn uniformly at random between 0 and 1. A correlation of 0.3 was ensured across all features. By default, the error variance in the Friedman procedure is set to $\sigma^2 = 1$, which produces an irreducible error of less than 5% of the total variance. We therefore chose $\sigma^2 = 100$, which produces about 80% of irreducible error, for a more realistic setting.

We varied sample size n = 100, 300, 500, 1'000, 3'000, 5'000 and dimensionality p = 10, 30. For each combination of n and p, the fitting was repeated on five simulated training datasets and predictive performance was assessed on a test dataset of size 10'000, common across all replicates. The experiment was analogously repeated for the case of logistic regression, where the outcome was

```
Algorithm 2 Estimating interaction Shapley values \{\phi_{j,k}(x^*)\}_{j,k} for F(x) = \prod_{l=1}^p R_l(x_l)
Require:
   R_1(x_1^{(1)}), \dots, R_p(x_p^{(1)}), \dots, R_1(x_1^{(n)}), \dots, R_p(x_p^{(n)}) \in \{0, 1\}
   R_1(x_1^*), \ldots, R_p(x_n^*) \in \{0, 1\}
Ensure:
   q^* \leftarrow \sum_{l=1}^p R_l(x_l^*)
   phiSum_{1,1} \leftarrow \cdots \leftarrow phiSum_{1,p} \cdots \leftarrow phiSum_{p,p} \leftarrow 0  > Preallocate summations as in formula
   for i=1,\ldots,n do
                                                                                                          ▶ Loop over points used for estimates
         if \sum_{l=1}^{p} (1 - R_l(x_l^{(i)}))(1 - R_l(x_l^*)) = 0 then \triangleright Check if point contributes to estimates
               q \leftarrow \sum_{l=1}^{p} R_l(x_l^{(i)}) for j = 1, \dots, p do
                     for k = 1, ..., p s.t. k \neq j do
phiSum_{j,k} \leftarrow phiSum_{j,k} + \frac{R_{j}(x_{j}^{*})R_{k}(x_{k}^{*}) + R_{j}(t_{j})R_{k}(t_{k}) - R_{j}(x_{j}^{*})R_{k}(t_{k}) - R_{j}(t_{j})R_{k}(x_{k}^{*})}{\binom{2p-q^{*}-q-3+R_{j}(x_{j}^{*})+R_{k}(x_{k}^{*})+R_{j}(t_{j})+R_{k}(t_{k})}{p-q^{*}+R_{j}(x_{j}^{*})+R_{k}(x_{k}^{*})}}
                     end for
               end for
         end if
   end for
   for j = 1, \ldots, p do
         for k = 1, \dots, p s.t. k \neq j do \phi_{j,k} \leftarrow \frac{phiSum_{j,k}}{n(p-1-q^*+R_j(x_j^*)+R_k(x_k^*))}
                                                                                        ▶ Rescale summations to obtain Shapley values
         end for
```

defined by:

end for

$$\eta = 10\sin(\pi x_1 x_2) + 20(x_3 - 0.5)^2 + 10x_4 + 5x_5,
p = \frac{exp(\eta - \overline{\eta})}{exp(\eta - \overline{\eta}) + 1},
y \sim \mathcal{B}\mathbf{e}(p),$$
(9)

with $\bar{\eta} \approx 14.4$ computed as the approximate mean of η under this data-generation scheme, in the case of independent features.

A Bayesian regression typically requires a check on the convergence of the estimates. However, as this simulation was repeated for many settings in multiple iterations, we simply used a very large number of MCMC samples to ensure convergence without the need for manual checks (22'000 samples drawn per model, out of which 2'000 were burn-in). The results were stable under replication, which we interpreted as a sign that the chains had indeed converged.

6.1.2 Results

The boxplots in Figures S1, S2, S3 and S4 in the Supplementary material compare the coefficients of the linear terms of the OLS linear regression, LASSO regression, RuleFit, HorseRule (both param-

eter settings) and RuleSHAP models. These are shown across the five replicates of the experiment, for features x_3 (purely nonlinear), x_4 (purely linear), x_5 (purely linear) and x_6 (noise). As expected, all models are able to correctly identify x_6 as noise, but RuleFit completely penalizes the linear terms out of the model, even for features x_4 and x_5 which induce a purely linear effect on the outcome. While relaxing the shrinkage on linear terms partially mitigates the problem, HorseRule does not induce a satisfactory improvement over RuleFit in this sense. RuleSHAP, on the other hand, is more prone to include linear terms, especially for the linear features x_4, x_5 and especially when n is larger.

In terms of predictive performance, RuleSHAP remains strongly competitive. The test MSEs for the case of a continuous outcome (Figure S5) and the test area under the ROC curve for the case of binary outcome (Figure S6) are shown in the Supplementary material. These figures show RuleSHAP's predictive performance to be up to par with all other models for all sample sizes.

Lastly, we used the simulated data to measure how well RuleSHAP reconstructs the effect of each feature. We focused on a continuous outcome, where predictions of Random Forest, HorseRule and RuleSHAP are all on the same scale. Shapley values were computed for each of the models fitted above, to evaluate the quality of the feature effect reconstruction. For each replicate, the mean squared distances between the true local effects and the estimated local effects were averaged across all datapoints. The boxplots in Figure 2 show the mean squared distances across replicates, for the most indicative sample sizes. To compensate for the fact that each feature's effect has a different scale, the squared distance of each signal feature was rescaled by the overall variance of that effect. The boxplots thus indicate the "fraction of unexplained effect variance". The full figure for all sample sizes is shown in the Supplementary material as Figure S7, while Figure S8 is shown in the Supplementary material for the data with p=30 features. From these visualizations we observe that while all methods improve with more observations, Random Forests remain unsatisfactory at effect reconstruction, even for settings with higher sample sizes or settings where their predictive performance is up to par with the other models. For low sample sizes, RuleSHAP better identifies noise, but does not detect the purely nonlinear effect of feature x_3 . For all other feature effects, RuleSHAP has better or up-to-par reconstruction. This reflects the main properties of RuleSHAP: the effects of features x_1, x_2, x_4, x_5 are (partially) linear and thus can be better reconstructed across all sample sizes. The effect of feature x_3 , on the other hand, may only be reconstructed by rules, and low sample sizes do not give enough certainty in the rule generation scheme for x_3 to emerge. This explains why many iterations show an unexplained feature effect variance of (approximately) 1, i.e. an estimated null effect of x_3 , for low sample sizes. HorseRule and Random Forest, on the other hand, employ a more uncertainty-insensitive rule-generation scheme, which thus "dares" to create more specific rules. This induces a better estimation of the effect of x_3 , but also a worse estimation of the (null) effect of noise, which in turn negatively affects the type I error rate, as we show with our next experiment. These trends might also be explained by RuleSHAP's beneficial ability to discourage spurious interactions between noise and signal features, since such interactions both increase the estimated effect of noise and dilute the signal effects.

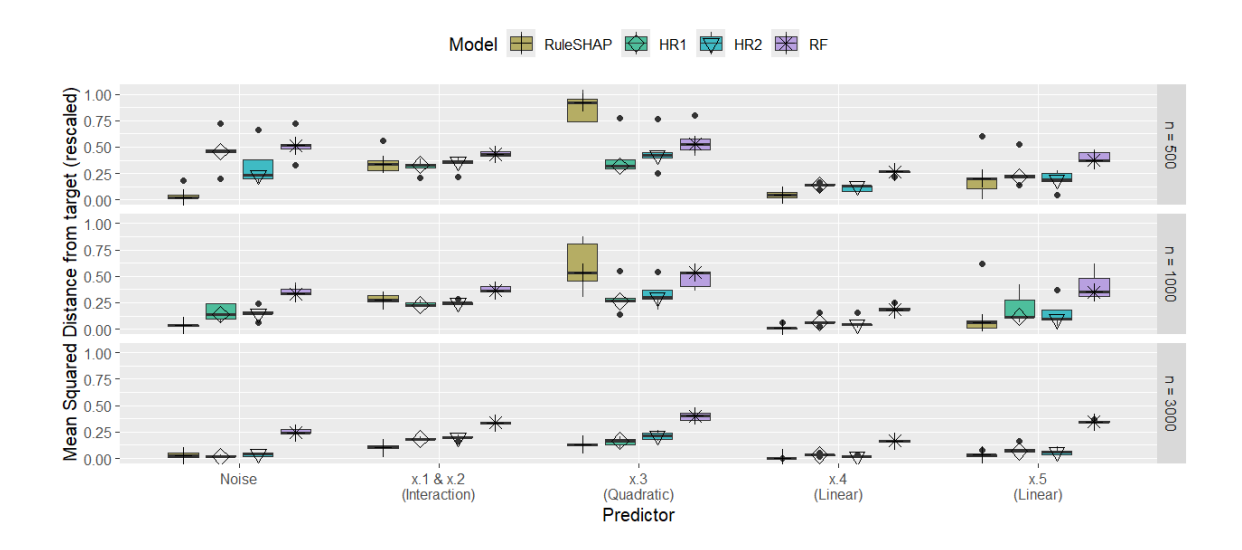


Figure 2: Rescaled mean squared distance between feature effects estimated by the model and the target effects for five replicates of different models fitted on Friedman-generated data, for p=10 features and some of the different sample sizes n. Full figure is shown in the Supplementary material as Figure S7. Estimated feature effects are computed as marginal Shapley values. Since x_1 and x_2 induce an interacting effect, their feature effects are analyzed jointly, as the sum of the Shapley values of the two features. The distance is averaged across all replicates of the experiment, across all points of the dataset. All noise features are averaged out together. Models are fitted on data generated from the Friedman generating function, with continuous outcome and p=10. To ease interpretation across different effect magnitudes, the squared distance of each signal feature was rescaled by the overall variance of that effect.

6.2 Evaluation of uncertainty quantification

6.2.1 Method

To evaluate uncertainty quantification in relation to feature selection, we compared RuleSHAP to BART and HorseRule, since all three may be combined with Shapley values to provide uncertainty estimates for local feature effects. As the n/p ratio changes, the goal of these models might change: while for high ratios one might be interested in a good reconstruction of the effects, a higher dimensionality might push for the use of uncertainty quantification to perform feature selection. For this reason this experiment explored the type I error rates and false discovery rates of all three approaches fitted to datasets generated with the Friedman generating function. We focused specifically on the setting with n = 1'000 observations and p = 10, 30, 50. The error variance and correlation across features were kept to $\sigma^2 = 100$ and $\rho = .3$ respectively, as in the previous experiments. A feature was considered to be flagged as "significant" by a model if the 95% credible interval for the Shapley value associated to the feature did not contain zero for at least one observation in the dataset. The experiment was replicated 100 times for each value of p.

6.2.2 Results

Table 1 shows the observed rejection rates for the null hypothesis of no effect. Results are averaged across signal features (x_1,\ldots,x_5) and noise features (x_6,\ldots,x_p) separately. The rejection frequencies are also used to compute the false discovery rates shown in Table 2. From these tables we see that while BART and HR1 have higher discovery power than RuleSHAP, they also have quite high type I error rates. The HR2 model seems to better control for type I error rates, but becomes overly confident for a high n/p ratio, where the estimated type I error rate lies quite above the nominal threshold of $\alpha=0.05$. RuleSHAP, on the other hand, seems to be the only method to have an at-most-nominal type I error rate, across all settings. It also seems to be strongly competitive in terms of false discovery rate, even when the noise features substantially outnumber the signal features. Overall, the rejection rates decrease for lower n/p ratios for all methods. To illustrate the reason behind the excessive rejection rates, Figure 3 shows the Shapley values produced by one of the BART and RuleSHAP fits respectively. As we can see, BART's feature effect estimations are much less stable and the underestimation of such instability yields a high type I error rate. This is prevented by RuleSHAP's stability in the rule generation, which makes the shape of the effects less erratic.

7 Risk and protective factors in Cardiovascular Health

To showcase its use in practice, we fitted RuleSHAP to a dataset from the HELIUS study [15], which collects information about physical and mental health across different ethnic groups in the Netherlands. The very large sample size of the HELIUS study (n=21'570) allowed us to explore the fitting and prediciton patterns of several models for different sample sizes. Following [37], we focused on two different outcomes: systolic blood pressure and cholesterol level. These were predicted from BMI, socio-demographic features (age, ethnicity, gender) and habits-related features (smoker Y/N, yearly cigarettes consumption, coffee drinker Y/N). As a form of negative control, we added four noise features drawn from a standard normal distributions to the dataset.

	Signal (x_1,\ldots,x_5)				Noise (x_6, \ldots, x_p)			
	BART	HR1	HR2	RuleSHAP	BART	HR1	HR2	RuleSHAP
p = 10	0.992	0.988	0.956	0.968	0.266	0.118	0.098	0.048
p = 30	0.974	0.978	0.864	0.888	0.010	0.073	0.020	0.006
p = 50	0.958	0.946	0.808	0.814	0.063	0.060	0.013	0.004

Table 1: Empirical rejection rates as observed from 100 independent replicates of using Shapley values to detect significant features from a RuleSHAP model, a BART model and two HorseRule models (HR1 for default settings, HR2 for settings similar to RuleSHAP). The models are fitted on n=1'000 observations generated from the Friedman data-generating scheme. The rates are aggregated across all noise features and across all signal features. The nominal type I error rate of the credible intervals is $\alpha=0.05$ for all models.

	BART	HR1	HR2	RuleSHAP
p = 10	0.211	0.107	0.093	0.047
p = 30	0.339	0.272	0.106	0.033
p = 50	0.371	0.365	0.126	0.040

Table 2: Empirical False Discovery Rates rates as observed from 100 independent replicates of using Shapley values to detect significant features from a RuleSHAP model, a BART model and two HorseRule models (HR1 for default settings, HR2 for settings similar to RuleSHAP). The models are fitted on n=1'000 observations generated from the Friedman data-generating scheme. The nominal type I error rate of the credible intervals is $\alpha=0.05$ for all models.

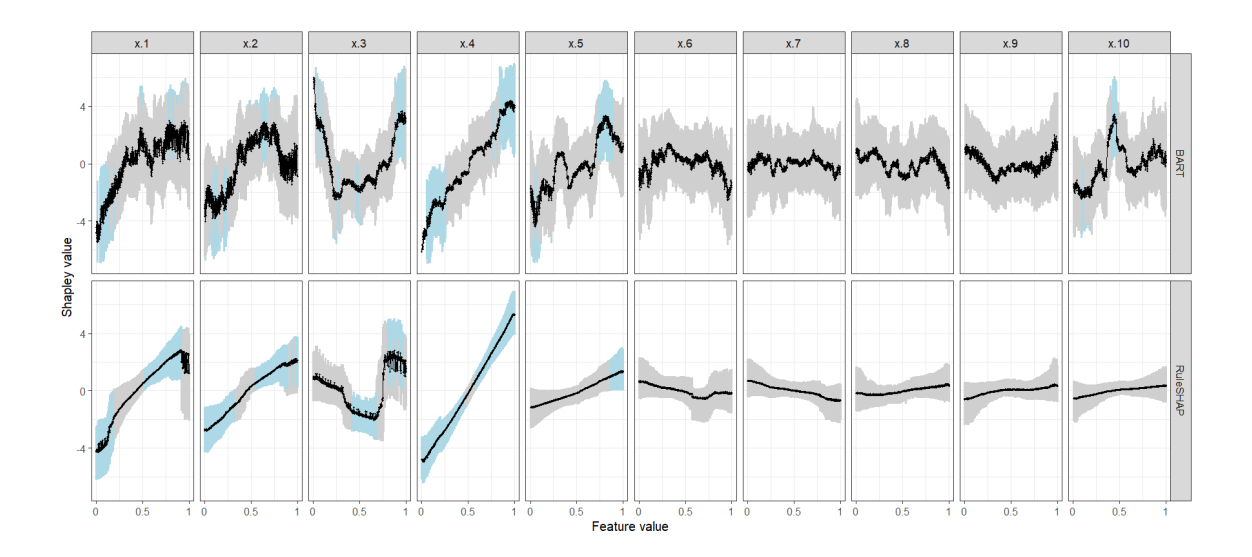


Figure 3: Example of Shapley values estimated from BART (top row) and RuleSHAP (bottom row) fitted on the same n=1'000 Friedman-generated observations. Point-wise credible intervals are color-coded based on whether they contain zero (grey) or not (light blue).

In order to fit the RuleSHAP model, the categorical features were dummy-coded. In the case of ethnicity, which presents five categories, we followed the same logic as contrast coding and coded each dummy variable with the values -0.5,2. By doing so, we ensured that the the dummy variables are standardized in the setting where the five categories are balanced. All other aspects of the experiment matched those of the simulation described in Section 5: for each of the two outcomes, we fitted different models (Ordinary Least Squares, Random Forest, HorseRule, RuleFit, LASSO regression, RuleSHAP) on a subsample of different sizes (n = 100, 300, 500, 1'000, 3'000, 5'000), and registered the estimated coefficients of the linear terms, the test predictive performance and the Shapley values of the RuleSHAP models. More specifically, 15'000 observations were retained for training, and the remaining 6'570 observations were used for testing. For sample sizes n = 100, 300, 500, 1'000, 3'000, five non-overlapping datasets were drawn from the 15'000 training observations, without replacement. For the sample size of n = 5'000, where 5 non-overlapping datasets would require 25'000 training observations, we allowed the datasets to overlap with eachother, while still ensuring that no observation would appear multiple times in the same dataset. A single fit on n = 10'000 of the training observations was also included in the experiment.

Predictive performance may be observed in Figure 4 for some indicative sample sizes and is fully shown in Figures S9 and S10 of the supplementary material: for the prediction of systolic blood pressure, which is already accurately described by a linear model, RuleSHAP relies more heavily on the linear terms, making it the method that most closely captures linear effects after OLS. For the prediction of cholesterol levels, on the other hand, linear fits are too rigid, and this is reflected in the much poorer predictive performance of the OLS model. This seems most adequately captured by RuleSHAP, which relies on rules to correct linear terms, only when necessary. This is not the case for RuleFit and HorseRule, which instead largely prefer rules over linear terms for both predicted outcomes. The problem is mitigated with careful tuning of the HorseRule hyperparameters (HR2 model) but remains present.

Figures 5 and 6 show the Shapley values from the RuleSHAP fit on n=10'000 observations, for both outcomes. We see heavy wiggliness in the marginal effects of some features. This does not denote instability, but rather the presence of meaningful interactions, for example, the effect of a certain value of age strongly oscillates across different ethnicities. The presence of interactions is also in accordance with the strikingly good predictive performance of a single conditional inference tree for higher sample sizes. The heatmap in Figures S11 and S12 in the Supplementary material use interaction Shapley values to produce a quick, global insight into the significant interaction trends estimated by RuleSHAP for both outcomes. These figures show several significant interaction effects between age and other features (ethnicity and sex for prediction of systolic blood pressure; glucose, BMI, ethnicity and sex for prediction of cholesterol). Using marginal Shapley values, these can be further explored. Figure 7, for instance, specifically focuses on the interaction between age and sex that is detected when predicting cholesterol level. Figure S13 in the Supplementary material explores the interaction between age and ethnicity for the prediction of systolic blood pressure.

8 Discussion

We have shown how RuleSHAP combines the strengths of RuleFit, HorseRule and Shapley values to enable local inference for feature importance measures. We developed an improved rule-generation procedure that better accounts for uncertainty and counters overfitting, and we derived an explicit

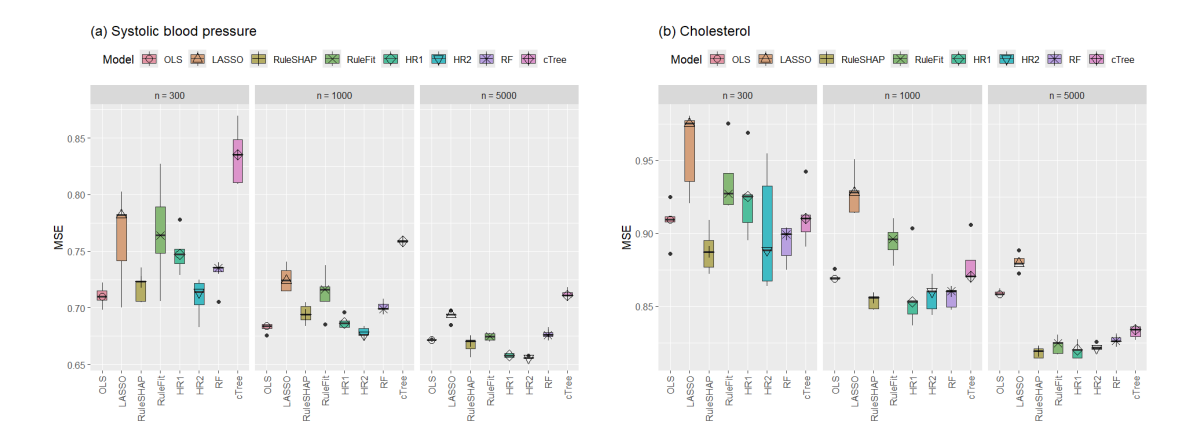


Figure 4: Test MSE across five fits of OLS linear regression, LASSO regression, RuleFit regression, HorseRule regression (HR1 for default settings; HR2 for custom settings), RuleSHAP regression and Random Forest. These models are fitted on subsamples of different sizes n taken from the the HELIUS study data, with predicted outcome of systolic blood pressure (panel a) or cholesterol (panel b).

formula for efficient computation of Shapley values. The simulations and the application to the from the HELIUS data suggest that RuleSHAP strikes a better balance between linear terms and rules, especially for larger sample sizes. This sets RuleSHAP apart from its predecessors, since both RuleFit and HorseRule seemed mostly unable to accurately recognize linear signal, even when the underlying generating function was purely linear. This pattern confirms the findings in [11], where the presence of linear terms in the HorseRule model was not relevant for predictive performance. By contrast, RuleSHAP more heavily relies on linear terms, which produces a model whose predictive performance is competitive both in small and large sample sizes. While our simulations show that good predictive performance is not necessarily an indicator of valid feature effect reconstruction (as was the case for Random Forests), RuleSHAP seems to still be competitive (when not superior) in both regards.

The main advantage of RuleSHAP is that it allows for more reliable detection and inference of beyond-linear trends and that the latter can be performed on a local level. Many other ML alternatives are also typically considered for this context, but to our knowledge none of them can produce satisfactory results, especially at the level of individual effects. Generalized Additive Models (GAMs), for instance, can detect nonlinear effects and test them. However, such testing is only valid on a global level, since the credible intervals for local effects are still in need of improvement [38]. Most importantly, GAMs require manual specification of any interaction terms, as for a linear model. These two elements impede discovery and reliable statistical inference for novel local effects. Tree ensembles, on the other hand, capture both nonlinearity and interaction effects and, in the context of Random Forests, include importance measures with uncertainty quantifications [39]. These measures, however, are also limited to a global setting. Furthermore, they join the marginal and the interaction effects in one single number, the estimated increase in MSE, which is not the effect of the covariates on the outcome. This makes any interpretation of what is being tested far

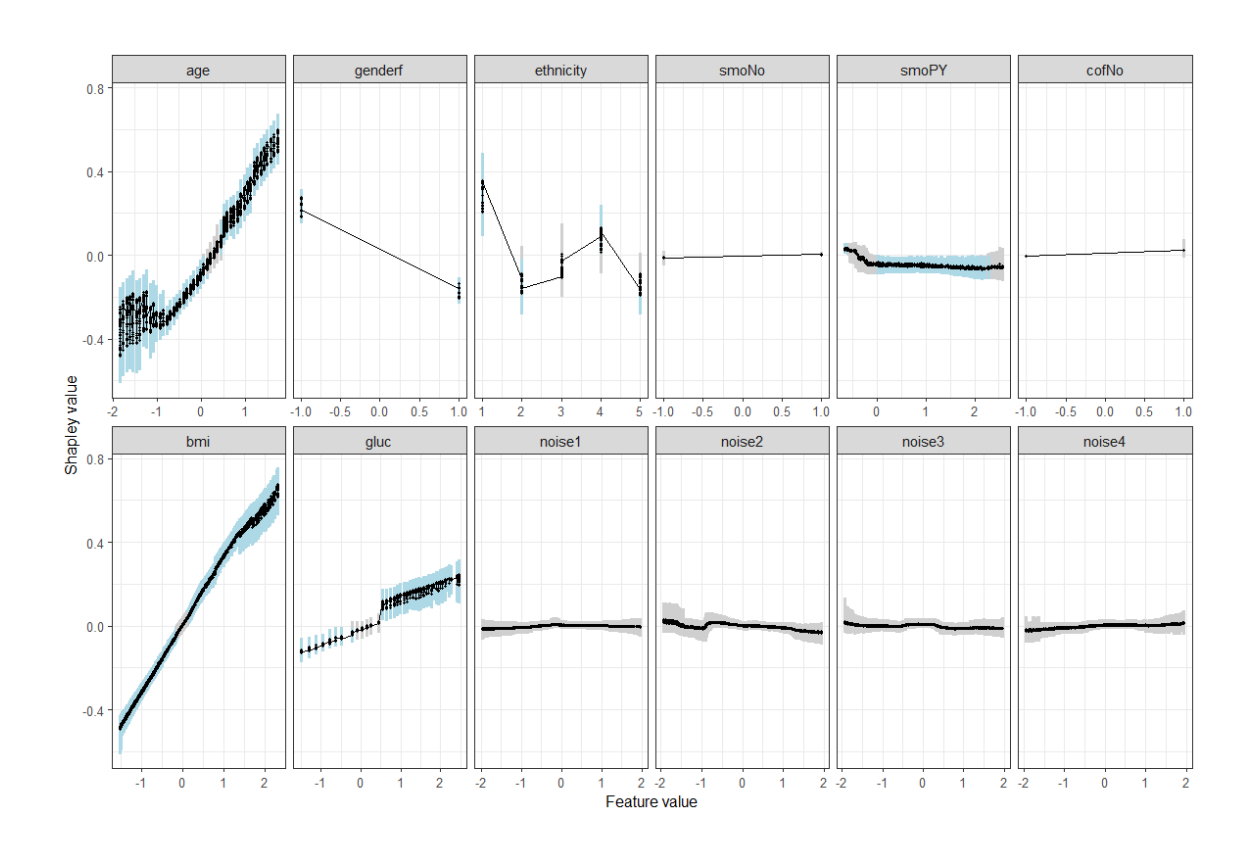


Figure 5: Shapley values computed from a RuleSHAP model fitted on n=10'000 observations from the HELIUS study, to predict systolic blood pressure. Point-wise 95% credible intervals are shown and color-coded based on whether they contain zero (grey) or not (light blue).

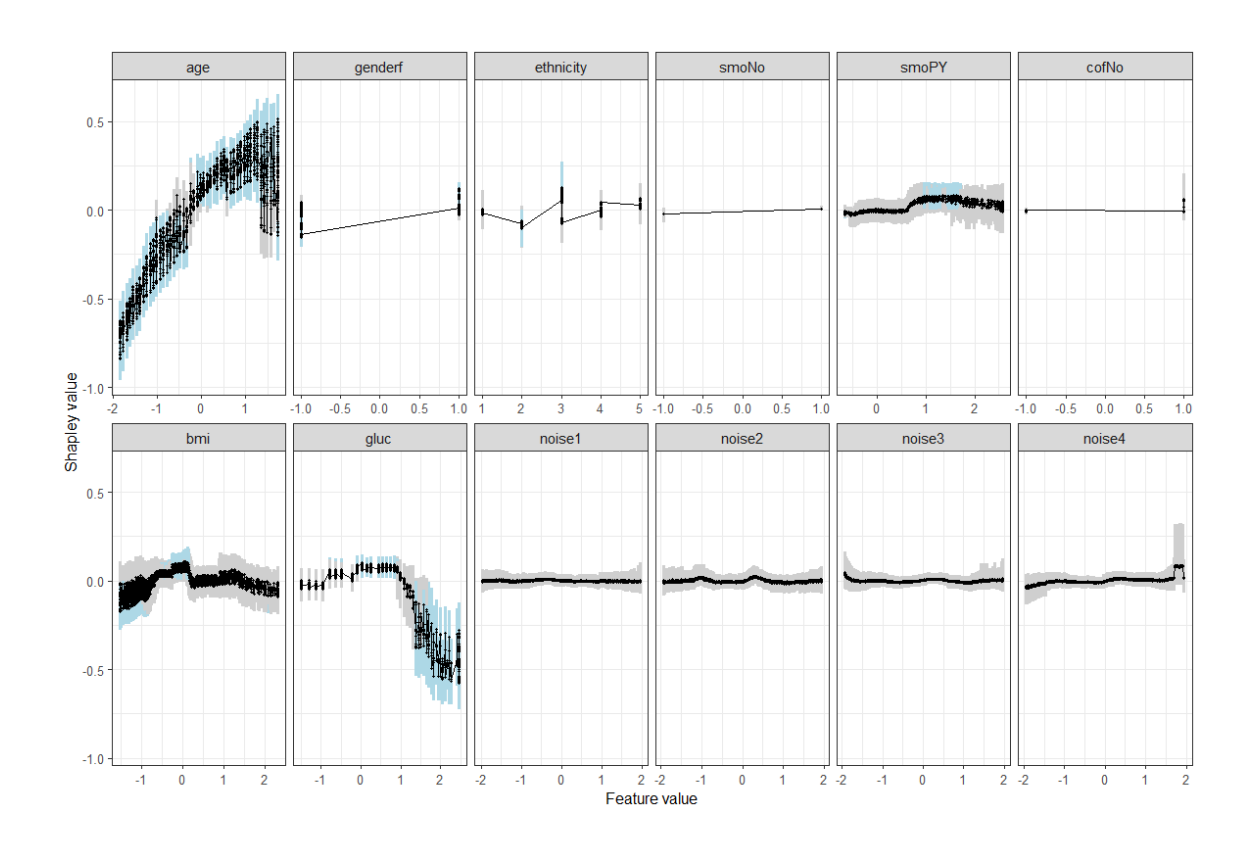


Figure 6: Shapley values computed from a RuleSHAP model fitted on n=10'000 observations from the HELIUS study, to predict cholesterol. Point-wise 95% credible intervals are shown and color-coded based on whether they contain zero (grey) or not (light blue).

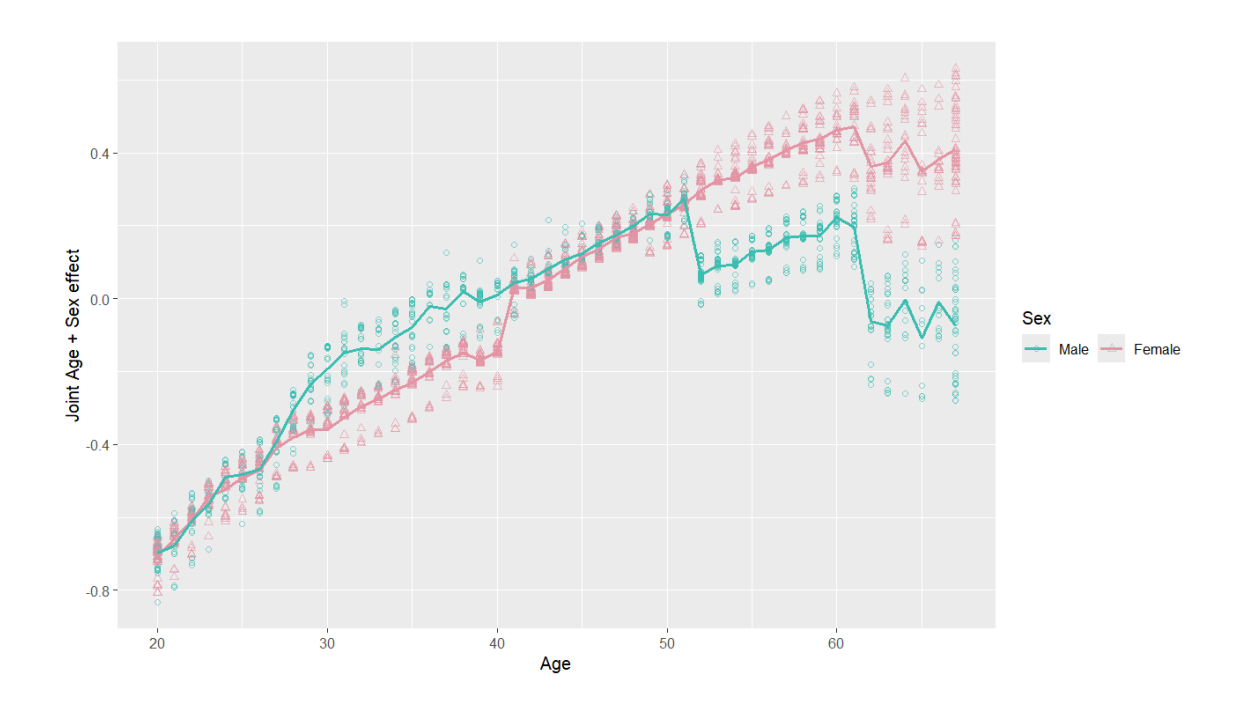


Figure 7: Marginal Shapley values computed from a RuleSHAP model fitted on n=10'000 observations from the HELIUS study, to predict cholesterol, stratified by sex. The marginal Shapley values of sex and age are summed up together for each observation, so that their joint effect may be visualized. Lines show the overall trend of the mean joint contribution. The individual joint contributions, which oscillate between observations due to the other interaction effects of age, are represented by dots and triangles.

from straightforward. The coverage of these intervals also requires carefulness, as the Out-Of-Bag estimation that they rely upon is similar to a nesting of bootstrapping and cross-validation. The bias of cross-validation can be non-negligible [40] and thus influence the bootstrapped variance of its point estimates, i.e. the uncertainty quantification. The underestimated uncertainty of these importance measures leads to much higher type I error rates (see Example 3 in the Supplementary material).

8.1 Related methods

Other approaches are more directly related to RuleSHAP and quantify the uncertainty when combining ML models with local importance measures such as Shapley values or LIME. In the past few years, there has been a considerable effort into studying uncertainty at the level of the importance measures themselves [41] [42] [43]. However, this work is either only applicable at the whole population level [43] or, more often, only focuses on ensuring that the "true" Shapley values of a fixed, specific model are covered by the confidence/credible intervals. This means that the variance of the model itself is not taken into account, thus underestimating the overall uncertainty of these measures. To overcome this issue and account for uncertainty in the model fit, a Bayesian Additive Regression Tree (BART) has also been used as a way to propagate model uncertainty to the Shapley values [7]. However, due to their complex nature, BART models tend to require more observations in order to work well. Furthermore, the intricacy of the model makes it difficult to specify a prior which can ensure valid coverage and inferential properties: earlier work shows its coverage to be suboptimal [8] and to induce false positives, especially with smaller sample sizes [9]. Valid coverage for spike-and-tree variations of BART have been proven on an asymptotic level [44] but not on realistic sample sizes as is instead the case for the horseshoe prior [12]. Furthermore, while the horseshoe prior guarantees good coverage at the level of the coefficients (and therefore at the level of the feature effects) the uncertainty of BART and variations thereof is only expressed in terms of predicted outcome, which thus gives no guarantee of satisfactory coverage for the effect of individual features. Our simulated experiment confirmed the unsatisfactory coverage of BART as it reported high type I error rates from feature selection performed using BART and Shapley values.

8.2 Limitations

The main limitation of RuleSHAP is its computational time, which grows quadratically with sample size for $n \lesssim 10'000$, and linearly thereafter. We relied on the use of a high performance cluster, where the computational time of fitting a single RuleSHAP model spanned from about 40 minutes for n=300 observations to short of five days for n=5'000 observations. A dataset of n=1'000 observations took approximately six hours to analyze. However, all these models comprised 20,000 MCMC samples to ensure the convergence of the Markov chain without the need to assess it manually. Since, for most practical settings, a Markov Chain would converge with much fewer samples, the estimated computational time might be much lower in practice. Breaking or parallelizing the Bayesian regression Markov Chain into multiple smaller chains allows for computation on larger sample sizes. For instance, RuleSHAP was fitted on n=10'000 observations by splitting the Markov chain into two sequential sub-chains. Computing time is relatively insensitive to p, as the number of terms in the model mostly depends on the number of rules that are generated. Nevertheless, as

for the other methods, a larger value of p would reduce the power to correctly identify signal features.

The interpretation of a RuleSHAP model should be performed with care: without appropriate modifications, the results cannot be interpreted in a causal sense, as this model currently lacks any adjustments for confounding. While confounding might appear in the form of interactions, a more structured approach such as propensity score matching is likely needed. Furthermore, the interpretation depends on the data at hand. In the HELIUS study, for example, self-sampling might also explain the interactions that we observed, since diabetes incidence varies with age and individuals with a diabetes diagnosis might be less inclined to participate to the study. These interactions are thus not necessarily meaningful in an etiological sense and might be specific tothe dataset that RuleSHAP was fitted on.

8.3 Outlook

Overall, these findings suggest that RuleSHAP is a valid tool both for epidemiological research, where inference options are strongly restrictive, and for transparent Machine Learning, where concerns for forms of bias or lack of transparency require optimal interpretability. These fields of application naturally inspire the need for further research and development. A thorough analysis of coverage, for instance, could further support the use of this method for hypothesis testing in scientific research. Furthermore, the natural decomposition into feature effects offered by Shapley values might make it more accessible to test for the significance of groups of features or interactions. Another point for future research is inspired by the limitations discussed above: a faster implementation of RuleSHAP could be explored, for instance through mini-batch Gibbs sampling [45] or with fast approximations of the Horseshoe regression [46]. Further research could focus on the direct formula that we produced for the computation of marginal Shapley values: replacing the regular sample means with importance-sampling based ones could extend our work to estimate non-marginal Shapley values.

9 Acknowledgements

We would like to thank Benny Markovitch for suggesting disaggregation of rules to improve separation of main and interaction effects. Marjolein Fokkema and Giorgio Spadaccini are supported by an NWO Vidi grant (number VI.Vidi.231G.065). The Amsterdam University Medical Centres and the Public Health Service of Amsterdam (GGD Amsterdam) provided core financial support for HELIUS. The HELIUS study is also funded by research grants of the Dutch Heart Foundation (Hartstichting; grant no. 2010T084), the Netherlands Organization for Health Research and Development (ZonMw; grant no. 200500003), the European Integration Fund (EIF; grant no. 2013EIF013) and the European Union (Seventh Framework Programme, FP-7; grant no. 278901). This work was performed using the computational resources from the Academic Leiden Interdisciplinary Cluster Environment (ALICE) provided by Leiden University.

10 Supplementary code

The R code used to run the experiments and analyses is available on github at the link https://github.com/GiorgioSpadaccini/ruleSHAP. The code to fit a RuleSHAP model has been converted into an R package which may be installed, for instance, using the <code>install_github</code> function from the <code>devtools</code> package. More details are available on the webpage linked above.

References

- [1] Angelo Del Parigi, Wenbo Tang, Dacheng Liu, Christopher Lee, and Richard Pratley. Machine learning to identify predictors of glycemic control in type 2 diabetes: an analysis of target HbA1c reduction using empagliflozin/linagliptin data. *Pharmaceutical Medicine*, 33:209–217, 2019.
- [2] Iqbal Madakkatel, Ang Zhou, Mark D McDonnell, and Elina Hyppönen. Combining machine learning and conventional statistical approaches for risk factor discovery in a large cohort study. *Scientific Reports*, 11(1):22997, 2021.
- [3] Xiaonan Liu, Davide Morelli, Thomas J Littlejohns, David A Clifton, and Lei Clifton. Combining machine learning with cox models to identify predictors for incident post-menopausal breast cancer in the UK Biobank. *Scientific Reports*, 13(1):9221, 2023.
- [4] Iqbal Madakkatel, Amanda L Lumsden, Anwar Mulugeta, Ian Olver, and Elina Hyppönen. Hypothesis-free discovery of novel cancer predictors using machine learning. *European Journal of Clinical Investigation*, 53(10):e14037, 2023.
- [5] SN Wood. Generalized additive models. Annual Review of Statistics and its Application, 2024.
- [6] Trevor J Hastie. Generalized additive models. In Statistical models in S, pages 249–307. Routledge, 2017.
- [7] Akira Horiguchi and Matthew T Pratola. Estimating Shapley effects in big-data emulation and regression settings using Bayesian Additive Regression Trees. arXiv preprint arXiv:2304.03809, 2023.
- [8] P Richard Hahn, Jared S Murray, and Carlos M Carvalho. Bayesian regression tree models for causal inference: Regularization, confounding, and heterogeneous effects (with discussion). *Bayesian Analysis*, 15(3):965–1056, 2020.
- [9] Rodney Sparapani, Charles Spanbauer, and Robert McCulloch. Nonparametric machine learning and efficient computation with Bayesian additive regression trees: The BART R package. Journal of Statistical Software, 97:1–66, 2021.
- [10] Jerome H Friedman and Bogdan E Popescu. Predictive learning via rule ensembles. *The Annals of Applied Statistics*, 2(3):916–954, 2008.
- [11] Malte Nalenz and Mattias Villani. Tree ensembles with rule structured horseshoe regularization. *The Annals of Applied Statistics*, 12(4):2379–2408, 2018.

- [12] Stéphanie van der Pas, Botond Szabó, and Aad van der Vaart. Uncertainty quantification for the horseshoe (with discussion). *Bayesian Analysis*, 12(4):1221–1274, 2017.
- [13] Lloyd S Shapley. A value for n-person games. Contributions to the Theory of Games, 2(28):307–317, 1953.
- [14] Erik Strumbelj and Igor Kononenko. An efficient explanation of individual classifications using game theory. The Journal of Machine Learning Research, 11:1–18, 2010.
- [15] Marieke B Snijder, Henrike Galenkamp, Maria Prins, Eske M Derks, Ron JG Peters, Aeilko H Zwinderman, and Karien Stronks. Cohort profile: the healthy life in an urban setting (HELIUS) study in Amsterdam, the Netherlands. *BMJ Open*, 7(12):e017873, 2017.
- [16] Marjolein Fokkema. Fitting prediction rule ensembles with R package pre. *Journal of Statistical Software*, 92:1–30, 2020.
- [17] Carlos M Carvalho, Nicholas G Polson, and James G Scott. The horseshoe estimator for sparse signals. *Biometrika*, 97(2):465–480, 2010.
- [18] Probal Chaudhuri, Wen-Da Lo, Wei-Yin Loh, and Ching-Ching Yang. Generalized regression trees. *Statistica Sinica*, pages 641–666, 1995.
- [19] Wei-Yin Loh. Regression tress with unbiased variable selection and interaction detection. *Statistica Sinica*, pages 361–386, 2002.
- [20] Elise Dusseldorp, Claudio Conversano, and Bart Jan Van Os. Combining an additive and tree-based regression model simultaneously: STIMA. *Journal of Computational and Graphical Statistics*, 19(3):514–530, 2010.
- [21] Enes Makalic and Daniel F Schmidt. A simple sampler for the horseshoe estimator. *IEEE Signal Processing Letters*, 23(1):179–182, 2015.
- [22] Stephanie van der Pas, James Scott, Antik Chakraborty, and Anirban Bhattacharya. horseshoe: Implementation of the Horseshoe Prior, 2019. R package version 0.2.0.
- [23] Maity Arnab Kumar, Carroll Raymond J., and Mallick Bani K. Integration of survival and binary data for variable selection and prediction: A Bayesian approach. *Journal of the Royal Statistical Society: Series C (Applied Statistics)*, 68(5):1577–1595, 2019.
- [24] Erik Štrumbelj and Igor Kononenko. Explaining prediction models and individual predictions with feature contributions. *Knowledge and Information Systems*, 41:647–665, 2014.
- [25] Scott M Lundberg, Gabriel G Erion, and Su-In Lee. Consistent individualized feature attribution for tree ensembles. arXiv preprint arXiv:1802.03888, 2018.
- [26] Hugh Chen, Joseph D Janizek, Scott Lundberg, and Su-In Lee. True to the model or true to the data? arXiv preprint arXiv:2006.16234, 2020.
- [27] Hugh Chen, Ian C. Covert, Scott M. Lundberg, and Su-In Lee. Algorithms to estimate shapley value feature attributions. *Nature Machine Intelligence*, 5(6):590–601, 2023.

- [28] Konrad Komisarczyk, Pawel Kozminski, Szymon Maksymiuk, and Przemyslaw Biecek. tree-shap: Compute SHAP Values for Your Tree-Based Models Using the 'TreeSHAP' Algorithm, 2024. R package version 0.3.1.
- [29] Scott M Lundberg, Gabriel Erion, Hugh Chen, Alex DeGrave, Jordan M Prutkin, Bala Nair, Ronit Katz, Jonathan Himmelfarb, Nisha Bansal, and Su-In Lee. From local explanations to global understanding with explainable AI for trees. *Nature machine intelligence*, 2(1):56–67, 2020.
- [30] Munir Hiabu, Enno Mammen, and Joseph T Meyer. Random planted forest: a directly interpretable tree ensemble. arXiv preprint arXiv:2012.14563, 2020.
- [31] Achim Zeileis, Torsten Hothorn, and Kurt Hornik. Model-based recursive partitioning. *Journal of Computational and Graphical Statistics*, 17(2):492–514, 2008.
- [32] Artjom Zern, Klaus Broelemann, and Gjergji Kasneci. Interventional SHAP values and interaction values for piecewise linear regression trees. In *Proceedings of the AAAI Conference on Artificial Intelligence*, volume 37, pages 11164–11173, 2023.
- [33] Trevor Hastie, Junyang Qian, and Kenneth Tay. An introduction to glmnet. CRAN R Repositary, 5:1–35, 2021.
- [34] Malte Nalenz and Mattias Villani. R package for the horserule model. https://github.com/mattiasvillani/horserule/, 2017.
- [35] Andy Liaw and Matthew Wiener. Classification and regression by randomforest. *R News*, 2(3):18–22, 2002.
- [36] Jerome H Friedman. Multivariate adaptive regression splines. *The Annals of Statistics*, 19(1):1–67, 1991.
- [37] Mark A van de Wiel, Matteo Amestoy, and Jeroen Hoogland. Linked shrinkage to improve estimation of interaction effects in regression models. *Epidemiologic Methods*, 13(1):20230039, 2024.
- [38] Giampiero Marra and Simon N Wood. Coverage properties of confidence intervals for generalized additive model components. *Scandinavian Journal of Statistics*, 39(1):53–74, 2012.
- [39] Hemant Ishwaran and Min Lu. Standard errors and confidence intervals for variable importance in random forest regression, classification, and survival. *Statistics in Medicine*, 38(4):558–582, 2019.
- [40] Stephen Bates, Trevor Hastie, and Robert Tibshirani. Cross-validation: what does it estimate and how well does it do it? Journal of the American Statistical Association, 119(546):1434– 1445, 2024.
- [41] David Watson, Joshua O'Hara, Niek Tax, Richard Mudd, and Ido Guy. Explaining predictive uncertainty with information theoretic Shapley values. *Advances in Neural Information Processing Systems*, 36, 2024.

- [42] Dylan Slack, Anna Hilgard, Sameer Singh, and Himabindu Lakkaraju. Reliable post hoc explanations: Modeling uncertainty in explainability. Advances in Neural Information Processing Systems, 34:9391–9404, 2021.
- [43] Brian Williamson and Jean Feng. Efficient nonparametric statistical inference on population feature importance using shapley values. In *International Conference on Machine Learning*, pages 10282–10291. PMLR, 2020.
- [44] Veronika Ročková and Stephanie Van der Pas. Posterior concentration for Bayesian regression trees and forests. *The Annals of Statistics*, 48(4):2108–2131, 2020.
- [45] Vadim Smolyakov, Qiang Liu, and John W Fisher III. Adaptive scan Gibbs sampler for large scale inference problems. arXiv preprint arXiv:1801.09144, 2018.
- [46] James Johndrow, Paulo Orenstein, and Anirban Bhattacharya. Scalable approximate mcmc algorithms for the horseshoe prior. *Journal of Machine Learning Research*, 21(73):1–61, 2020.
- [47] Tianqi Chen, Tong He, Michael Benesty, Vadim Khotilovich, Yuan Tang, Hyunsu Cho, Kailong Chen, Rory Mitchell, Ignacio Cano, Tianyi Zhou, Mu Li, Junyuan Xie, Min Lin, Yifeng Geng, Yutian Li, and Jiaming Yuan. *xgboost: Extreme Gradient Boosting*, 2024. R package version 1.7.8.1.

Supplementary material

10.1 Examples

Example 1. Partial Dependence Plots do not always pick up cooperation between features:

Consider a setting where $X_1, X_2 \sim \mathcal{N}(0,1)$ are independent features. Define the following prediction model:

$$F(x_1, x_2) = I(x_1 \cdot x_2 < 0).$$

The estimated PDP-based effects of the features X_1, X_2 would be null at every point x^* , which would wrongly suggest that no feature has an effect on this model.

Example 2. The feature importance measures $I_j(x)$ and I_j from Equations 2 and 3 may be misleading:

For a setting where $X_1, X_2, X_3 \sim \mathcal{N}(0, 1)$, consider the two models:

$$F(x_1, x_2, x_3) = x_1 + I(x_1 < -1) + I(x_2 < 3, x_3 \ge 0) = x_1 + r_1(x) + r_2(x)$$

$$G(x_1, x_2, x_3) = x_1 + I(x_3 \ge 0) = x_1 + r_3(x),$$

$$r_1(x) := I(x_1 < -1), \qquad r_2(x) := I(x_2 < 3, x_3 \ge 0), \qquad r_3(x) := I(x_3 \ge 0).$$

In this context, RuleFit measures the importance of feature X_1 to be higher in model F(x) than it is in model G(x), both locally and globally:

$$I_1^{(F)} = sd(x_1) + \sqrt{\overline{r}_1 \cdot (1 - \overline{r}_1)} > sd(x_1) = I_1^{(G)},$$

$$I_1^{(F)}(x^*) = |x_1^* - \overline{x}_1| + |r_1(x^*) - \overline{r}_1| > |x_1^* - \overline{x}_1| = I_1^{(G)}(x^*).$$

For this feature, however, the rule $r_1(x)$ has a dampening role on the effect of the term x_1 , so the importance of X_1 should be lower in the model F(x) than in the model G(x). While this issue could be resolved by removing the absolute values in the definition of the importance measures, notice that the concern of unfairly splitting the effect of interaction effects remains: with a probability higher than 99.5%, the rules $r_2(x)$ and $r_3(x)$ coincide, since the condition $X_2 < 3$ is very likely to be true. This means that X_2 technically appears in the model F(x), but is essentially not relevant in it, as in G(x). Furthermore, the importance of X_3 in the models F(x) and G(x) should be approximately the same. Yet, because RuleFit's feature importance measure splits the effect of an interaction equally between the involved features, these expectations are not met:

$$\begin{split} I_2^{(F)} &= \frac{\sqrt{\overline{r}_2 \cdot (1 - \overline{r}_2)}}{2} > 0 = I_2^{(G)}, \\ I_2^{(F)}(x) &= \frac{|r_2(x) - \overline{r}_2|}{2} > 0 = I_1^{(G)}(x), \\ I_3^{(F)} &= \frac{\sqrt{\overline{r}_2 \cdot (1 - \overline{r}_2)}}{2} \approx \frac{\sqrt{\overline{r}_3 \cdot (1 - \overline{r}_3)}}{2} < \sqrt{\overline{r}_3 \cdot (1 - \overline{r}_3)} = I_3^{(G)}, \\ I_3^{(F)}(x) &= \frac{|r_2(x) - \overline{r}_2|}{2} \approx \frac{|r_3(x) - \overline{r}_3|}{2} < |r_3(x) - \overline{r}_3| = I_1^{(G)}(x). \end{split}$$

Quantity	Model			
Quantity	RF-VImp	Two-step		
# Null hypothesis rejections for noise features	2'438	68		
# Tested noise features	2'500	309		
Estimated type I error rate	.9752	.2201		

Table 3: Observed frequencies of rejection of the null hypothesis for inference performed with Random Forest combined with RF-VImp and for inference performed with a two-step approach combining XGBoost and linear regression. Frequencies are summed across all 100 replicates of the experiment and type I error rate is estimated as the ratio between the times that the null hypothesis was rejected for any noise feature and the number of times that any noise feature was included in the testing model.

Example 3. The two-step procedure that selects features with a ML model and subsequently performs inference with an OLS fit on the same data could lead to high type I error rates. Performing inference using RF-VImp with a Random Forest might also lead to high type I error rates:

We set up an exemplary simulation to show the problems of this approach: more specifically, we simulated data under the Friedman generating function described in Equation 8. The dataset involved five signal features and 25 noise features, for a total of p=30 independent features and n=1'000 observations. The experiment was repeated 100 times. In each replicate, we fitted the two-step approach on the data. The approach involved fitting an XGBoost tree ensemble (package xgboost [47]). The eight features with highest average absolute shapley value were selected and used to fit a linear model on the same dataset (lm function in R). In each replicate, the linear model was used to test for significance on these eight features. Each replicate also included fitting a Random Forest, and using RF-VImp to estimate uncertainty and thus perform inference. As shown in Table 3, the type II error rate estimated across replicates is much higher than the nominal level of $\alpha=0.05$, for both approaches.

10.2 Other remarks

Remark 1. Standardizing or rescaling a feature is directly connected to its shrinkage in a horseshoe prior:

We refer to the horseshoe prior with structured shrinkage defined in Subsection 3.2. Given the feature vectors x_1, \ldots, x_p , which are columns of the design matrix X, one can rescale the features and turn them into $x'_1 = x_1/\alpha_1, \ldots, x'_p = x_p/\alpha_p$, columns of the design matrix X'. If one fits a Bayesian regression on such rescaled features and produces a coefficient vector estimate β' , then returning on the original scale means computing the vector $\beta = (\beta'_1/\alpha_1 \cdots \beta'_p/\alpha_p)^t$. In this case,

the probability density is:

$$\begin{split} \pi(\beta = b|X,y) &= \pi(\beta' = \alpha \odot b|X',y) \\ &\propto e^{-\frac{1}{2\sigma^2}||y - \sum_{j=1}^p \frac{x_j}{\alpha_j} \cdot \alpha_j b_j||^2} \cdot e^{-\frac{1}{2\tau^2} \left(\sum_{j=1}^p \frac{b_j^2 \alpha_j^2}{\lambda_j^2}\right)} \cdot \frac{1}{1+\tau^2} \cdot \prod_{j=1}^p \frac{1}{A_j^2 + \lambda_j^2} \\ &\propto e^{-\frac{1}{2\sigma^2}||y - \sum_{j=1}^p x_j b_j||^2} \cdot e^{-\frac{1}{2\tau^2} \left(\sum_{j=1}^p \frac{b_j^2}{(\lambda_j/\alpha_j)^2}\right)} \cdot \frac{1}{1+\tau^2} \cdot \prod_{j=1}^p \frac{1}{(A_j/\alpha_j)^2 + (\lambda_j/\alpha_j)^2} \end{split}$$

which, up to re-parametrizing $\lambda_j \leftarrow \lambda_j/\alpha_j$, is equivalent to the same prior as in HorseRule, but with the structured shrinkage parameter A_j being replaced by A_j/α_j . If we consider the specific setting of HorseRule where a rule term $r_k(x)$ would be rescaled by its standard deviation, this means replacing A_k with:

$$\begin{split} A_k' &= \frac{A_k}{sd(r_k)} \\ &= \frac{A_k}{\sqrt{\overline{r}_k(1-\overline{r}_k)}} \\ &= \frac{(2\min(\overline{r}_k,1-\overline{r}_k))^\mu}{m_k^\eta\sqrt{\overline{r}_k(1-\overline{r}_k)}} \\ &= \frac{(2\min(\overline{r}_k,1-\overline{r}_k))^{\mu-0.5}}{m_k^\eta} \cdot \sqrt{\frac{2\min(\overline{r}_k,1-\overline{r}_k)}{\overline{r}_k(1-\overline{r}_k)}} \\ &= \frac{(2\min(\overline{r}_k,1-\overline{r}_k))^{\mu-0.5}}{m_k^\eta} \cdot \sqrt{\frac{2}{\max(\overline{r}_k,1-\overline{r}_k)}}. \end{split}$$

10.3 Figures and results

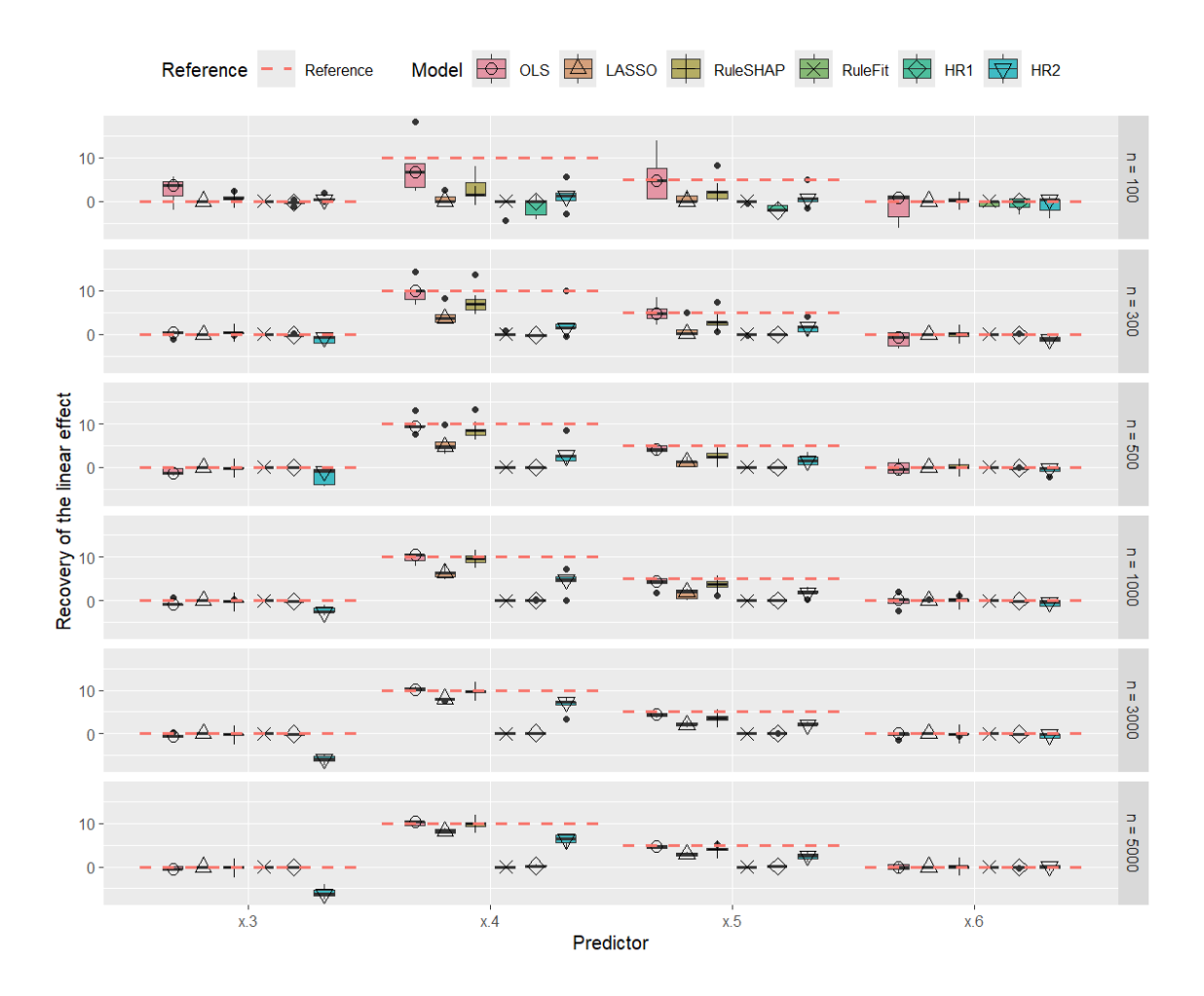


Figure S1: Coefficients of linear terms across five fits of OLS linear regression, LASSO regression, RuleFit regression, HorseRule regression (HR1 for default settings; HR2 for custom settings) and RuleSHAP regression. These models are fitted on the Friedman-generated data with continuous outcome and p=10, across different values of n. Target coefficients are presented with dashed red lines. Note that the boxplots do not represent uncertainty, but rather variation across the five replicates of the experiment.

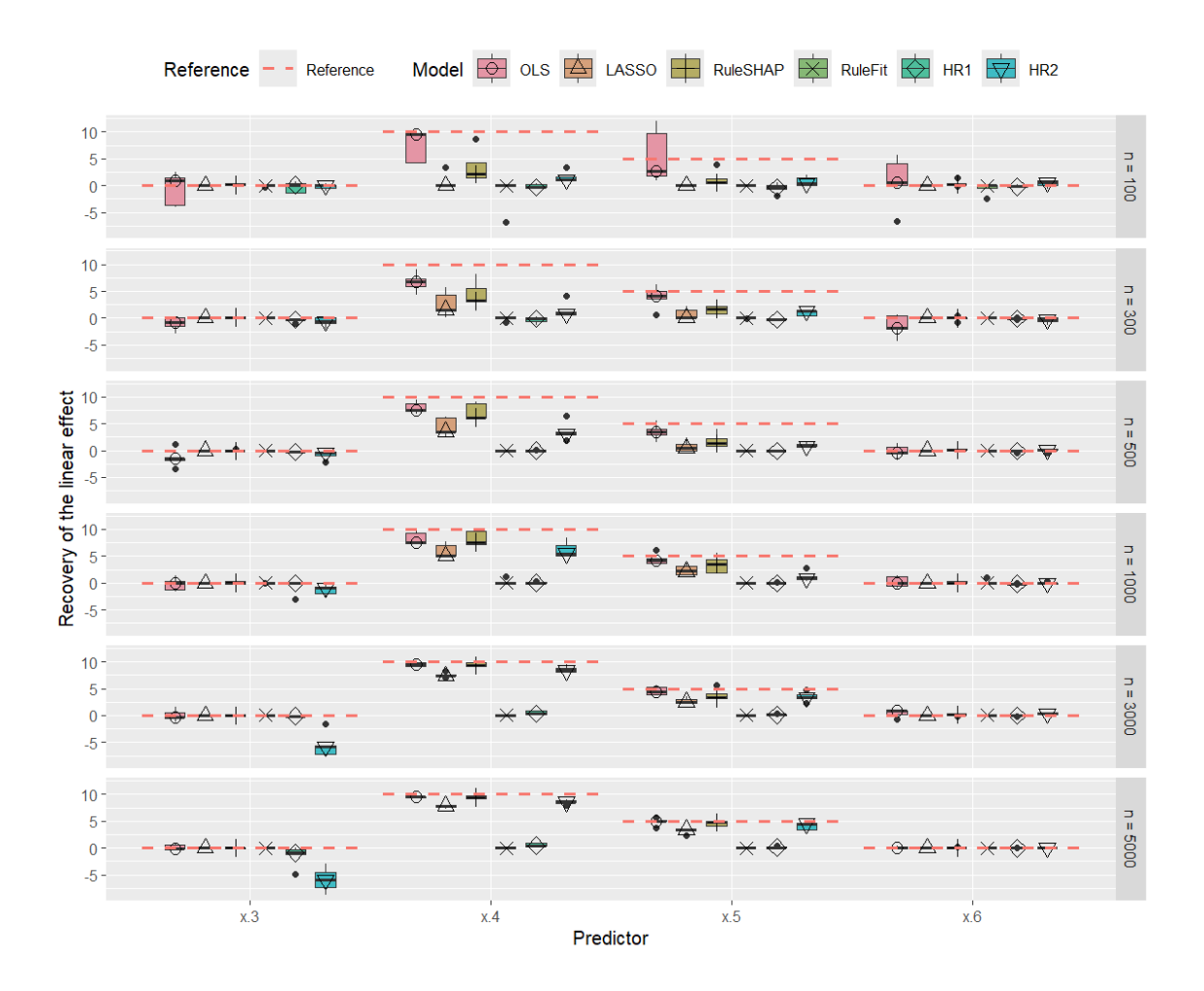


Figure S2: Coefficients of linear terms across five fits of OLS linear regression, LASSO regression, RuleFit regression, HorseRule regression (HR1 for default settings; HR2 for custom settings) and RuleSHAP regression. These models are fitted on the Friedman-generated data with continuous outcome and p=30, across different values of n. Target coefficients are presented with dashed red lines. Note that the boxplots do not represent uncertainty, but rather variation across the five replicates of the experiment.

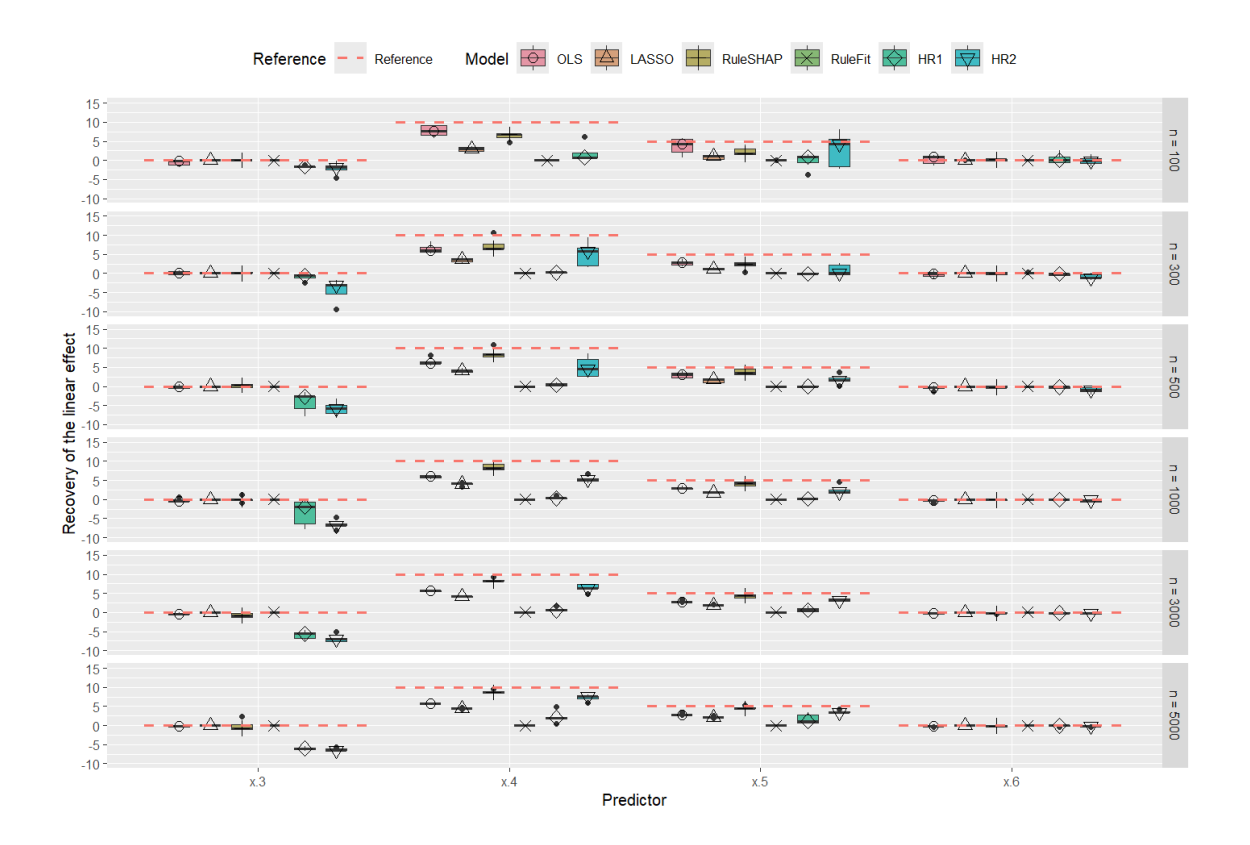


Figure S3: Coefficients of linear terms across five fits of logistic linear regression, LASSO logistic regression, RuleFit logistic regression, HorseRule logistic regression (HR1 for default settings; HR2 for custom settings) and RuleSHAP logistic regression. These models are fitted on the Friedmangenerated data with binary outcome and p=10, across different values of n. Target level is presented with dashed red lines. Note that the boxplot does not represent uncertainty quantifications, but rather the variation across the five replicates of the experiment.

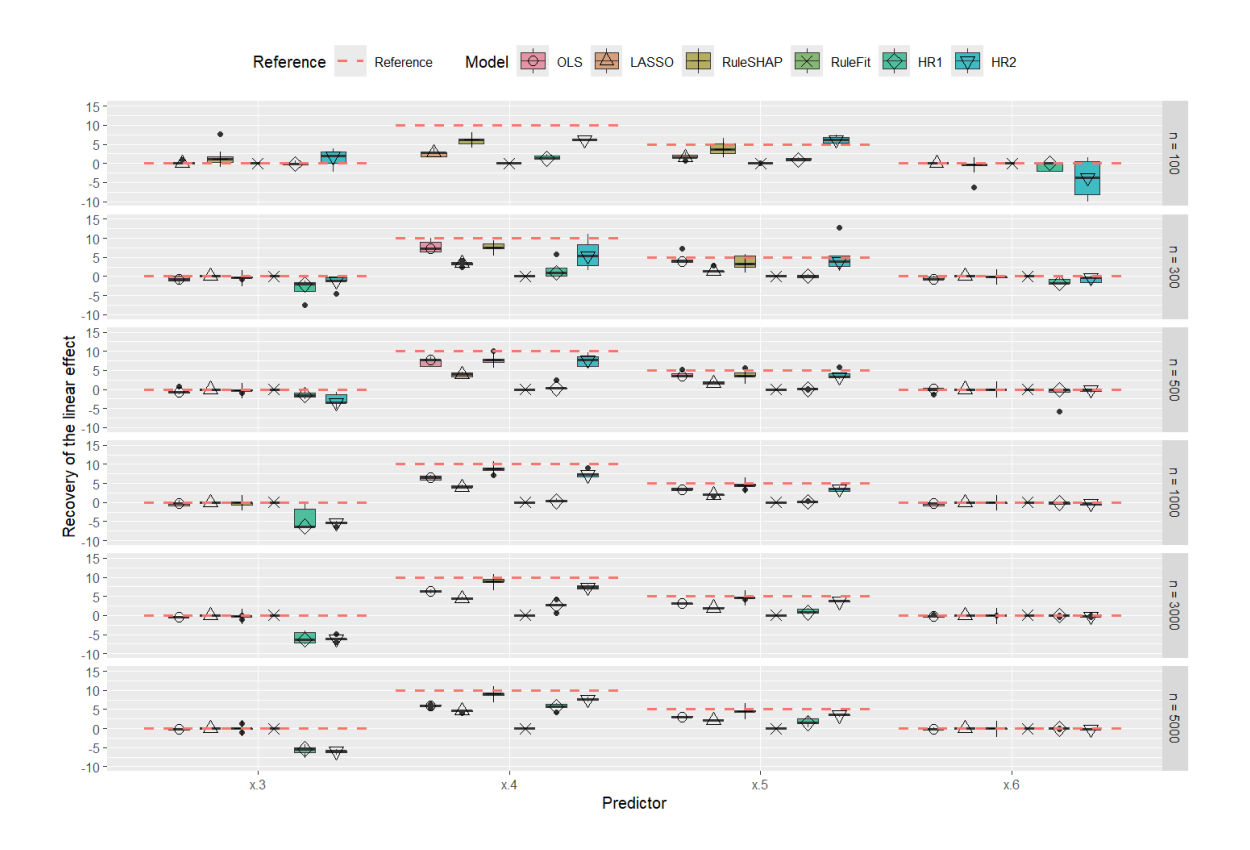


Figure S4: Coefficients of linear terms across five fits of logistic linear regression, LASSO logistic regression, RuleFit logistic regression, HorseRule logistic regression (HR1 for default settings; HR2 for custom settings) and RuleSHAP logistic regression. These models are fitted on the Friedmangenerated data with binary outcome and p=30, across different values of n. Target level is presented with dashed red lines. Note that the boxplot does not represent uncertainty quantifications, but rather the variation across the five replicates of the experiment.

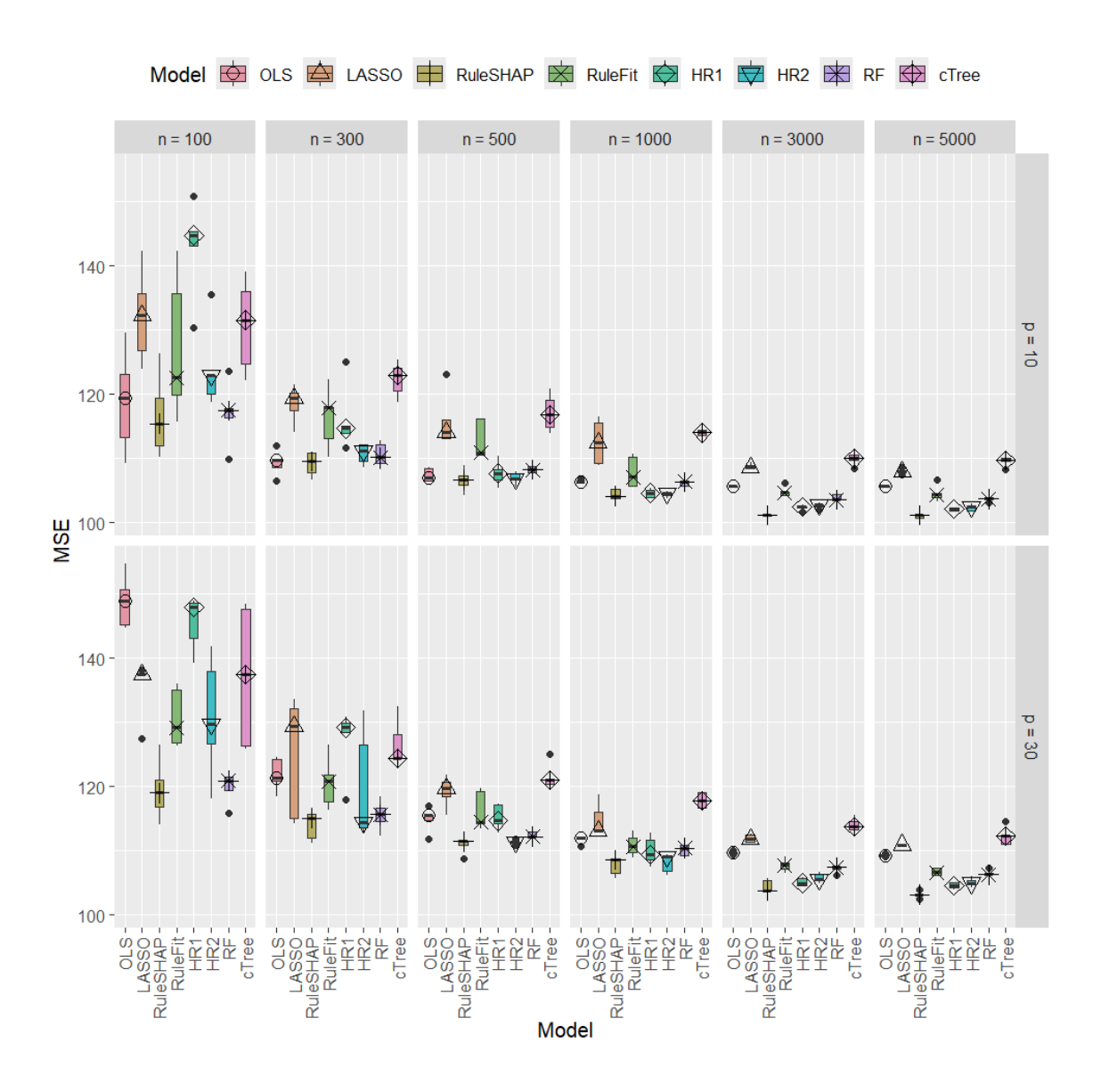


Figure S5: Test MSE across five fits of OLS linear regression, LASSO regression, RuleFit regression, HorseRule regression (HR1 for default settings; HR2 for custom settings), RuleSHAP regression and Random Forest. These models are fitted on the Friedman-generated data with continuous outcome, across different values of n and p.

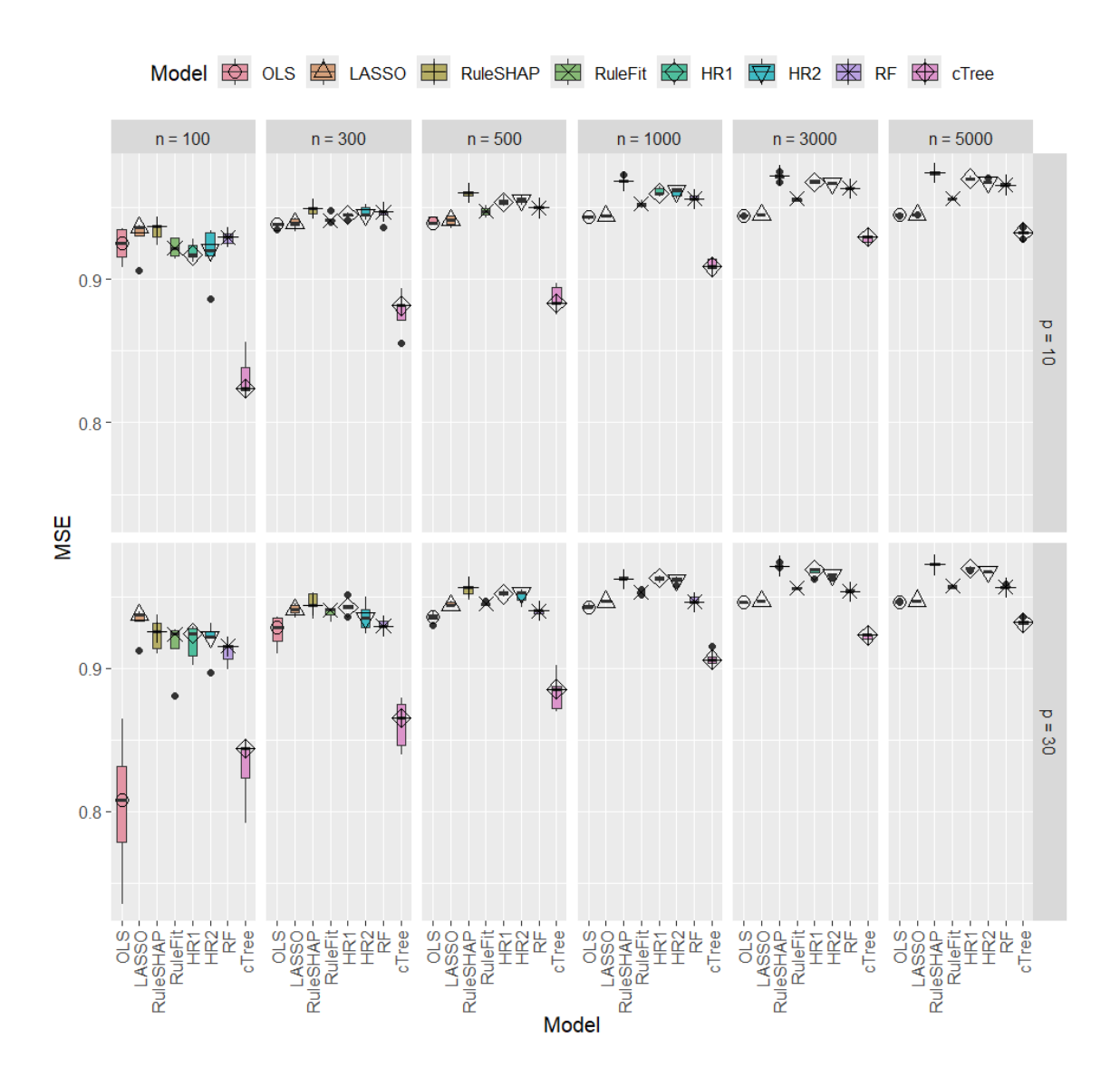


Figure S6: Test Area Under the ROC Curve (AUC) across five fits of logistic linear regression, LASSO logistic regression, RuleFit logistic regression, HorseRule logistic regression (HR1 for default settings; HR2 for custom settings), RuleSHAP logistic regression and Random Forest. These models are fitted on the Friedman-generated data with binary outcome, across different values of n and p.

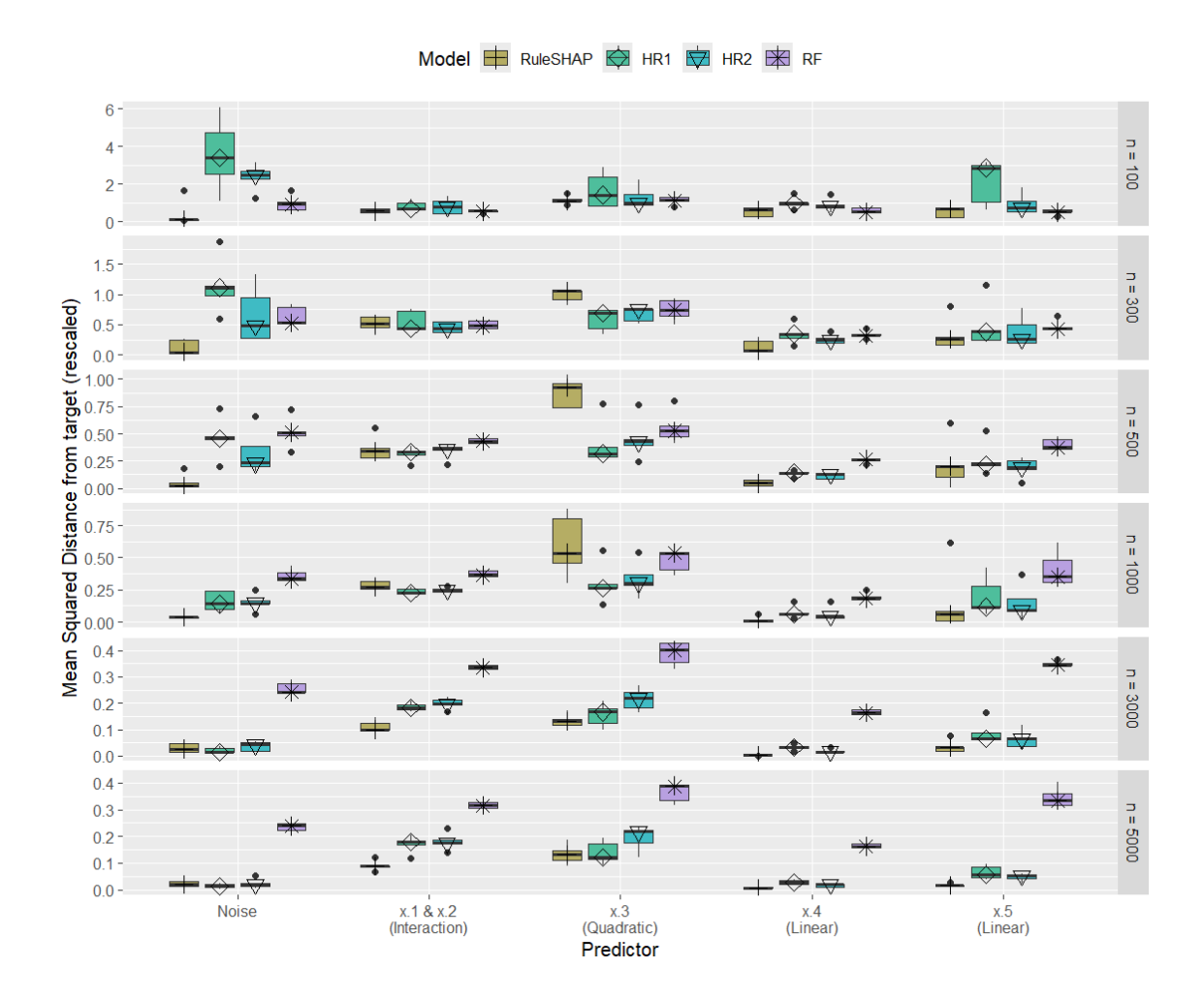


Figure S7: Re-scaled mean squared distance between feature effects estimated by the model and the target effects for five replicates of different models fitted on Friedman-generated data, for p=10 features and different sample sizes n. Estimated feature effects are computed as marginal Shapley values. Since x_1 and x_2 induce an interacting effect, their feature effects are analyzed jointly, as the sum of the Shapley values of the two features. The distance is averaged across all replicates of the experiment, across all points of the dataset. All noise features are averaged out together. Models are fitted on data generated from the Friedman generating function, with continuous outcome and p=10. To ease interpretation across different effect magnitudes, the squared distance of each signal feature was rescaled by the overall variance of that effect. The scale on the y axis varies across plots.

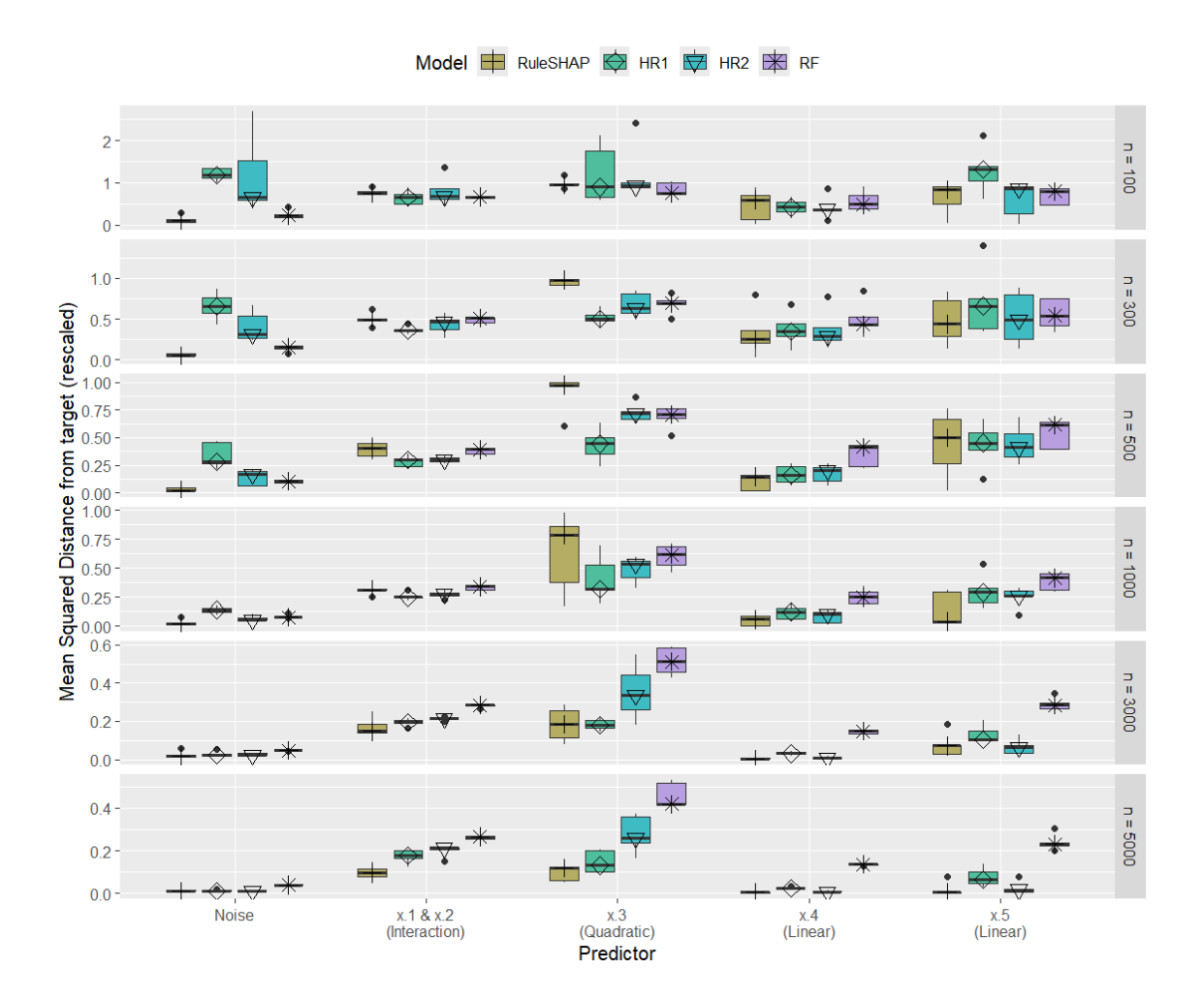


Figure S8: Re-scaled mean squared distance between feature effects estimated by the model and the target effects for five replicates of different models fitted on Friedman-generated data, for p=10 features and different sample sizes n. Estimated feature effects are computed as marginal Shapley values. Since x_1 and x_2 induce an interacting effect, their feature effects are analyzed jointly, as the sum of the Shapley values of the two features. The distance is averaged across all replicates of the experiment, across all points of the dataset. All noise features are averaged out together. Models are fitted on data generated from the Friedman generating function, with continuous outcome and p=30. To ease interpretation across different effect magnitudes, the squared distance of each signal feature was rescaled by the overall variance of that effect. The scale on the y axis varies across plots.

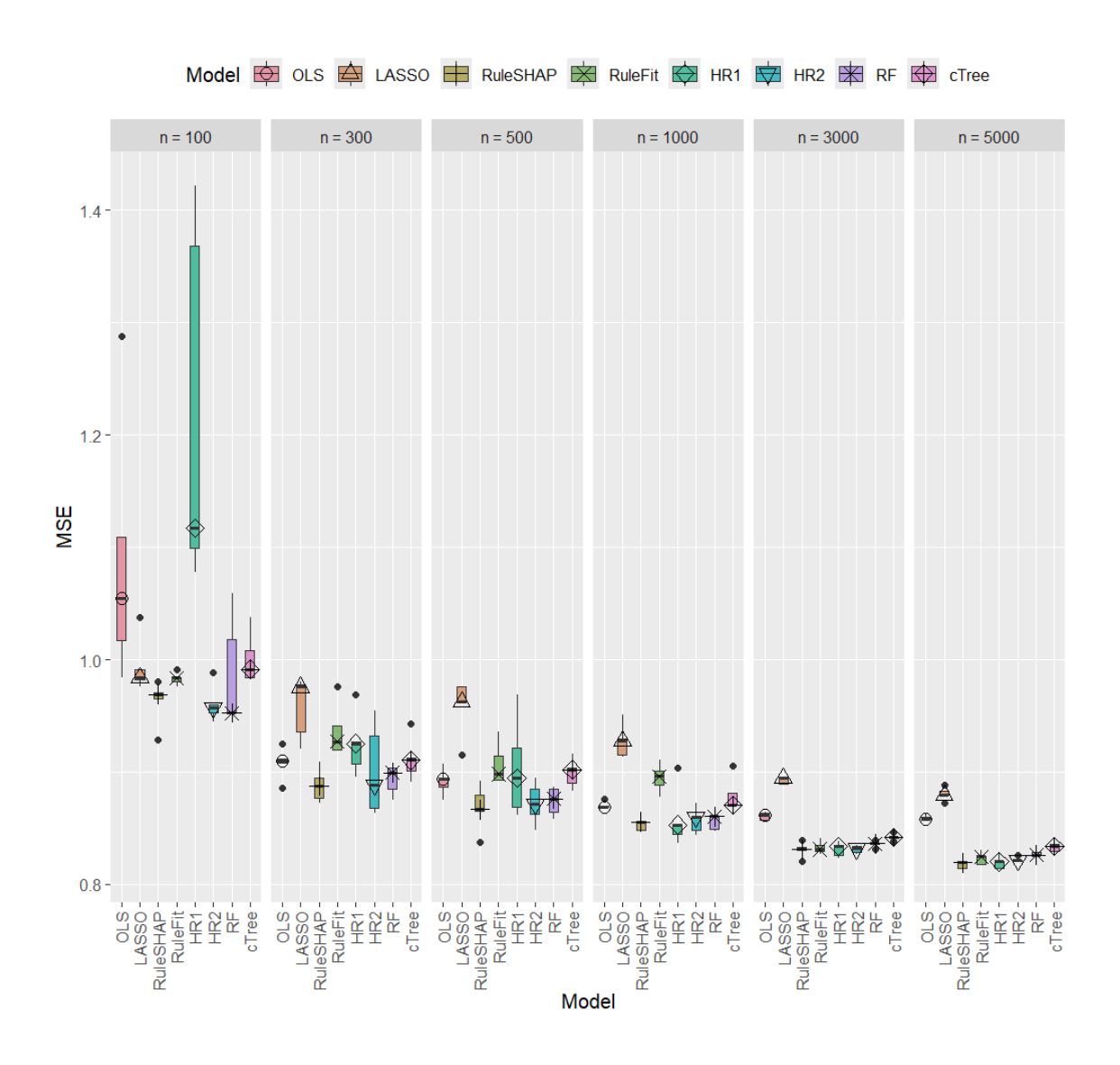


Figure S9: Test MSE across five fits of OLS linear regression, LASSO regression, RuleFit regression, HorseRule regression (HR1 for default settings; HR2 for custom settings), RuleSHAP regression and Random Forest. These models are fitted on subsamples of different sizes n taken from the the HELIUS study data, with **cholesterol** as predicted outcome.

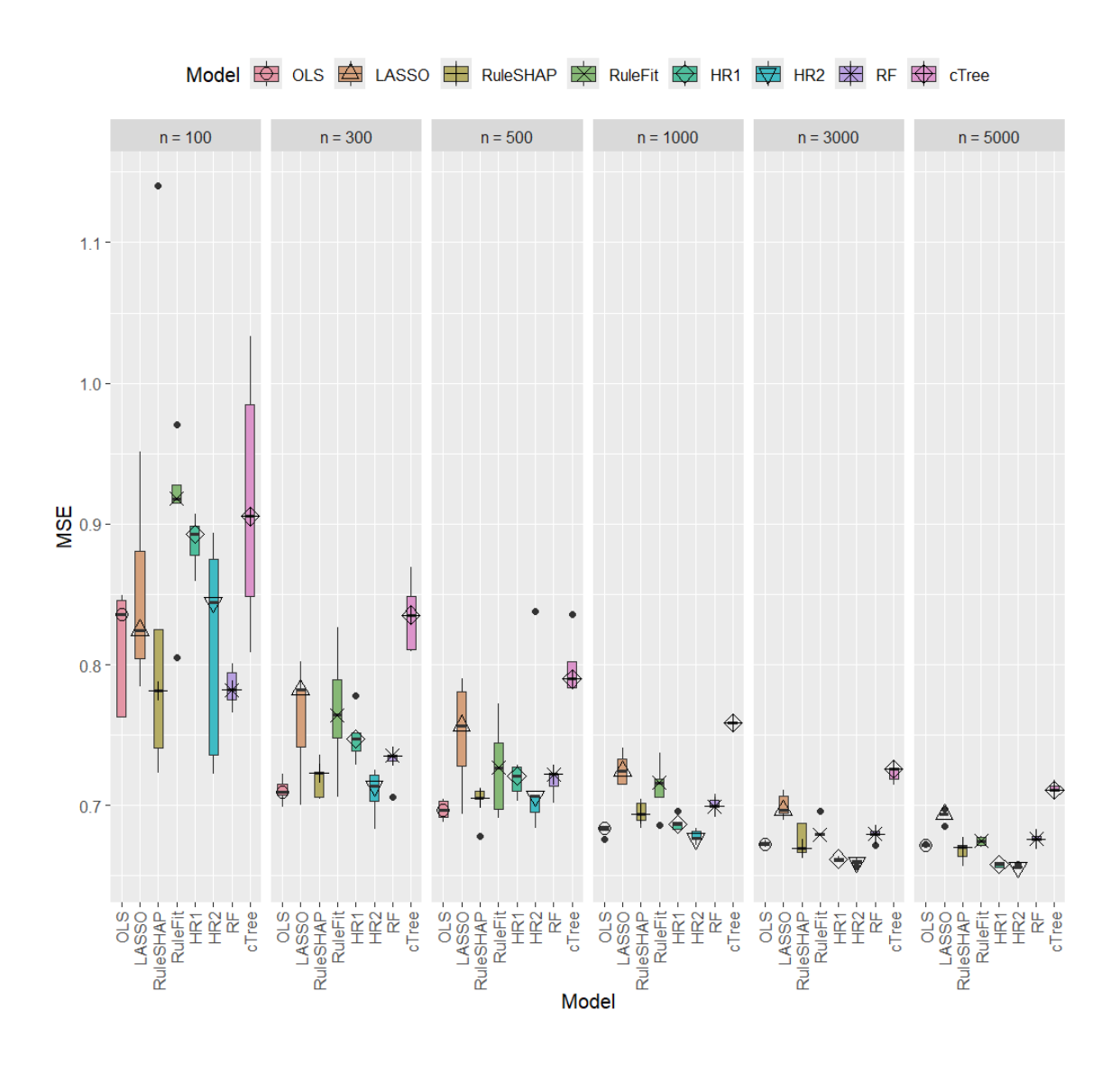


Figure S10: Test MSE across five fits of OLS linear regression, LASSO regression, RuleFit regression, HorseRule regression (HR1 for default settings; HR2 for custom settings), RuleSHAP regression and Random Forest. These models are fitted on subsamples of different sizes n taken from the the HELIUS study data, with **systolic blood pressure** as predicted outcome.

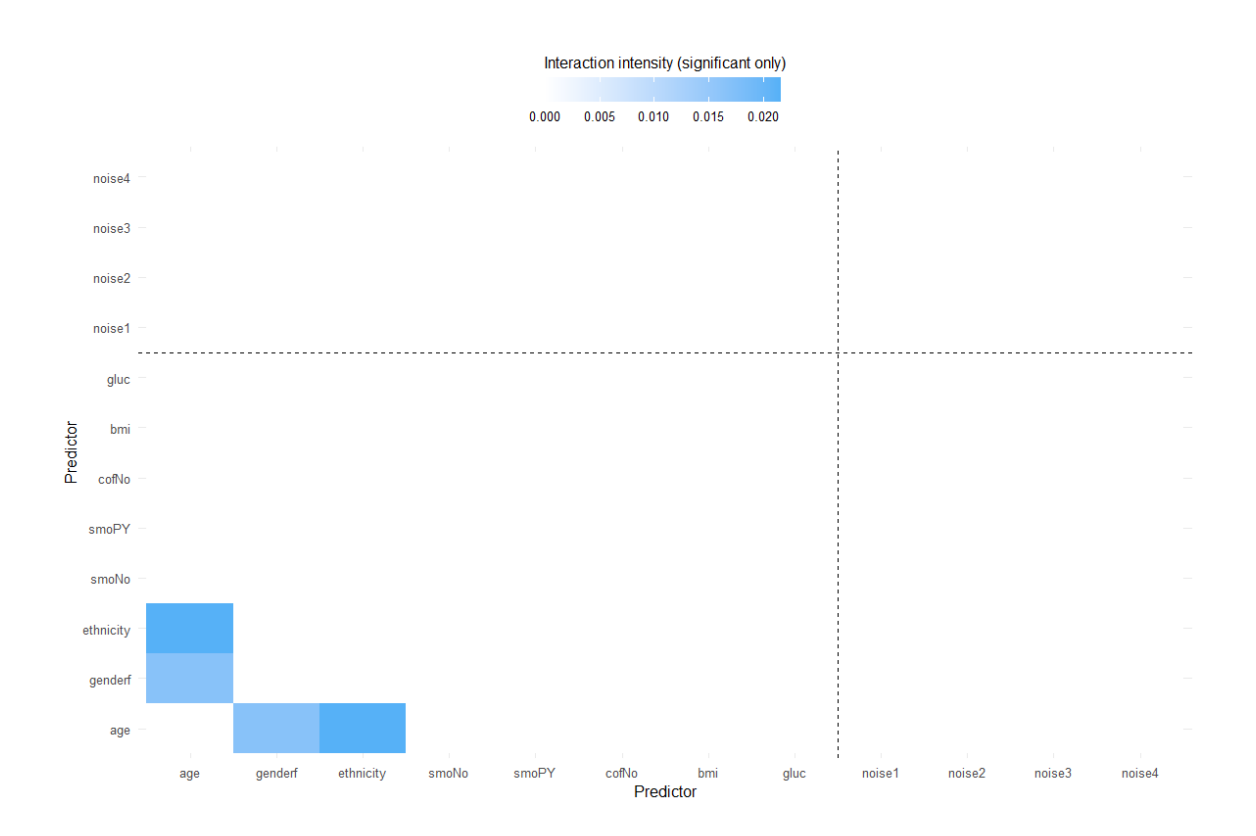


Figure S11: Interaction Shapley values computed from a RuleSHAP model fitted on n=10'000 observations from the HELIUS study, to predict **systolic blood pressure**. Point-wise 95% credible intervals are used to determine significance of interactions, and only significant interactions are shown in the form of mean absolute values. Dashed line separates artificial noise features from the rest.

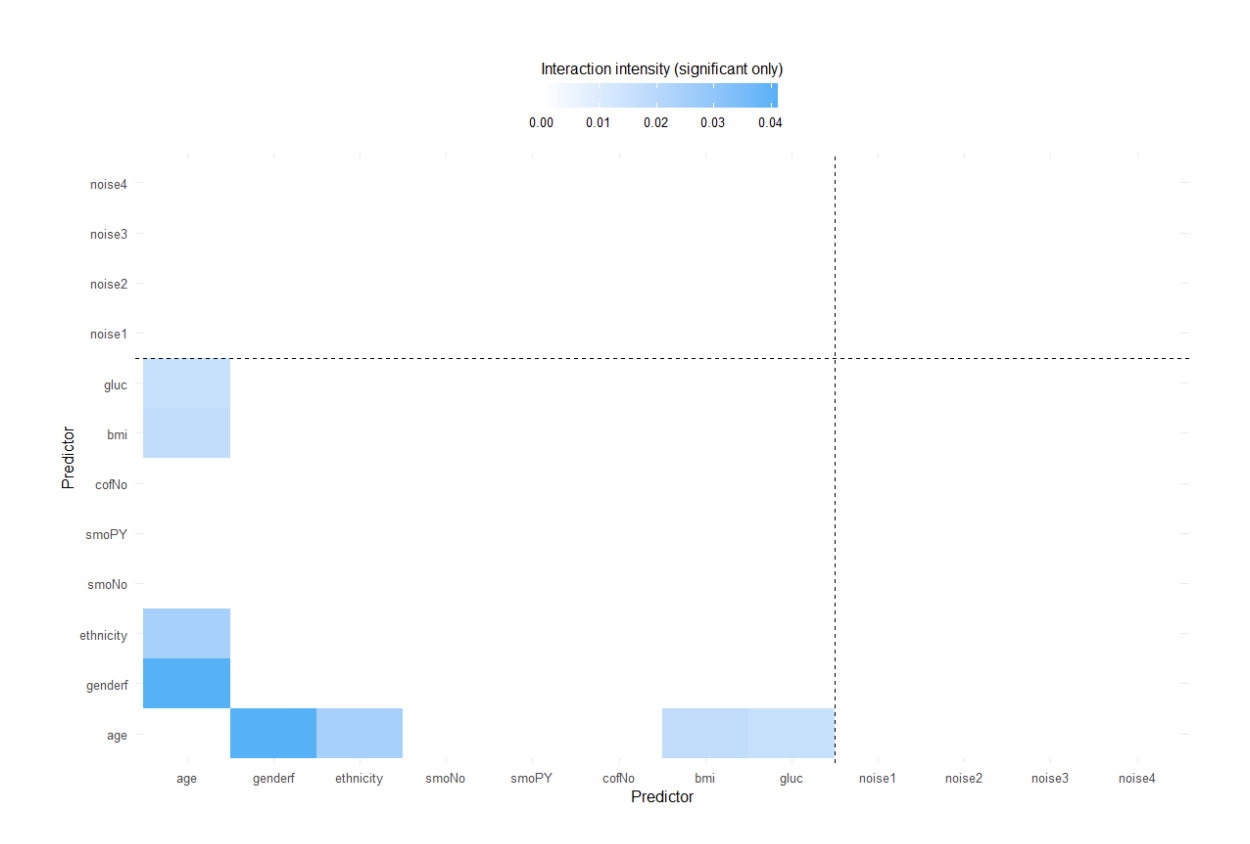


Figure S12: Interaction Shapley values computed from a RuleSHAP model fitted on n=10'000 observations from the HELIUS study, to predict **cholesterol**. Point-wise 95% credible intervals are used to determine significance of interactions, and only significant interactions are shown in the form of mean absolute values. Dashed line separates artificial noise features from the rest.

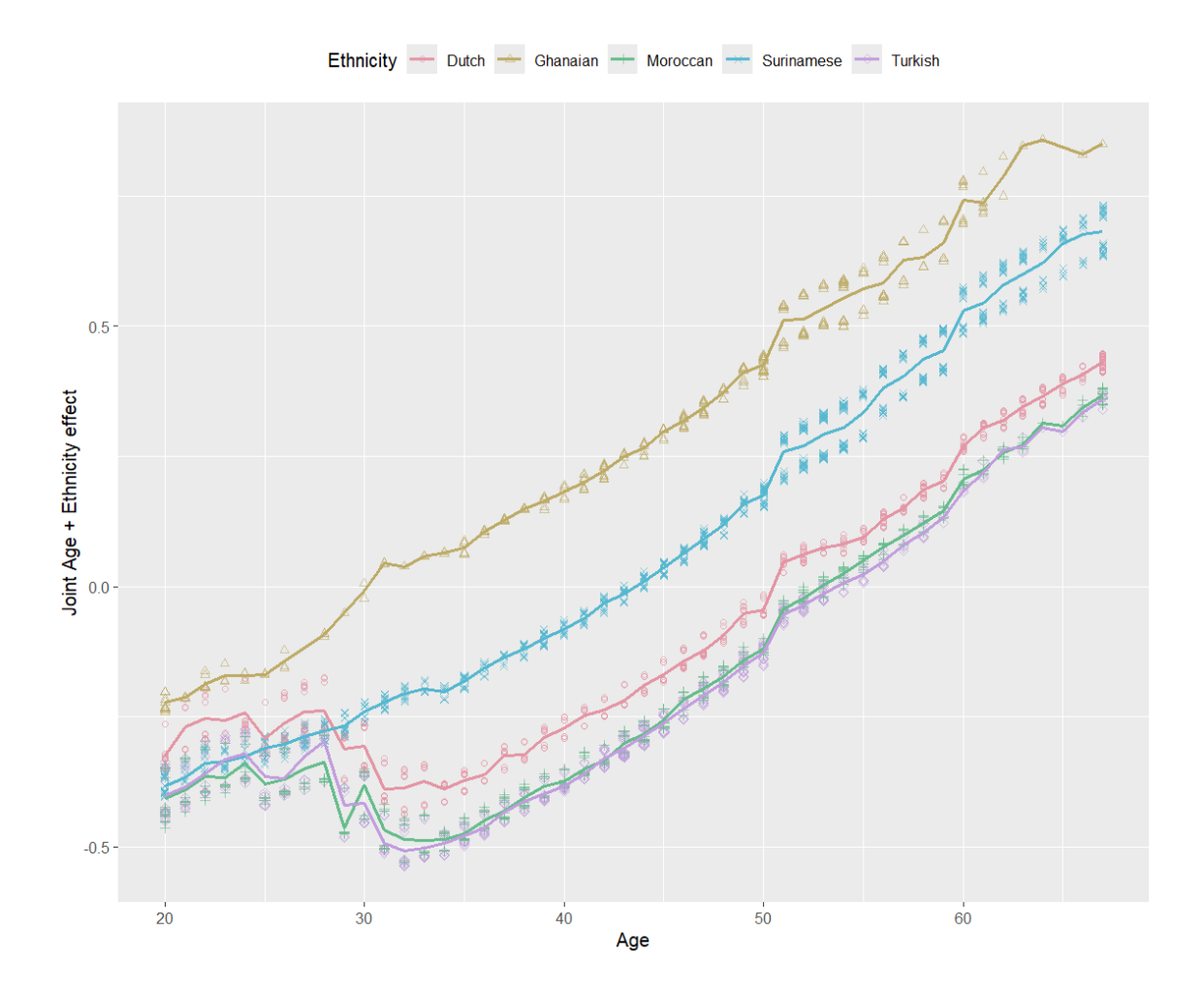


Figure S13: Marginal Shapley values computed from a RuleSHAP model fitted on n=10'000 observations from the HELIUS study, to predict systolic blood pressure, stratified by ethnicity. The marginal Shapley values of ethnicity and age are summed up together for each observation, so that their joint effect may be visualized. Lines show the overall trend of the mean joint contribution. The individual joint contributions, which (weakly) oscillate between observations due to the other interaction effects of age, are represented by dots.

10.4 Theoretical results

Lemma 3. (Variation of Vandermonde's identity) For any $a, b, c \in \mathbb{N}$ such that $c \leq b$, the following equality holds:

$$\sum_{l=0}^{c} \binom{a+l}{l} \binom{b-l}{c-l} = \binom{a+b+1}{c}.$$

Proof. We firstly produce the following intermediate formula with a combinatorial argument:

$$\binom{a+b}{c} = \sum_{l=0}^{c} \binom{a+l}{l} \binom{b-l}{c-l} - \sum_{l=0}^{c-1} \binom{a+l}{l} \binom{b-l-1}{c-l-1}.$$

Notice that the result holds straightforwardly for values of a=0 or b=0 or b=c. For the remaining cases, we rely on two ways to compute the number of subsets. Consider the set $G=\{1,\ldots,a+b\}$. Then the number of all possible subsets $S\subseteq G$ of size c is precisely $\binom{a+b}{c}$. On the other hand, consider the following disjoint partitions of G into $G_1^{(l)}$ and $G_2^{(l)}$ for any index $l\in\{0,\ldots,c\}$:

$$G_1^{(0)} = \{1, \dots, a\}, \qquad G_2^{(0)} = \{a+1, \dots, a+b\},$$

$$G_1^{(1)} = \{1, \dots, a+1\}, \qquad G_2^{(1)} = \{a+2, \dots, a+b\},$$

$$\vdots$$

$$G_1^{(l)} = \{1, \dots, a+l\}, \qquad G_2^{(l)} = \{a+l+1, \dots, a+b\},$$

$$\vdots$$

$$G_1^{(c)} = \{1, \dots, a+c\}, \qquad G_2^{(c)} = \{a+c+1, \dots, a+b\}.$$

A simple induction on b can show that any subset of G of size c can be represented as a set S which shares l elements with $G_1^{(l)}$ and c-l elements with $G_2^{(l)}$, for at least one index l. For a given value of l, notice that there are:

$$\binom{|G_1^{(l)}|}{l} \cdot \binom{|G_2^{(l)}|}{c-l} = \binom{a+l}{l} \cdot \binom{b-l}{c-l}$$

such sets. One can therefore sum over all indices l and count the number of subsets S that take l elements from $G_1^{(l)}$ and c-l elements with $G_2^{(l)}$. This count would include all of the $\binom{a+b}{c}$ subsets $S\subseteq G$. However, this could count the same subset multiple times, so for the summation to be equal to $\binom{a+b}{c}$ one needs to subtract the subsets counted multiple times. More specifically notice that, due to the sequential nature of the partitions, a set S being decomposed in the aforementioned form also takes a sequential nature: if S may be written as l' elements from $G_1^{(l')}$ and c-l' elements from $G_2^{(l'')}$, then this also holds for any other value of l between l' and l''. In particular, this means that for any fixed l one may simply count all $\binom{a+l}{l} \cdot \binom{b-l}{c-l}$ subsets and then subtract the ones that will also be counted for the value l+1. This way, no multiple copies are included. For a fixed l, the sets that will also be counted

again at the next iteration with l+1, and that therefore need to be subtracted from the count, are the ones that have exactly l elements in $G_1^{(l)}$ but then will also have exactly l+1 elements in $G_1^{(l+1)}$. This happens (only) when the element "a+l+1" is in the subset S. Therefore, such type of double-counted subset contains:

the element "a+l+1" any l elements in $G_1^{(l)}$ any c-l-1 elements in $G_2^{(l+1)}$

Figure S14 shows an example.

This means that for every index l there are $\binom{a+l}{l}\binom{b-l-1}{c-l-1}$ subsets that need to be removed from the count because they will also be counted at the next index, i.e. for l+1. This quantity is not subtracted at the last index, i.e. for l=c, as there will be no next index to double-count the subsets. This means that we can write:

$$\binom{a+b}{c} = \sum_{l=0}^{c} \binom{a+l}{l} \binom{b-l}{c-l} - \sum_{l=0}^{c-1} \binom{a+l}{l} \binom{b-l-1}{c-l-1}$$

Now that we have this formula, we can prove the Lemma by induction on c. For c=0, we have:

$$\sum_{l=0}^{0} \binom{a+l}{l} \binom{b-l}{c-l} = \binom{a}{0} \binom{b}{0} = 1 = \binom{a+b+1}{0} = \binom{a+b+1}{c}$$

So equality holds. For the induction step, we isolate the last term of the summation:

$$\sum_{l=0}^{c} \binom{a+l}{l} \binom{b-l}{c-l} = \binom{a+b}{c} + \sum_{l=0}^{c-1} \binom{a+l}{l} \binom{b-l-1}{c-l-1} = \binom{a+b}{c} + \binom{a+b}{c-1}$$

The last equality holds by induction, since $\sum_{l=0}^{c-1} {a+l \choose l} {b-l-1 \choose c-l-1}$ is exactly the summation we are inductively calculating, but with b-1 instead of b and with c-1 instead of c. Using Pascal's rule, we conclude that $\sum_{l=0}^{c} {a+l \choose l} {b-l \choose c-l} = {a+b+1 \choose c}$

Lemma 4. Consider a function $F: \mathbb{R}^p \to \mathbb{R}$, and take q < p such that $F(x_1, \ldots, x_p)$ only depends on q of the p total features, say x_{j_1}, \ldots, x_{j_q} . Then the marginal Shapley values for F may be computed by only focusing on x_{j_1}, \ldots, x_{j_q} : if $j \in \{j_1, \ldots, j_q\}$, then:

$$\phi_j(x^*) = \sum_{S \subseteq \{j_1, \dots, j_q\} \setminus \{j\}} \frac{1}{q\binom{q-1}{|S|}} \Big(\mathbb{E}[F(x_1, \dots, x_p) | x_j = x_j^*, x_S = x_S^*] - \mathbb{E}[F(x_1, \dots, x_p) | x_S = x_S^*] \Big).$$

If
$$j \notin \{j_1, ..., j_q\}$$
, then $\phi_j(x^*) = 0$.

Proof. Without loss of generality, we may assume that $j_1 = 1, ..., j_q = q$. Furthermore, it suffices to prove this Lemma for q = p - 1. If we then iterate the argument multiple times and remove all

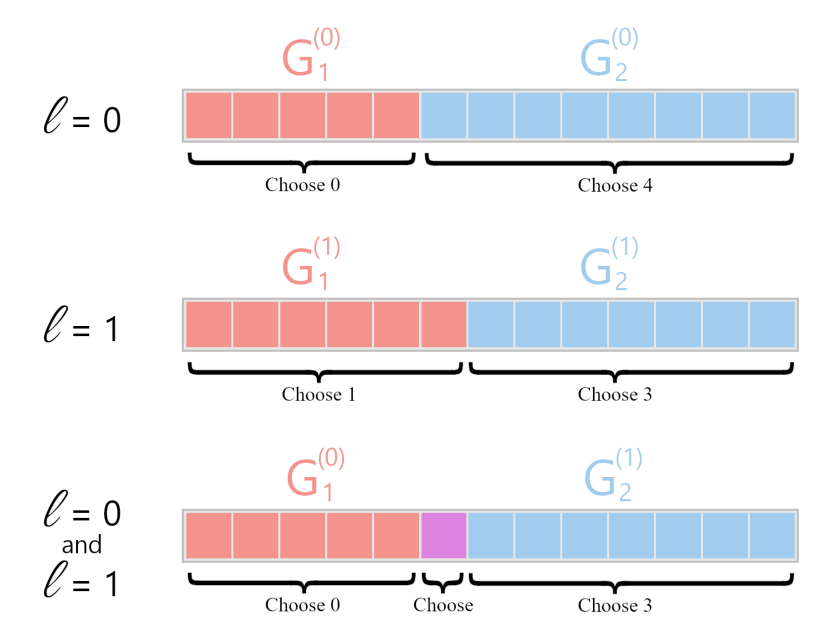


Figure S14: Example of subsets being counted twice for a=5,b=8,c=4 and $l\in\{0,1\}$. A subset here is counted twice if it has no elements in $G_1^{(0)}$ and one element in $G_1^{(1)}$, four elements in $G_2^{(0)}$ and three elements in $G_2^{(1)}$. This happens when the purple element is in the set, then no elements are on its left and 3=c-1 elements are on the right.

non-contributing features one by one, the argument is generally proven. Let us also use the notation:

$$\Delta \mathbb{E}_S := \mathbb{E}[F(x_1, \dots, x_p) | x_j = x_j^*, x_S = x_S^*] - \mathbb{E}[F(x_1, \dots, x_p) | x_S = x_S^*].$$

Note that $\phi_p(x^*) = 0$ is trivial, since the independence of F from x_p means that $\Delta \mathbb{E}_S = 0 \forall S$. For the remaining cases, let us assume that we need to compute the Shapley value for the first feature, for simplicity.

Now we can write:

$$\phi_1(x^*) = \sum_{S \subseteq \{2,\dots,p\}} \frac{1}{p\binom{p-1}{|S|}} \Delta \mathbb{E}_S$$

$$= \sum_{\substack{S \subseteq \{2,\dots,p\}\\S \not\ni p}} \frac{1}{p\binom{p-1}{|S|}} \Delta \mathbb{E}_S + \sum_{\substack{S \subseteq \{2,\dots,p\}\\S \ni p}} \frac{1}{p\binom{p-1}{|S|}} \Delta \mathbb{E}_S$$

Now let us write the subsets $S \subseteq \{2, ..., p\}$ containing p as $S = Z \cup \{p\}$. For these subsets, |S| = 1 + |Z|. Furthermore, since F does not depend on x_p , we know that $\Delta \mathbb{E}_S = \Delta \mathbb{E}_Z$.

$$\phi_1(x^*) = \sum_{S \subseteq \{2, \dots, p-1\}} \frac{1}{p\binom{p-1}{|S|}} \Delta \mathbb{E}_S + \sum_{Z \subseteq \{2, \dots, p-1\}} \frac{1}{p\binom{p-1}{1+|Z|}} \Delta \mathbb{E}_Z.$$

Now both summations are over the same subsets, so we can join them:

$$\phi_{j}(x^{*}) = \sum_{S \subseteq \{2, \dots, p-1\}} \frac{1}{p} \left(\frac{1}{\binom{p-1}{|S|}} + \frac{1}{\binom{p-1}{1+|S|}} \right) \Delta \mathbb{E}_{S}$$

$$= \sum_{S \subseteq \{2, \dots, p-1\}} \frac{1}{p!} \left(|S|!(p-1-|S|)! + (|S|+1)!(p-2-|S|)! \right) \Delta \mathbb{E}_{S}$$

$$= \sum_{S \subseteq \{2, \dots, p-1\}} \frac{|S|!(p-2-|S|)!}{p!} \left((p-1-|S|) + (|S|+1) \right) \Delta \mathbb{E}_{S}$$

$$= \sum_{S \subseteq \{2, \dots, p-1\}} \frac{|S|!(p-2-|S|)! \cdot p}{p!} \Delta \mathbb{E}_{S}$$

$$= \sum_{S \subseteq \{2, \dots, p-1\}} \frac{|S|!(p-2-|S|)!}{(p-1)!} \Delta \mathbb{E}_{S}$$

$$= \sum_{S \subseteq \{2, \dots, p-1\}} \frac{1}{(p-1)\binom{p-1}{|S|}} \Delta \mathbb{E}_{S}.$$

This concludes the proof, as the last step is precisely the formula for Shapley values for the features x_1, \ldots, x_{p-1} .

Theorem. Assume to have a dataset \mathcal{T} of size n. Consider a 0-1 coded rule of the form $r(x_1, \ldots, x_p) = \prod_{j=1}^p R_j(x_j)$, with $R_j : \mathbb{R} \to \{0,1\}$. Consider any real-valued function $\varphi : \mathbb{R} \to \mathbb{R}$. Given

 $l, k \in \{1, ..., p\}$, an unbiased estimator of the marginal Shapley value of $F(x) = \beta \varphi(x_l) r(x)$ for the k-th feature and the datapoint x^* is, for $k \neq l$:

$$\widehat{\phi}_k(x^*) = \beta \cdot \left(\frac{1}{n} \sum_{\substack{t \in \mathcal{T}s.t. \\ R_j(t_j) = 1 \lor R_j(x_j^*) = 1 \lor j}} \frac{\left(R_k(x_k^*) - R_k(t_k)\right) \cdot \left(\frac{\varphi(x_l^*)R_l(x_l^*)}{p - 1 - q(x^*) + R_l(x_l^*) + R_k(x_k^*)} + \frac{\varphi(t_l)R_l(t_l)}{p - 1 - q(t) + R_l(t_l) + R_k(t_k)}\right)}{\left(\frac{2p - q(x^*) - q(t) - 2 + R_l(x_l^*) + R_k(x_k^*) + R_l(t_l) + R_k(t_k)}{p - 1 - q(x^*) + R_l(x_l^*) + R_k(x_k^*)}\right)}.$$

For k = l, an unbiased estimator of the marginal Shapley value for the l-th feature is:

$$\widehat{\phi}_{l}(x^{*}) = \beta \cdot \left(\frac{1}{n(p - q(x^{*}) + R_{l}(x_{l}^{*}))} \sum_{\substack{t \in \mathcal{T}s.t. \\ R_{i}(t) = 1 \lor R_{i}(x^{*}) = 1 \lor j}} \frac{\varphi(x_{l}^{*})R_{l}(x_{l}^{*}) - \varphi(t_{l})R_{l}(t_{l})}{(2p - q(x^{*}) - q(t) - 1 + R_{l}(x_{l}^{*}) + R_{l}(t_{l}))} \right)$$

where $q: \mathbb{R} \to \mathbb{N}$ is defined as $q(x) = \sum_{j=1}^{p} R_j(x_j)$.

Proof. By linearity of marginal Shapley values, we can assume $\beta = 1$. For simplicity of notation, let us assume that l = 1.

Let us first cover the case k = l = 1 and write $S' := \{2, \ldots, p\} \setminus S$, for any subset $S \subseteq \{2, \ldots, p\}$. For any subset of active players S, we have:

$$\mathbb{E}[\varphi(x_1)r(x)|x_S = x_S^*] = \mathbb{E}[\varphi(x_1) \prod_{j=1}^p R_j(x_j)|x_S = x_S^*]$$

$$= \prod_{j \in S} R_j(x_j^*) \mathbb{E}[\varphi(x_1) \prod_{j \in \{1, \dots, p\} \setminus S} R_j(x_j)|x_S = x_S^*]$$

$$= \prod_{j \in S} R_j(x_j^*) \mathbb{E}[\varphi(x_1) \prod_{j \in \{1, \dots, p\} \setminus S} R_j(x_j)].$$

Analogously, we have:

$$\mathbb{E}[\varphi(x_1)r(x)|x_S = x_S^*, x_1 = x_1^*] = \varphi(x_1^*) \prod_{j \in S \cup \{1\}} R_j(x_j^*) \mathbb{E}[\prod_{j \in S'} R_j(x_j)]$$

We write these products more compactly by grouping up the indices: define $R_S(x_S^*) := \prod_{j \in S} R_j(x_j^*)$ and, consequently, $R_{S'}(x_{S'}) := \prod_{j \in S'} R_j(x_j)$. Then $\phi_1(x^*)$ may be re-written as:

$$\phi_{1}(x^{*}) = \sum_{S \subseteq \{2,...,p\}} w(S) \Big(\mathbb{E}[\varphi(x_{1})r(x)|x_{S} = x_{S}^{*}, x_{1} = x_{1}^{*}] - \mathbb{E}[\varphi(x_{1})r(x)|x_{S} = x_{S}^{*}] \Big)$$

$$= \sum_{S \subseteq \{2,...,p\}} w(S) \mathbb{E}[\varphi(x_{1})r(x)|x_{S} = x_{S}^{*}, x_{1} = x_{1}^{*}]$$

$$- \sum_{S \subseteq \{2,...,p\}} w(S) \mathbb{E}[\varphi(x_{1})r(x)|x_{S} = x_{S}^{*}]$$

$$= \sum_{S \subseteq \{2,...,p\}} w(S)\varphi(x_{1}^{*})R_{1}(x_{1}^{*})R_{S}(x_{S}^{*})\mathbb{E}[R_{S'}(x_{S'})]$$

$$- \sum_{S \subseteq \{2,...,p\}} w(S)R_{S}(x_{S}^{*})\mathbb{E}[\varphi(x_{1})R_{S' \cup \{1\}}(x_{S' \cup \{1\}})].$$

Let us treat the two summations separately; define the following:

$$\mathcal{A} = \sum_{S \subseteq \{2,\dots,p\}} w(S)\varphi(x_1^*)R_1(x_1^*)R_S(x_S^*)\mathbb{E}[R_{S'}(x_{S'})],$$

$$\mathcal{B} = \sum_{S \subseteq \{2, \dots, p\}} w(S) R_S(x_S^*) \mathbb{E}[\varphi(x_1) R_{S' \cup \{1\}}(x_{S' \cup \{1\}})].$$

Note that the expectations that appear in these formulas may be unbiasedly estimated by their sample means over the set \mathcal{T} . Let us focus on the first summation \mathcal{A} , which is therefore approximated by:

$$\widehat{\mathcal{A}} = \sum_{S \not\ni 1} w(S) \varphi(x_1^*) R_1(x_1^*) R_S(x_S^*) \widehat{\mathbb{E}}[R_{S'}(x_{S'})]$$

$$= \sum_{S \not\ni 1} w(S) \varphi(x_1^*) R_1(x_1^*) R_S(x_S^*) \frac{1}{n} \sum_{t \in \mathcal{T}} R_{S'}(t_{S'})$$

$$= \varphi(x_1^*) R_1(x_1^*) \cdot \frac{1}{n} \sum_{t \in \mathcal{T}} \sum_{S \not\ni 1} w(S) R_S(x_S^*) R_{S'}(t_{S'}).$$

Now let us focus on $\mathcal{C} := \sum_{S \not\supseteq 1} w(S) R_S(x_S^*) R_{S'}(t_{S'})$, for a fixed datapoint t. For any datapoint x, define the following:

$$\Omega_1(x) := \{ j \in \{2, \dots, p\} | R_j(x) = 1 \}, \qquad q_1(x) = |\Omega_1(x)|.$$

By definition of Ω_1 , we have:

$$R_{S}(x_{S}^{*})R_{S'}(t_{S'}) \neq 0 \iff \begin{cases} R_{S}(x_{S}^{*}) = 1 \\ R_{S'}(t_{S'}) = 1 \end{cases}$$

$$\iff \begin{cases} S \subseteq \Omega_{1}(x^{*}) \\ S' \subseteq \Omega_{1}(t) \end{cases}$$

$$\iff \begin{cases} S \subseteq \Omega_{1}(x^{*}) \\ \Omega_{1}(t)' \subseteq S \end{cases},$$

where $\Omega_1(t)'$ is meant as the complementary set of $\Omega_1(t)$ with respect to $\{2,\ldots,p\}$. This means that $w(S)R_S(x_S^*)R_{S'}(z_{S'})$ only gives a non-zero effect for the datapoints t such that $\Omega_1(t)'\subseteq\Omega_1(x^*)$, in which case the (only) subsets S that contribute are the ones such that $\Omega_1(t)'\subseteq S\subseteq\Omega_1(x^*)$. Since all such sets S contain $\Omega_1(t)'$, they can all be uniquely identified by the indices that they have besides those in $\Omega_1(t)'$. In other words, each S may be (uniquely) re-written as $S=\Omega_1(t)'\cup Z$, with $Z\subseteq\Omega_1(x^*)\setminus\Omega_1(t)'$. For every size |Z|=l, there are exactly $\binom{|\Omega_1(x^*)\setminus\Omega_1(t)'|}{l}=\binom{q_1(x^*)+q_1(t)-p+1}{l}$ possible choices of Z, and they all have the same effect $w(S)=\frac{1}{p\binom{p-1}{l-1}}=\frac{1}{p\binom{p-1}{l-1}-q_1(t)+l}$.

This means that we can write:

$$\begin{split} &\mathcal{C} = \sum_{S \not\ni 1} w(S) R_S(x_S^*) R_{S'}(t_{S'}) \\ &= \sum_{l=0}^{|\Omega_1(x^*) \setminus \Omega_1(t)|} \frac{\left(q_1(x^*) + q_1(t) - p + 1\right)}{p(l_{+p-1-q_1(t)})} \\ &= \sum_{l=0}^{q_1(x^*) + q_1(t) - p + 1} \frac{\left(q_1(x^*) + q_1(t) - p + 1\right)}{p(l_{+p-1-q_1(t)})} \\ &= \frac{\left(q_1(x^*) + q_1(t) - p + 1\right)!}{p!} \\ & \cdot \sum_{l=0}^{q_1(x^*) + q_1(t) - p + 1} \frac{\left(q_1(t) - l\right)!(p - 1 - q_1(t) + l)!}{\left(q_1(x^*) + q_1(t) - p + 1 - l\right)!l!} \\ &= \frac{\left(q_1(x^*) + q_1(t) - p + 1\right)!}{p!} \\ & \cdot \sum_{l=0}^{q_1(x^*) + q_1(t) - p + 1} \left[\binom{q_1(t) - l}{q_1(x^*) + q_1(t) - p + 1 - l} (p - 1 - q_1(x^*))! \\ & \cdot \binom{p - 1 - q_1(t) + l}{l} (p - 1 - q_1(t))! \right] \\ &= \frac{\left(q_1(x^*) + q_1(t) - p + 1\right)!(p - 1 - q_1(t))!(p - 1 - q_1(t))!}{p!} \\ & \cdot \sum_{l=0}^{q_1(x^*) + q_1(t) - p + 1} \binom{q_1(t) - l}{q_1(x^*) + q_1(t) - p + 1 - l} \binom{p - 1 - q_1(t) + l}{l}. \end{split}$$

Using Lemma 3 with $a = p - 1 - q_1(t)$, $b = q_1(t)$, $c = q_1(x^*) + q_1(t) - p + 1$, we conclude:

$$C = \sum_{S \not\supseteq 1} w(S) R_S(x_S^*) R_{S'}(t_{S'})$$

$$= \frac{(q_1(x^*) + q_1(t) - p + 1)!(p - 1 - q_1(t))!(p - 1 - q_1(x^*))!}{p!} \cdot \binom{p}{q_1(x^*) + q_1(t) - p + 1}$$

$$= \frac{(p - 1 - q_1(t))!(p - 1 - q_1(x^*))!}{(2p - q_1(x^*) - q_1(t) - 1)!}$$

$$= \frac{1}{(p - q_1(x^*))} \cdot \frac{1}{\binom{2p - q_1(x^*) - q_1(t) - 1}{p - q_1(x^*)}}.$$

This allows us to conclude that:

$$\widehat{\mathcal{A}} = \varphi(x_1^*) R_1(x_1^*) \cdot \frac{1}{n(p - q_1(x^*))} \sum_{\substack{t \in \mathcal{T} \text{ s.t.} \\ \Omega_1(t)' \subseteq \Omega_1(x^*)}} \frac{1}{\binom{2p - q_1(x^*) - q_1(t) - 1}{p - q_1(x^*)}}.$$

The sum is only over the datapoints with $\Omega_1(t)' \subseteq \Omega_1(x^*)$, as the other datapoints have a null effect. In a similar fashion, let us compute $\widehat{\mathcal{B}}$:

$$\widehat{\mathcal{B}} = \sum_{S \not\ni 1} w(S) R_S(x_S^*) \mathbb{E}[\varphi(x_1) R_{S' \cup \{p\}}(x_{S' \cup \{p\}})]$$

$$= \sum_{S \not\ni 1} w(S) R_S(x_S^*) \frac{1}{n} \sum_{t \in \mathcal{T}} \varphi(t_1) R_{S' \cup \{p\}}(t_{S' \cup \{p\}})$$

$$= \sum_{S \not\ni 1} w(S) R_S(x_S^*) \frac{1}{n} \sum_{t \in \mathcal{T}} R_S(x_S^*) \varphi(t_1) R_{S'}(t_{S'}) R_1(t_1)$$

$$= \frac{1}{n} \sum_{t \in \mathcal{T}} \varphi(t_1) R_1(t_1) \sum_{S \not\ni 1} w(S) R_S(x_S^*) R_{S'}(t_{S'}).$$

As we can see, the expression now contains the exact same summation as before, which immediately allows us to conclude that:

$$\widehat{\mathcal{B}} = \frac{1}{n(p - q_1(x^*))} \sum_{\substack{t \in \mathcal{T} \text{ s.t.} \\ \Omega_1(t)' \subseteq \Omega_1(x^*)}} \frac{\varphi(t_1) R_1(t_1)}{\binom{2p - q_1(x^*) - q_1(t) - 1}{p - q_1(x^*)}}.$$

Combining the two expressions together gives us the formula:

$$\widehat{\phi_1}(x^*) = \widehat{\mathcal{A}} - \widehat{\mathcal{B}} = \frac{1}{n(p - q_1(x^*))} \sum_{\substack{t \in \mathcal{T} \text{ s.t.} \\ \Omega_1(t)' \subset \Omega_1(x^*)}} \frac{\varphi(x_1^*) R_1(x_1^*) - \varphi(t_1) R_1(t_1)}{\binom{2p - q_1(x^*) - q_1(t) - 1}{p - q_1(x^*)}}.$$

To obtain the formula stated in the Theorem, notice that $q(x) = q_1(x) + R_1(x)$ and that the condition $\Omega_1(t)' \subseteq \Omega_1(x^*)$ in the summation may be replaced with the condition $R_j(t) = 1 \vee R_j(x_j^*) = 1 \forall j$: the only datapoints for which the two conditions differ are the points for which $R_1(t_1) = R_1(x_1^*) = 0$. For such datapoints, the effect is null and thus does not affect the formula.

Now let us consider the case $k \neq l = 1$. For simplicity, let's assume k = p. For any subset $V \subseteq \{2, \ldots, p-1\}$, define V'' as $\{2, \ldots, p-1\} \setminus V$. By separating the cases $1 \in S$ and $1 \notin S$,

Shapley values may be re-written as:

$$\begin{split} \phi_p(x^*) &= \sum_{S \subseteq \{1, \dots, p-1\}} w(S) \Big(\mathbb{E}[\varphi(x_1) r(x) | x_S = x_S^*, x_p = x_p^*] - \mathbb{E}[\varphi(x_1) r(x) | x_S = x_S^*] \Big) \\ &= \sum_{V \subseteq \{2, \dots, p-1\}} w(V \cup \{1\}) \Big(\mathbb{E}[\varphi(x_1) r(x) | x_V = x_V^*, x_1 = x_1^*, x_p = x_p^*] - \mathbb{E}[\varphi(x_1) r(x) | x_V = x_V^*, x_1 = x_1^*] \Big) \\ &\quad + \sum_{V \subseteq \{2, \dots, p-1\}} w(V) \Big(\mathbb{E}[\varphi(x_1) r(x) | x_V = x_V^*, x_p = x_p^*] - \mathbb{E}[\varphi(x_1) r(x) | x_V = x_V^*] \Big) \\ &= \sum_{V \subseteq \{2, \dots, p-1\}} w(V \cup \{1\}) \mathbb{E}[\varphi(x_1) r(x) | x_V = x_V^*, x_1 = x_1^*, x_p = x_p^*] \\ &\quad - \sum_{V \subseteq \{2, \dots, p-1\}} w(V) \mathbb{E}[\varphi(x_1) r(x) | x_V = x_V^*, x_p = x_p^*] \\ &\quad + \sum_{V \subseteq \{2, \dots, p-1\}} w(V) \mathbb{E}[\varphi(x_1) r(x) | x_V = x_V^*, x_p = x_p^*] \\ &\quad - \sum_{V \subseteq \{2, \dots, p-1\}} w(V) \mathbb{E}[\varphi(x_1) r(x) | x_V = x_V^*] \\ &= \sum_{V \subseteq \{2, \dots, p-1\}} w(V \cup \{1\}) \varphi(x_1^*) R_1(x_1^*) R_V(x_V^*) \mathbb{E}[R_{V''}(x_{V''})] \\ &\quad - \sum_{V \subseteq \{2, \dots, p-1\}} w(V) \mathbb{E}[\varphi(x_1) R_1(x_1^*) R_V(x_V^*) \mathbb{E}[R_{V'' \cup \{1\}})] \\ &\quad + \sum_{V \subseteq \{2, \dots, p-1\}} w(V) R_V(x_V^*) \mathbb{E}[\varphi(x_1) R_{V'' \cup \{1\}} (x_{V'' \cup \{1\}})] \\ &\quad - \sum_{V \subseteq \{2, \dots, p-1\}} w(V) R_V(x_V^*) \mathbb{E}[\varphi(x_1) R_{V'' \cup \{1, p\}} (x_{V'' \cup \{1, p\}})] \end{aligned}$$

Let us treat the four summations separately; define the following:

$$\mathcal{D} = \sum_{V \subseteq \{2, \dots, p-1\}} w(V \cup \{1\}) \varphi(x_1^*) R_1(x_1^*) R_V(x_V^*) R_p(x_p^*) \mathbb{E}[R_{V''}(x_{V''})],$$

$$\mathcal{E} = \sum_{V \subseteq \{2, \dots, p-1\}} w(V \cup \{1\}) \varphi(x_1^*) R_1(x_1^*) R_V(x_V^*) \mathbb{E}[R_{V'' \cup \{p\}}(x_{V'' \cup \{p\}})],$$

$$\mathcal{F} = \sum_{V \subseteq \{2, \dots, p-1\}} w(V) R_V(x_V^*) R_p(x_p^*) \mathbb{E}[\varphi(x_1) R_{V'' \cup \{1\}}(x_{V'' \cup \{1\}})],$$

$$\mathcal{G} = \sum_{V \subseteq \{2, \dots, p-1\}} w(V) R_V(x_V^*) \mathbb{E}[\varphi(x_1) R_{V'' \cup \{1, p\}}(x_{V'' \cup \{1, p\}})].$$

With a similar argument as above, they can be approximated without bias by:

$$\widehat{\mathcal{D}} = \sum_{V \subseteq \{2, \dots, p-1\}} w(V \cup \{1\}) \varphi(x_1^*) R_1(x_1^*) R_V(x_V^*) R_p(x_p^*) \frac{1}{n} \sum_{t \in \mathcal{T}} R_{V''}(t_{V''})$$

$$= \frac{1}{n} \sum_{t \in \mathcal{T}} x_1^* R_1(x_1^*) R_p(x_p^*) \sum_{V \subseteq \{2, \dots, p-1\}} w(V \cup \{1\}) R_V(x_V^*) R_{V''}(t_{V''})$$

$$\widehat{\mathcal{E}} = \sum_{V \subseteq \{2, \dots, p-1\}} w(V \cup \{1\}) \varphi(x_1^*) R_1(x_1^*) R_V(x_V^*) \frac{1}{n} \sum_{t \in \mathcal{T}} R_{V'' \cup \{p\}}(t_{V'' \cup \{p\}})$$

$$= \frac{1}{n} \sum_{t \in \mathcal{T}} x_1^* R_1(x_1^*) R_p(t_p) \sum_{V \subseteq \{2, \dots, p-1\}} w(V \cup \{1\}) R_V(x_V^*) R_{V''}(t_{V''})$$

$$\widehat{\mathcal{F}} = \sum_{V \subseteq \{2, \dots, p-1\}} w(V) R_V(x_V^*) R_p(x_p^*) \frac{1}{n} \sum_{t \in \mathcal{T}} \varphi(t_1) R_{V'' \cup \{1\}}(t_{V'' \cup \{1\}})$$

$$= \frac{1}{n} \sum_{t \in \mathcal{T}} \varphi(t_1) R_1(t_1) R_p(x_p^*) \sum_{V \subseteq \{2, \dots, p-1\}} w(V) R_V(x_V^*) R_{V''}(t_{V''})$$

$$\widehat{\mathcal{G}} = \sum_{V \subseteq \{2, \dots, p-1\}} w(V) R_V(x_V^*) \frac{1}{n} \sum_{t \in \mathcal{T}} \varphi(t_1) R_{V'' \cup \{1, p\}} (t_{V'' \cup \{1, p\}})$$

$$= \frac{1}{n} \sum_{t \in \mathcal{T}} \varphi(t_1) R_1(t_1) R_p(t_p) \sum_{V \subseteq \{2, \dots, p-1\}} w(V) R_V(x_V^*) R_{V''}(t_{V''})$$

In order to compute these, we re-write the two summations over the sets V that appear above: for any datapoint x, define the following:

$$\Omega_{1,p}(x) := \{ j \in \{2, \dots, p-1\} | R_j(x) = 1 \}, \qquad q_{1,p}(x) = |\Omega_{1,p}(x)|.$$

Then the terms $R_V(x_V^*)R_{V''}(t_{V''})$ are again non-zero exactly when $\Omega_{1,p}(x^*)$ contains $\Omega_{1,p}(t)''$, and

only for the sets in between these two, so:

$$\begin{split} \mathcal{H} &:= \sum_{V \subseteq \{2, \dots, p-1\}} w(V \cup \{1\}) R_V(x_V^*) R_{V''}(t_{V''}) \\ &= \sum_{l=0}^{|\Omega_{1,p}(x^*) \setminus \Omega_{1,p}(t)''|} \frac{\left(q_{1,p}(x^*) + q_{1,p}(t) - p + 2\right)}{p\left(l_{1+p-1} - q_{1,p}(t)\right)} \\ &= \sum_{l=0}^{q_{1,p}(x^*) + q_{1,p}(t) - p + 2} \frac{\left(q_{1,p}(x^*) + q_{1,p}(t) - p + 2\right)}{p\left(l_{1+p-1} - q_{1,p}(t)\right)} \\ &= \frac{\left(q_{1,p}(x^*) + q_{1,p}(t) - p + 2\right)!}{p!} \\ & \cdot \sum_{l=0}^{q_{1,p}(x^*) + q_{1,p}(t) - p + 2} \frac{\left(q_{1,p}(t) - l\right)!(p - 1 - q_{1,p}(t) + l)!}{\left(q_{1,p}(x^*) + q_{1,p}(t) - p + 2 - l\right)!l!} \\ &= \frac{\left(q_{1,p}(x^*) + q_{1,p}(t) - p + 2\right)!}{p!} \\ & \cdot \sum_{l=0}^{q_{1,p}(x^*) + q_{1,p}(t) - p + 2} \left[\left(q_{1,p}(x^*) + q_{1,p}(t) - p + 2 - l\right) (p - 2 - q_{1,p}(x^*))! \\ & \cdot \left(p - 1 - q_{1,p}(t) + l\right) (p - 1 - q_{1,p}(t))! \right] \\ &= \frac{\left(q_{1,p}(x^*) + q_{1,p}(t) - p + 2\right)!(p - 1 - q_{1,p}(t))!(p - 2 - q_{1,p}(x^*))!}{p!} \\ & \cdot \sum_{l=0}^{q_{1,p}(x^*) + q_{1,p}(t) - p + 2} \left(q_{1,p}(x^*) + q_{1,p}(t) - p + 2 - l\right) \left(p - 1 - q_{1,p}(t) + l\right). \end{split}$$

Using Lemma 3 with $a = p - 1 - q_{1,p}(t)$, $b = q_{1,p}(t)$ and $c = q_{1,p}(x^*) + q_{1,p}(t) - p + 2$, we conclude:

$$\mathcal{H} = \sum_{\substack{V \subseteq \{2, \dots, p-1\} \\ V \subseteq \{2, \dots, p-1\} \\ }} w(V \cup \{1\}) R_V(x_V^*) R_{V''}(t_{V''})$$

$$= \frac{(q_{1,p}(x^*) + q_{1,p}(t) - p + 2)!(p - 1 - q_{1,p}(t))!(p - 2 - q_{1,p}(x^*))!}{p!} \cdot \begin{pmatrix} p \\ q_{1,p}(x^*) + q_{1,p}(t) - p + 2 \end{pmatrix}$$

$$= \frac{(p - 1 - q_{1,p}(t))!(p - 2 - q_{1,p}(x^*))!}{(2p - q_{1,p}(x^*) - q_{1,p}(t) - 2)!}$$

$$= \frac{1}{(p - 1 - q_{1,p}(x^*))} \cdot \frac{1}{\binom{2p - q_{1,p}(x^*) - q_{1,p}(t) - 2}{p - 1 - q_{1,p}(x^*)}}.$$

Similarly, the other summation can be written as:

$$\begin{split} &\mathcal{I} := \sum_{V \subseteq \{2, \dots, p-1\}} w(V) R_V(x_V^*) R_{V''}(t_{V''}) \\ &= \sum_{l=0}^{|\Omega_{1,p}(x^*) \setminus \Omega_{1,p}(t)|} \frac{\left(q_{1,p}(x^*) + q_{1,p}(t) - p + 2\right)}{p\left(l_{1+p-2-q_{1,p}(t)}\right)} \\ &= \sum_{l=0}^{q_{1,p}(x^*) + q_{1,p}(t) - p + 2} \frac{\left(q_{1,p}(x^*) + q_{1,p}(t) - p + 2\right)}{p\left(l_{1+p-2-q_{1,p}(t)}\right)} \\ &= \frac{\left(q_{1,p}(x^*) + q_{1,p}(t) - p + 2\right)!}{p!} \\ & \cdot \sum_{l=0}^{q_{1,p}(x^*) + q_{1,p}(t) - p + 2} \frac{\left(q_{1,p}(t) + 1 - l\right)!(p - 2 - q_{1,p}(t) + l)!}{(q_{1,p}(x^*) + q_{1,p}(t) - p + 2 - l)!l!} \\ &= \frac{\left(q_{1,p}(x^*) + q_{1,p}(t) - p + 2\right)!}{p!} \\ & \cdot \sum_{l=0}^{q_{1,p}(x^*) + q_{1,p}(t) - p + 2} \left[\left(q_{1,p}(t) + 1 - l\right) (p - 1 - q_{1,p}(x^*))! \\ & \cdot \left(p - 2 - q_{1,p}(t) + l\right) (p - 2 - q_{1,p}(t))! \right] \\ &= \frac{\left(q_{1,p}(x^*) + q_{1,p}(t) - p + 2\right)!(p - 2 - q_{1,p}(t))!(p - 1 - q_{1,p}(x^*))!}{p!} \\ & \cdot \sum_{l=0}^{q_{1,p}(x^*) + q_{1,p}(t) - p + 2} \left(q_{1,p}(t) + 1 - l\right) \left(p - 2 - q_{1,p}(t) + l\right) \cdot \sum_{l=0}^{q_{1,p}(x^*) + q_{1,p}(t) - p + 2 - l} \left(q_{1,p}(x^*) + q_{1,p}(t) - p + 2 - l\right) \left(p - 2 - q_{1,p}(t) + l\right). \end{split}$$

Using Lemma 3 with $a = p - 2 - q_{1,p}(t)$, $b = q_{1,p}(t) + 1$ and $c = q_{1,p}(x^*) + q_{1,p}(t) - p + 2$, we conclude:

$$\begin{split} \mathcal{I} &= \sum_{V \subseteq \{2, \dots, p-1\}} w(V) R_V(x_V^*) R_{V''}(t_{V''}) \\ &= \frac{(q_{1,p}(x^*) + q_{1,p}(t) - p + 2)!(p - 2 - q_{1,p}(t))!(p - 1 - q_{1,p}(x^*))!}{p!} \\ & \cdot \binom{p}{q_{1,p}(x^*) + q_{1,p}(t) - p + 2} \\ &= \frac{(p - 2 - q_{1,p}(t))!(p - 1 - q_{1,p}(x^*))!}{(2p - q_{1,p}(x^*) - q_{1,p}(t) - 2)!} \\ &= \frac{1}{(p - 1 - q_{1,p}(t))} \cdot \frac{1}{\binom{2p - q_{1,p}(x^*) - q_{1,p}(t) - 2}{p - 1 - q_{1,p}(x^*)}}. \end{split}$$

These allow us to conclude that:

$$\begin{split} \widehat{\mathcal{D}} &= \frac{1}{n} \sum_{\substack{t \in \mathcal{T} \text{s.t.} \\ \Omega_{1,p}(t)' \subseteq \Omega_{1,p}(x^*)}} \frac{1}{\binom{2p - q_{1,p}(x^*) - q_{1,p}(t) - 2}{p - 1 - q_{1,p}(x^*)}} \cdot \frac{\varphi(x_1^*) R_1(x_1^*) R_p(x_p^*)}{p - 1 - q_{1,p}(x^*)} \\ \widehat{\mathcal{E}} &= \frac{1}{n} \sum_{\substack{t \in \mathcal{T} \text{s.t.} \\ \Omega_{1,p}(t)' \subseteq \Omega_{1,p}(x^*)}} \frac{1}{\binom{2p - q_{1,p}(x^*) - q_{1,p}(t) - 2}{p - 1 - q_{1,p}(x^*)}} \cdot \frac{\varphi(x_1^*) R_1(x_1^*) R_p(t_p)}{p - 1 - q_{1,p}(x^*)} \\ \widehat{\mathcal{F}} &= \frac{1}{n} \sum_{\substack{t \in \mathcal{T} \text{s.t.} \\ \Omega_{1,p}(t)' \subseteq \Omega_{1,p}(x^*)}} \frac{1}{\binom{2p - q_{1,p}(x^*) - q_{1,p}(t) - 2}{p - 1 - q_{1,p}(x^*)}} \cdot \frac{\varphi(t_1) R_1(t_1) R_p(x_p^*)}{p - 1 - q_{1,p}(t)} \\ \widehat{\mathcal{G}} &= \frac{1}{n} \sum_{\substack{t \in \mathcal{T} \text{s.t.} \\ \Omega_{1,p}(t)' \subseteq \Omega_{1,p}(x^*)}} \frac{1}{\binom{2p - q_{1,p}(x^*) - q_{1,p}(t) - 2}{p - 1 - q_{1,p}(x^*)}} \cdot \frac{\varphi(t_1) R_1(t_1) R_p(t_p)}{p - 1 - q_{1,p}(t)} \end{split}$$

Putting the four pieces together, we obtain:

$$\widehat{\phi_p}(x^*) = \widehat{\mathcal{D}} - \widehat{\mathcal{E}} + \widehat{\mathcal{F}} - \widehat{\mathcal{G}}$$

$$= \frac{1}{n} \sum_{\substack{t \in \mathcal{T} \text{s.t.} \\ \Omega_{1,p}(t)' \subseteq \Omega_{1,p}(x^*)}} \frac{\varphi(x_1^*) R_1(x_1^*) \frac{R_p(x_p^*) - R_p(t_p)}{p - 1 - q_{1,p}(x^*)} + \varphi(t_1) R_1(t_1) \frac{R_p(x_p^*) - R_p(t_p)}{p - 1 - q_{1,p}(t)}}{\binom{2p - q_{1,p}(x^*) - q_{1,p}(t) - 2}{p - 1 - q_{1,p}(x^*)}}.$$

To obtain the formula stated in the Theorem, notice that $q(x) = q_1(x) + R_1(x)$ and that the condition $\Omega_1(t)' \subseteq \Omega_1(x^*)$ in the summation may be replaced with the condition $R_j(t) = 1 \vee R_j(x_j^*) = 1 \forall j$: the only datapoints for which the two conditions differ are the points for which $R_1(t_1) = R_1(x_1^*) = 0$. For such datapoints, the effect is null and thus does not affect the formula.

Theorem. Assume to have a dataset \mathcal{T} of size n. Consider a 0-1 coded rule of the form $r(x_1, \ldots, x_p) = \prod_{j=1}^p R_j(x_j)$, with $R_j : \mathbb{R} \to \{0,1\}$. Consider any real-valued function $\varphi : \mathbb{R} \to \mathbb{R}$. Given $l, k, k' \in \{1, \ldots, p\}$ with $k \neq k'$ and $k \neq l$, an unbiased estimator of the marginal interaction Shapley value of $F(x) = \beta \varphi(x_l) r(x)$ for the k-th and k'-th features and the datapoint x^* is, for $k' \neq l$:

$$\widehat{\phi}_{k,k'}(x^*) = \beta \cdot \frac{1}{2n} \sum_{\substack{t \in \mathcal{T}s.t. \\ R_j(t_j) = 1 \lor R_j(x_j^*) = 1 \lor j}} \frac{\frac{\varphi(x_l^*)R_l(x_l^*)}{p - 2 - q(x^*) + R_l(x_l^*) + R_k(x_k^*)} + \frac{\varphi(t_l)R_l(t_l)}{p - 2 - q(t) + R_l(t_l) + R_{k'}(t_{k'}) + R_k(t_k)}}{\frac{(2p - q(x^*) + R_l(x_l^*) + R_{k'}(x_{k'}^*) + R_k(x_k^*) - q(t) + R_l(t_l) + R_{k'}(t_{k'}) + R_k(t_k) - q(t)}{p - 2 - q(x^*) + R_l(x_l^*) + R_{k'}(x_{k'}^*) + R_k(x_k^*)}} \cdot \left(R_{k'}(x_{k'}^*) R_k(x_k^*) - R_{k'}(x_{k'}^*) R_k(t_k) - R_{k'}(t_{k'}) R_k(x_k^*) + R_{k'}(t_{k'}) R_k(t_k) \right).$$

For k' = l, an unbiased estimator of the marginal interaction Shapley value for the l-th and k-th feature is:

$$\widehat{\phi}_{l,k}(x^*) = \beta \cdot \frac{1}{2n(p-1-q(x^*)+R_l(x_l^*))} \cdot \sum_{\substack{t \in \mathcal{T}_{s.t.} \\ R_j(t)=1 \lor R_j(x^*)=1 \lor j}} \frac{\varphi(x_l^*)R_l(x_l^*)R_k(x_k^*) - \varphi(x_l^*)R_l(x_l^*)R_k(t_k) - \varphi(t_l)R_l(t_l)R_k(x_k^*) + \varphi(t_l)R_l(t_l)R_k(t_k)}{\binom{2p-q(x^*)-q(t)-1+R_l(x_l^*)+R_k(x_k^*)+R_l(t_k)+R_l(t_k)}{p-q(x^*)+R_l(x_l^*)+R_l(x_k^*)}},$$

where $q: \mathbb{R} \to \mathbb{N}$ is defined as $q(x) = \sum_{j=1}^{p} R_j(x_j)$.

Proof. By linearity of marginal Shapley values, we can assume $\beta = 1$. For simplicity of notation, let us assume that l = 1 and k = p.

Let us first cover the case k'=l=1 and write $S':=\{2,\ldots,p-1\}\setminus S$, for any subset $S\subseteq\{2,\ldots,p-1\}$. For any subset of active players S, we have:

$$\mathbb{E}[\varphi(x_1)r(x)|x_S = x_S^*] = \mathbb{E}[\varphi(x_1) \prod_{j=1}^p R_j(x_j)|x_S = x_S^*]$$

$$= \prod_{j \in S} R_j(x_j^*) \mathbb{E}[\varphi(x_1) \prod_{j \in \{1, \dots, p\} \setminus S} R_j(x_j)|x_S = x_S^*]$$

$$= \prod_{j \in S} R_j(x_j^*) \mathbb{E}[\varphi(x_1) \prod_{j \in \{1, \dots, p\} \setminus S} R_j(x_j)].$$

Analogously, we have:

$$\mathbb{E}[\varphi(x_1)r(x)|x_S = x_S^*, x_1 = x_1^*, x_p = x_p^*] = \varphi(x_1^*) \prod_{j \in S \cup \{1, p\}} R_j(x_j^*) \mathbb{E}[\prod_{j \in S'} R_j(x_j)]$$

$$\mathbb{E}[\varphi(x_1)r(x)|x_S = x_S^*, x_1 = x_1^*] = \varphi(x_1^*) \prod_{j \in S \cup \{1\}} R_j(x_j^*) \mathbb{E}[\prod_{j \in S' \cup \{p\}} R_j(x_j)]$$

$$\mathbb{E}[\varphi(x_1)r(x)|x_S = x_S^*, x_p = x_p^*] = \prod_{j \in S \cup \{p\}} R_j(x_j^*) \mathbb{E}[\varphi(x_1^*) \prod_{j \in S' \cup \{1\}} R_j(x_j)]$$

We write these products more compactly by grouping up the indices: define $R_S(x_S^*) := \prod_{j \in S} R_j(x_j^*)$

and, consequently, $R_{S'}(x_{S'}) := \prod_{j \in S'} R_j(x_j)$. Then $\phi_{1,p}(x^*)$ may be re-written as:

$$\begin{split} \phi_{1,p}(x^*) &= \sum_{S \subseteq \{2,...,p-1\}} w(S) \Big(\mathbb{E}[\varphi(x_1)r(x)|x_S = x_S^*, x_1 = x_1^*, x_p = x_p^*] \\ &- \mathbb{E}[\varphi(x_1)r(x)|x_S = x_S^*, x_1 = x_1^*] - \mathbb{E}[\varphi(x_1)r(x)|x_S = x_S^*, x_p = x_p^*] \\ &+ \mathbb{E}[\varphi(x_1)r(x)|x_S = x_S^*] \Big) \\ &= \sum_{S \subseteq \{2,...,p-2\}} w(S) \mathbb{E}[\varphi(x_1)r(x)|x_S = x_S^*, x_1 = x_1^*, x_p = x_p^*] \\ &- \sum_{S \subseteq \{2,...,p-2\}} w(S) \mathbb{E}[\varphi(x_1)r(x)|x_S = x_S^*, x_1 = x_1^*] \\ &- \sum_{S \subseteq \{2,...,p-2\}} w(S) \mathbb{E}[\varphi(x_1)r(x)|x_S = x_S^*, x_p = x_p^*] \\ &+ \sum_{S \subseteq \{2,...,p-2\}} w(S) \mathbb{E}[\varphi(x_1)r(x)|x_S = x_S^*] \\ &= \sum_{S \subseteq \{2,...,p-2\}} w(S) \varphi(x_1^*) R_1(x_1^*) R_p(x_p^*) R_S(x_S^*) \mathbb{E}[R_{S'}(x_{S'})] \\ &- \sum_{S \subseteq \{2,...,p-2\}} w(S) \varphi(x_1^*) R_1(x_1^*) R_S(x_S^*) \mathbb{E}[R_{S' \cup \{p\}}(x_{S' \cup \{p\}})] \\ &- \sum_{S \subseteq \{2,...,p-2\}} w(S) R_p(x_p^*) R_S(x_S^*) \mathbb{E}[\varphi(x_1) R_{S' \cup \{1\}}(x_{S' \cup \{1\}})] \\ &+ \sum_{S \subseteq \{2,...,p-2\}} w(S) R_S(x_S^*) \mathbb{E}[\varphi(x_1) R_{S' \cup \{1,p\}}(x_{S' \cup \{1,p\}})]. \end{split}$$

Let us treat the four summations separately; define the following:

$$\mathcal{A} = \sum_{S \subseteq \{2, \dots, p-2\}} w(S)\varphi(x_1^*)R_1(x_1^*)R_p(x_p^*)R_S(x_S^*)\mathbb{E}[R_{S'}(x_{S'})],$$

$$\mathcal{B} = \sum_{S \subseteq \{2, \dots, p-2\}} w(S)\varphi(x_1^*)R_1(x_1^*)R_S(x_S^*)\mathbb{E}[R_{S' \cup \{p\}}(x_{S' \cup \{p\}})],$$

$$\mathcal{C} = \sum_{S \subseteq \{2, \dots, p-2\}} w(S)R_p(x_p^*)R_S(x_S^*)\mathbb{E}[\varphi(x_1)R_{S' \cup \{1\}}(x_{S' \cup \{1\}})],$$

$$\mathcal{D} = \sum_{S \subseteq \{2, \dots, p-2\}} w(S)R_S(x_S^*)\mathbb{E}[\varphi(x_1)R_{S' \cup \{1, p\}}(x_{S' \cup \{1, p\}})].$$

Note that the expectations that appear in these formulas may be unbiasedly estimated by their sample means over the set \mathcal{T} . Let us focus on the first summation \mathcal{A} , which is therefore approximated

by:

$$\begin{split} \widehat{\mathcal{A}} &= \sum_{S \subseteq \{2, \dots, p-2\}} w(S) \varphi(x_1^*) R_1(x_1^*) R_p(x_p^*) R_S(x_S^*) \widehat{\mathbb{E}}[R_{S'}(x_{S'})] \\ &= \sum_{S \subseteq \{2, \dots, p-2\}} w(S) \varphi(x_1^*) R_1(x_1^*) R_p(x_p^*) R_S(x_S^*) \frac{1}{n} \sum_{t \in \mathcal{T}} R_{S'}(t_{S'}) \\ &= \varphi(x_1^*) R_1(x_1^*) R_p(x_p^*) \cdot \frac{1}{n} \sum_{t \in \mathcal{T}} \sum_{S \subseteq \{2, \dots, p-2\}} w(S) R_S(x_S^*) R_{S'}(t_{S'}). \end{split}$$

Now let us focus on $\mathcal{E} := \sum_{S \subseteq \{2,...,p-2\}} w(S) R_S(x_S^*) R_{S'}(t_{S'})$, for a fixed datapoint t. For any datapoint x, define the following:

$$\Omega_{1,p}(x) := \{ j \in \{2, \dots, p-2\} | R_j(x) = 1 \}, \qquad q_{1,p}(x) = |\Omega_{1,p}(x)|.$$

By definition of $\Omega_{1,p}$, we have:

$$R_{S}(x_{S}^{*})R_{S'}(t_{S'}) \neq 0 \iff \begin{cases} R_{S}(x_{S}^{*}) = 1 \\ R_{S'}(t_{S'}) = 1 \end{cases}$$

$$\iff \begin{cases} S \subseteq \Omega_{1,p}(x^{*}) \\ S' \subseteq \Omega_{1,p}(t) \end{cases}$$

$$\iff \begin{cases} S \subseteq \Omega_{1,p}(x^{*}) \\ \Omega_{1,p}(t)' \subseteq S \end{cases},$$

where $\Omega_{1,p}(t)'$ is meant as the complementary set of $\Omega_{1,p}(t)$ with respect to $\{2,\ldots,p-2\}$. This means that $w(S)R_S(x_S^*)R_{S'}(z_{S'})$ only gives a non-zero effect for the datapoints t such that $\Omega_{1,p}(t)'\subseteq\Omega_{1,p}(x^*)$, in which case the (only) subsets S that contribute are the ones such that $\Omega_{1,p}(t)'\subseteq S\subseteq\Omega_{1,p}(x^*)$. Since all such sets S contain $\Omega_{1,p}(t)'$, they can all be uniquely identified by the indices that they have besides those in $\Omega_{1,p}(t)'$. In other words, each S may be (uniquely) re-written as $S=\Omega_{1,p}(t)'\cup Z$, with $Z\subseteq\Omega_{1,p}(x^*)\setminus\Omega_{1,p}(t)'$. For every size |Z|=l, there are exactly $\binom{|\Omega_{1,p}(x^*)\setminus\Omega_{1,p}(t)'|}{l}=\binom{q_{1,p}(x^*)+q_{1,p}(t)-p+2}{l}$ possible choices of Z, and they all have the same effect $w(S)=\frac{1}{2(p-1)\binom{p-2}{|S|}}=\frac{1}{2(p-1)\binom{p-2}{p-2-q_{1,p}(t)+l}}$.

This means that we can write:

$$\begin{split} \mathcal{E} &= \sum_{S \subseteq \{2, \dots, p-2\}} w(S) R_S(x_S^*) R_{S'}(t_{S'}) \\ &= \sum_{l=0}^{|\Omega_{1,p}(x^*) \setminus \Omega_{1,p}(t)|} \frac{\left(q_{1,p}(x^*) + q_{1,p}(t) - p + 2\right)}{2(p-1) \left(p-2 - q_{1,p}(t) + l\right)} \\ &= \sum_{l=0}^{q_{1,p}(x^*) + q_{1,p}(t) - p + 2} \frac{\left(q_{1,p}(x^*) + q_{1,p}(t) - p + 2\right)}{2(p-1) \left(p-2 - q_{1,p}(t) + l\right)} \\ &= \frac{\left(q_{1,p}(x^*) + q_{1,p}(t) - p + 2\right)!}{2(p-1)!} \\ &\cdot \sum_{l=0}^{q_{1,p}(x^*) + q_{1,p}(t) - p + 2} \frac{\left(q_{1,p}(t) - l\right)!(p-2 - q_{1,p}(t) + l)!}{(q_{1,p}(x^*) + q_{1,p}(t) - p + 2 - l)!l!} \\ &= \frac{\left(q_{1,p}(x^*) + q_{1,p}(t) - p + 2\right)!}{2(p-1)!} \\ &\cdot \sum_{l=0}^{q_{1,p}(x^*) + q_{1,p}(t) - p + 2} \left[\binom{q_{1,p}(t) - l}{q_{1,p}(x^*) + q_{1,p}(t) - p + 2 - l} (p-2 - q_{1,p}(t))!\right] \\ &= \frac{\left(q_{1,p}(x^*) + q_{1,p}(t) - p + 2\right)!(p-2 - q_{1,p}(t) + l)}{2(p-1)!} \\ &\cdot \sum_{l=0}^{q_{1,p}(x^*) + q_{1,p}(t) - p + 2} \binom{q_{1,p}(t) - l}{2(p-1)!} \\ &\cdot \sum_{l=0}^{q_{1,p}(x^*) + q_{1,p}(t) - p + 2} \binom{q_{1,p}(t) - l}{q_{1,p}(x^*) + q_{1,p}(t) - p + 2 - l} \binom{p-2 - q_{1,p}(t) + l}{l}. \end{split}$$

Using Lemma 3 with $a = p - 2 - q_{1,p}(t)$, $b = q_{1,p}(t)$, $c = q_{1,p}(x^*) + q_{1,p}(t) - p + 2$, we conclude:

$$\mathcal{E} = \sum_{S \subseteq \{2, \dots, p-2\}} w(S) R_S(x_S^*) R_{S'}(t_{S'})$$

$$= \frac{(q_{1,p}(x^*) + q_{1,p}(t) - p + 2)! (p - 2 - q_{1,p}(x^*))! (p - 2 - q_{1,p}(t))!}{2(p - 1)!} \cdot \binom{p - 1}{q_{1,p}(x^*) + q_{1,p}(t) - p + 2}$$

$$= \frac{(p - 2 - q_{1,p}(x^*))! (p - 2 - q_{1,p}(t))!}{2(2p - q_{1,p}(x^*) - q_{1,p}(t) - 3)!}$$

$$= \frac{1}{2(p - 1 - q_{1,p}(x^*))} \cdot \frac{1}{\binom{2p - q_{1,p}(x^*) - q_{1,p}(t) - 1}{p - 1 - q_{1,p}(x^*)}}.$$

This allows us to conclude that:

$$\widehat{\mathcal{A}} = \frac{1}{2n(p-1-q_{1,p}(x^*))} \sum_{\substack{t \in \mathcal{T} \text{ s.t.} \\ \Omega_{1,p}(t)' \subseteq \Omega_{1,p}(x^*)}} \frac{\varphi(x_1^*)R_1(x_1^*)R_p(x_p^*)}{\binom{2p-q_{1,p}(x^*)-q_{1,p}(t)-1}{p-q_{1,p}(x^*)}}.$$

The sum is only over the datapoints with $\Omega_{1,p}(t)' \subseteq \Omega_{1,p}(x^*)$, as the other datapoints have a null effect. In a similar fashion, let us compute $\widehat{\mathcal{B}}, \widehat{\mathcal{C}}, \widehat{\mathcal{D}}$:

$$\begin{split} \widehat{\mathcal{B}} &= \sum_{S \subseteq \{2, \dots, p-2\}} w(S) \varphi(x_1^*) R_1(x_1^*) R_S(x_S^*) \frac{1}{n} \sum_{t \in \mathcal{T}} R_{S' \cup \{p\}}(t_{S' \cup \{p\}}) \\ &= \varphi(x_1^*) R_1(x_1^*) \frac{1}{n} \sum_{t \in \mathcal{T}} R_p(t_p) \sum_{S \subseteq \{2, \dots, p-2\}} w(S) R_S(x_S^*) R_{S'}(t_{S'}) \\ &= \frac{1}{2n(p-1-q_{1,p}(x^*))} \sum_{\substack{t \in \mathcal{T} \text{ s.t.} \\ \Omega_{1,p}(t)' \subseteq \Omega_{1,p}(x^*)}} \frac{\varphi(x_1^*) R_1(x_1^*) R_p(t_p)}{\binom{2p-q_{1,p}(x^*)-q_{1,p}(t)-1}}, \\ \widehat{\mathcal{C}} &= \sum_{S \subseteq \{2, \dots, p-2\}} w(S) R_p(x_p^*) R_S(x_S^*) \frac{1}{n} \sum_{t \in \mathcal{T}} \varphi(t_1) R_{S' \cup \{1\}}(t_{S' \cup \{1\}}) \\ &= R_p(x_p^*) \frac{1}{n} \sum_{t \in \mathcal{T}} \varphi(t_1) R_1(t_1) \sum_{S \subseteq \{2, \dots, p-2\}} w(S) R_S(x_S^*) R_{S'}(t_{S'}) \\ &= \frac{1}{2n(p-1-q_{1,p}(x^*))} \sum_{\substack{t \in \mathcal{T} \text{ s.t.} \\ \Omega_{1,p}(t)' \subseteq \Omega_{1,p}(x^*)}} \frac{\varphi(t_1) R_1(t_1) R_p(x_p^*)}{\binom{2p-q_{1,p}(x^*)-q_{1,p}(t)-1}}, \\ \widehat{\mathcal{D}} &= \sum_{S \subseteq \{2, \dots, p-2\}} w(S) R_S(x_S^*) \frac{1}{n} \sum_{t \in \mathcal{T} \text{ s.t.}} \varphi(t_1) R_{S' \cup \{1,p\}}(t_{S' \cup \{1,p\}}) \\ &= \frac{1}{n} \sum_{t \in \mathcal{T}} \varphi(t_1) R_1(t_1) R_p(t_p) \sum_{S \subseteq \{2, \dots, p-2\}} w(S) R_S(x_S^*) R_{S'}(t_{S'}) \\ &= \frac{1}{2n(p-1-q_{1,p}(x^*))} \sum_{\substack{t \in \mathcal{T} \text{ s.t.} \\ V \in \mathcal{D} \\ (x_t^*) \subseteq \Omega_{1,p}(x^*)}} \frac{\varphi(t_1) R_1(t_1) R_p(t_p)}{\frac{(2p-q_{1,p}(x^*)-q_{1,p}(t)-1)}{(2p-q_{1,p}(x^*)}}, \end{split}$$

Combining the expressions together gives us the formula:

$$\begin{split} \widehat{\phi}_{1,p}(x^*) &= \widehat{\mathcal{A}} - \widehat{\mathcal{B}} - \widehat{\mathcal{C}} + \widehat{\mathcal{D}} \\ &= \frac{1}{2n(p-1-q_{1,p}(x^*))} \\ &\cdot \sum_{\substack{t \in \mathcal{T} \text{ s.t.} \\ \Omega_{1,p}(t)' \subseteq \Omega_{1,p}(x^*)}} \frac{\varphi(x_1^*)R_1(x_1^*)R_p(x_p^*) - \varphi(x_1^*)R_1(x_1^*)R_p(t_p) - \varphi(t_1)R_1(t_1)R_p(x_p^*) + \varphi(t_1)R_1(t_1)R_p(t_p)}{\binom{2p-q_{1,p}(x^*)-q_{1,p}(t^*)-1}{p-q_{1,p}(x^*)}}. \end{split}$$

To obtain the formula stated in the Theorem, notice that $q(x) = q_{1,p}(x) + R_1(x) + R_p(x)$ and that the condition $\Omega_{1,p}(t)' \subseteq \Omega_{1,p}(x^*)$ in the summation may be replaced with the condition $R_j(t) = 1 \vee R_j(x_j^*) = 1 \forall j$: the only datapoints for which the two conditions differ are the points for which $R_1(t_1) = R_1(x_1^*) = 0$ or $R_p(t_p) = R_p(x_p^*) = 0$. For such datapoints, the effect is null and thus does not affect the formula.

Now let us consider the case $k' \neq l = 1$. For simplicity, let's assume k' = p - 1. For any subset $V \subseteq \{2, \ldots, p-2\}$, define V'' as $\{2, \ldots, p-2\} \setminus V$. By separating the cases $1 \in S$ and $1 \notin S$,

Shapley values may be re-written as:

$$\begin{split} \phi_{p-1,p}(x^*) &= \sum_{S\subseteq \{1,\dots,p-2\}} w(S) \Big(\mathbb{E}[\varphi(x_1)r(x)|x_S = x_S^*, x_{p-1} = x_{p-1}^*, x_p = x_p^*] \\ &- \mathbb{E}[\varphi(x_1)r(x)|x_S = x_S^*, x_{p-1} = x_{p-1}^*] - \mathbb{E}[\varphi(x_1)r(x)|x_S = x_S^*, x_p = x_p^*] \\ &+ \mathbb{E}[\varphi(x_1)r(x)|x_S = x_S^*] \Big) \\ &= \sum_{V\subseteq \{2,\dots,p-2\}} w(V \cup \{1\}) \Big(\mathbb{E}[\varphi(x_1)r(x)|x_S = x_S^*, x_1 = x_1^*, x_{p-1} = x_{p-1}^*, x_p = x_p^*] \\ &- \mathbb{E}[\varphi(x_1)r(x)|x_S = x_S^*, x_1 = x_1^*, x_{p-1} = x_{p-1}^*] - \mathbb{E}[\varphi(x_1)r(x)|x_S = x_S^*, x_1 = x_1^*, x_p = x_p^*] \\ &+ \mathbb{E}[\varphi(x_1)r(x)|x_S = x_S^*, x_1 = x_1^*] \Big) \\ &+ \sum_{V\subseteq \{2,\dots,p-2\}} w(V) \Big(\mathbb{E}[\varphi(x_1)r(x)|x_S = x_S^*, x_{p-1} = x_{p-1}^*, x_p = x_p^*] \\ &- \mathbb{E}[\varphi(x_1)r(x)|x_S = x_S^*, x_{p-1} = x_{p-1}^*] - \mathbb{E}[\varphi(x_1)r(x)|x_S = x_S^*, x_p = x_p^*] \\ &+ \mathbb{E}[\varphi(x_1)r(x)|x_S = x_S^*] \Big) \\ \\ &= \sum_{V\subseteq \{2,\dots,p-2\}} w(V \cup \{1\})\varphi(x_1^*)R_1(x_1^*)R_{p-1}(x_{p-1}^*)R_p(x_p^*)R_V(x_V^*)\mathbb{E}[R_{V''\cup\{p\}})] \\ &- \sum_{V\subseteq \{2,\dots,p-2\}} w(V \cup \{1\})\varphi(x_1^*)R_1(x_1^*)R_{p-1}(x_{p-1}^*)R_V(x_V^*)\mathbb{E}[R_{V''\cup\{p-1,p\}}(x_{V''\cup\{p-1,p\}})] \\ &+ \sum_{V\subseteq \{2,\dots,p-2\}} w(V \cup \{1\})\varphi(x_1^*)R_1(x_1^*)R_V(x_V^*)\mathbb{E}[R_{V''\cup\{p-1,p\}}(x_{V''\cup\{p-1,p\}})] \\ &+ \sum_{V\subseteq \{2,\dots,p-2\}} w(V)R_{p-1}(x_{p-1}^*)R_p(x_p^*)R_V(x_V^*)\mathbb{E}[\varphi(x_1)R_{V''\cup\{1,p}(x_1)(x_1)(x_1)\}] \\ &- \sum_{V\subseteq \{2,\dots,p-2\}} w(V)R_{p-1}(x_{p-1}^*)R_V(x_V^*)\mathbb{E}[\varphi(x_1)R_{V''\cup\{1,p}(x_1)(x_1,p-1,p\}})] \\ &- \sum_{V\subseteq \{2,\dots,p-2\}} w(V)R_{p-1}(x_p^*)R_V(x_V^*)\mathbb{E}[\varphi(x_1)R_{V''\cup\{1,p-1,p\}}(x_{V''\cup\{1,p-1,p\}})] \\ &- \sum_{V\subseteq \{2,\dots,p-2\}} w(V)R_{p-1}(x_p^*)R_V(x_V^*)\mathbb{E}[\varphi(x_1)R_{V''\cup\{1,p-1,p\}}(x_{V''\cup\{1,p-1,p\}})] \\ &+ \sum_{V\subseteq \{2,\dots,p-2\}} w(V)R_{p-1}(x_v^*)\mathbb{E}[\varphi(x_1)R_{V''\cup\{1,p-1,p\}}(x_{V''\cup\{1,p-1,p\}})] \\ &+ \sum_{V\subseteq \{2,\dots,p-2\}} w(V)R_{p-1}(x_v^*)\mathbb{E}[\varphi(x_1)R_{V''\cup\{1,p-1,p\}}(x_{V''\cup\{1,p-1,p\}})] \\ &+ \sum_{V\subseteq \{2,\dots,p-2\}} w(V)R_{p-1}(x_v^*)\mathbb{E}[\varphi(x_1)R_{V''\cup\{1,p-1,p\}}(x_{V''\cup\{1,p-1,p$$

Let us treat the eight summations separately; define the following:

$$\mathcal{F} = \sum_{V \subseteq \{2, \dots, p-2\}} w(V \cup \{1\}) \varphi(x_1^*) R_1(x_1^*) R_{p-1}(x_{p-1}^*) R_p(x_p^*) R_V(x_V^*) \mathbb{E}[R_{V''}(x_{V''})],$$

$$\mathcal{G} = \sum_{V \subseteq \{2, \dots, p-2\}} w(V \cup \{1\}) \varphi(x_1^*) R_1(x_1^*) R_{p-1}(x_{p-1}^*) R_V(x_V^*) \mathbb{E}[R_{V'' \cup \{p\}}(x_{V'' \cup \{p\}})],$$

$$\mathcal{H} = \sum_{V \subseteq \{2, \dots, p-2\}} w(V \cup \{1\}) \varphi(x_1^*) R_1(x_1^*) R_p(x_p^*) R_V(x_V^*) \mathbb{E}[R_{V'' \cup \{p-1\}}(x_{V'' \cup \{p-1\}})],$$

$$\mathcal{I} = \sum_{V \subseteq \{2, \dots, p-2\}} w(V \cup \{1\}) \varphi(x_1^*) R_1(x_1^*) R_V(x_V^*) \mathbb{E}[R_{V'' \cup \{p-1, p\}}(x_{V'' \cup \{p-1, p\}})],$$

$$\mathcal{I} = \sum_{V \subseteq \{2, \dots, p-2\}} w(V) R_{p-1}(x_{p-1}^*) R_p(x_p^*) R_V(x_V^*) \mathbb{E}[\varphi(x_1) R_{V'' \cup \{1\}}(x_{V'' \cup \{1\}})],$$

$$\mathcal{K} = \sum_{V \subseteq \{2, \dots, p-2\}} w(V) R_{p-1}(x_{p-1}^*) R_V(x_V^*) \mathbb{E}[\varphi(x_1) R_{V'' \cup \{1, p-1\}}(x_{V'' \cup \{1, p-1\}})],$$

$$\mathcal{L} = \sum_{V \subseteq \{2, \dots, p-2\}} w(V) R_p(x_p^*) R_V(x_V^*) \mathbb{E}[\varphi(x_1) R_{V'' \cup \{1, p-1\}}(x_{V'' \cup \{1, p-1\}})],$$

$$\mathcal{M} = \sum_{V \subseteq \{2, \dots, p-2\}} w(V) R_V(x_V^*) \mathbb{E}[\varphi(x_1) R_{V'' \cup \{1, p-1, p\}}(x_{V'' \cup \{1, p-1, p\}})].$$

With a similar argument as above, they can be approximated without bias by:

$$\widehat{\mathcal{F}} = \sum_{V \subseteq \{2, \dots, p-2\}} w(V \cup \{1\}) \varphi(x_1^*) R_1(x_1^*) R_{p-1}(x_{p-1}^*) R_p(x_p^*) R_V(x_V^*) \frac{1}{n} \sum_{t \in \mathcal{T}} R_{V''}(t_{V''})$$

$$= \frac{1}{n} \sum_{t \in \mathcal{T}} \varphi(x_1^*) R_1(x_1^*) R_{p-1}(x_{p-1}^*) R_p(x_p^*) \sum_{V \subseteq \{2, \dots, p-2\}} w(V \cup \{1\}) R_V(x_V^*) R_{V''}(t_{V''})$$

$$\widehat{\mathcal{G}} = \sum_{V \subseteq \{2, \dots, p-2\}} w(V \cup \{1\}) \varphi(x_1^*) R_1(x_1^*) R_{p-1}(x_{p-1}^*) R_V(x_V^*) \frac{1}{n} \sum_{t \in \mathcal{T}} R_{V'' \cup \{p\}}(t_{V'' \cup \{p\}})$$

$$= \frac{1}{n} \sum_{t \in \mathcal{T}} \varphi(x_1^*) R_1(x_1^*) R_{p-1}(x_{p-1}^*) R_p(t_p) \sum_{V \subseteq \{2, \dots, p-2\}} w(V \cup \{1\}) R_V(x_V^*) R_{V''}(t_{V''})$$

$$\widehat{\mathcal{H}} = \sum_{V \subseteq \{2, \dots, p-2\}} w(V \cup \{1\}) \varphi(x_1^*) R_1(x_1^*) R_p(x_p^*) R_V(x_V^*) \frac{1}{n} \sum_{t \in \mathcal{T}} R_{V'' \cup \{p-1\}} (t_{V'' \cup \{p-1\}})$$

$$= \frac{1}{n} \sum_{t \in \mathcal{T}} \varphi(x_1^*) R_1(x_1^*) R_{p-1}(t_{p-1}) R_p(x_p^*) \sum_{V \subseteq \{2, \dots, p-2\}} w(V \cup \{1\}) R_V(x_V^*) R_{V''}(t_{V''})$$

$$\widehat{\mathcal{I}} = \sum_{V \subseteq \{2, \dots, p-2\}} w(V \cup \{1\}) \varphi(x_1^*) R_1(x_1^*) R_V(x_V^*) \frac{1}{n} \sum_{t \in \mathcal{T}} R_{V'' \cup \{p-1, p\}} (t_{V'' \cup \{p-1, p\}})$$

$$= \frac{1}{n} \sum_{t \in \mathcal{T}} \varphi(x_1^*) R_1(x_1^*) R_{p-1}(t_{p-1}) R_p(t_p) \sum_{V \subseteq \{2, \dots, p-2\}} w(V \cup \{1\}) R_V(x_V^*) R_{V''}(t_{V''})$$

$$\widehat{\mathcal{J}} = \sum_{V \subseteq \{2, \dots, p-2\}} w(V) R_{p-1}(x_{p-1}^*) R_p(x_p^*) R_V(x_V^*) \frac{1}{n} \sum_{t \in \mathcal{T}} \varphi(t_1) R_{V'' \cup \{1\}}(t_{V'' \cup \{1\}})$$

$$= \frac{1}{n} \sum_{t \in \mathcal{T}} \varphi(t_1) R_1(t_1) R_{p-1}(x_{p-1}^*) R_p(x_p^*) \sum_{V \subseteq \{2, \dots, p-2\}} w(V) R_V(x_V^*) R_{V''}(t_{V''})$$

$$\widehat{\mathcal{K}} = \sum_{V \subseteq \{2, \dots, p-2\}} w(V) R_{p-1}(x_{p-1}^*) R_V(x_V^*) \frac{1}{n} \sum_{t \in \mathcal{T}} \varphi(t_1) R_{V'' \cup \{1, p\}}(t_{V'' \cup \{1, p\}})$$

$$= \frac{1}{n} \sum_{t \in \mathcal{T}} \varphi(t_1) R_1(t_1) R_{p-1}(x_{p-1}^*) R_p(t_p) \sum_{V \subseteq \{2, \dots, p-2\}} w(V) R_V(x_V^*) R_{V''}(t_{V''})$$

$$\begin{split} \widehat{\mathcal{L}} &= \sum_{V \subseteq \{2, \dots, p-2\}} w(V) R_p(x_p^*) R_V(x_V^*) \frac{1}{n} \sum_{t \in \mathcal{T}} R_{V'' \cup \{1, p-1\}} (t_{V'' \cup \{1, p-1\}}) \\ &= \frac{1}{n} \sum_{t \in \mathcal{T}} \varphi(t_1) R_1(t_1) R_{p-1}(t_{p-1}) R_p(x_p^*) \sum_{V \subseteq \{2, \dots, p-2\}} w(V) R_V(x_V^*) R_{V''}(t_{V''}) \end{split}$$

$$\widehat{\mathcal{M}} = \sum_{V \subseteq \{2, \dots, p-2\}} w(V) R_V(x_V^*) \frac{1}{n} \sum_{t \in \mathcal{T}} \varphi(t_1) R_{V'' \cup \{1, p-1, p\}} (t_{V'' \cup \{1, p-1, p\}})$$

$$= \frac{1}{n} \sum_{t \in \mathcal{T}} \varphi(t_1) R_1(t_1) R_{p-1}(t_{p-1}) R_p(t_p) \sum_{V \subseteq \{2, \dots, p-2\}} w(V) R_V(x_V^*) R_{V''}(t_{V''})$$

Notice that the way that the weights w(V) are defined for interactions Shapley values is so that the summations over V that appear in these expressions are the same as those computed for the proof of Theorem 1, except that here they use a set of p-1 features instead of a set of p features and up to multiplicative a factor of $\frac{1}{2}$. Using that same calculation, we thus deduce:

$$\widehat{\mathcal{F}} = \frac{1}{2n(p-2-q_{1,p-1,p}(x^*))} \sum_{\substack{t \in \mathcal{T}\text{s.t.} \\ \Omega_{1,p-1,p}(t)' \subseteq \Omega_{1,p-1,p}(x^*)}} \frac{\varphi(x_1^*)R_1(x_1^*)R_{p-1}(x_{p-1}^*)R_p(x_p^*)}{\binom{2p-q_{1,p-1,p}(x^*)-q_{1,p-1,p}(t)-4}{p-2-q_{1,p-1,p}(x^*)}}$$

$$\begin{split} \widehat{\mathcal{G}} &= \frac{1}{2n(p-2-q_{1,p-1,p}(x^*))} \sum_{\substack{t \in \mathcal{T}\text{s.t.} \\ \Omega_{1,p-1,p}(t)' \subseteq \Omega_{1,p-1,p}(x^*)}} \frac{\varphi(x_1^*)R_1(x_1^*)R_{p-1}(x_{p-1}^*)R_p(t_p)}{\binom{2p-q_{1,p-1,p}(x^*)-q_{1,p-1,p}(t)-4}{p-2-q_{1,p-1,p}(x^*)}} \\ \widehat{\mathcal{H}} &= \frac{1}{2n(p-2-q_{1,p-1,p}(x^*))} \sum_{\substack{t \in \mathcal{T}\text{s.t.} \\ \Omega_{1,p-1,p}(t)' \subseteq \Omega_{1,p-1,p}(x^*)}} \frac{\varphi(x_1^*)R_1(x_1^*)R_{p-1}(t_{p-1})R_p(t_p)}{\binom{2p-q_{1,p-1,p}(x^*)-q_{1,p-1,p}(t)-4}{p-2-q_{1,p-1,p}(x^*)}} \\ \widehat{\mathcal{I}} &= \frac{1}{2n(p-2-q_{1,p-1,p}(x^*))} \sum_{\substack{t \in \mathcal{T}\text{s.t.} \\ \Omega_{1,p-1,p}(t)' \subseteq \Omega_{1,p-1,p}(x^*)}} \frac{\varphi(x_1^*)R_1(x_1^*)R_{p-1}(t_{p-1})R_p(x_p^*)}{\binom{2p-q_{1,p-1,p}(x^*)-q_{1,p-1,p}(t)-4}{p-2-q_{1,p-1,p}(x^*)}} \\ \widehat{\mathcal{J}} &= \sum_{\substack{t \in \mathcal{T}\text{s.t.} \\ \Omega_{1,p-1,p}(t)' \subseteq \Omega_{1,p-1,p}(x^*)}} \frac{1}{2n(p-2-q_{1,p-1,p}(t))} \cdot \frac{\varphi(t_1)R_1(t_1)R_{p-1}(x_{p-1}^*)R_p(x_p^*)}{\binom{2p-q_{1,p-1,p}(x^*)-q_{1,p-1,p}(t)-4}{p-2-q_{1,p-1,p}(x^*)}} \\ \widehat{\mathcal{L}} &= \sum_{\substack{t \in \mathcal{T}\text{s.t.} \\ \Omega_{1,p-1,p}(t)' \subseteq \Omega_{1,p-1,p}(x^*)}} \frac{1}{2n(p-2-q_{1,p-1,p}(t))} \cdot \frac{\varphi(t_1)R_1(t_1)R_{p-1}(x_{p-1}^*)R_p(t_p)}{\binom{2p-q_{1,p-1,p}(x^*)-q_{1,p-1,p}(t)-4}{p-2-q_{1,p-1,p}(x^*)}} \\ \widehat{\mathcal{F}} &= \sum_{\substack{t \in \mathcal{T}\text{s.t.} \\ \Omega_{1,p-1,p}(t)' \subseteq \Omega_{1,p-1,p}(x^*)}} \frac{1}{2n(p-2-q_{1,p-1,p}(t))} \cdot \frac{\varphi(t_1)R_1(t_1)R_{p-1}(t_{p-1})R_p(t_p)}{\binom{2p-q_{1,p-1,p}(x^*)-q_{1,p-1,p}(t)-4}{p-2-q_{1,p-1,p}(x^*)}} \\ \widehat{\mathcal{F}} &= \sum_{\substack{t \in \mathcal{T}\text{s.t.} \\ \Omega_{1,p-1,p}(t)' \subseteq \Omega_{1,p-1,p}(x^*)}} \frac{1}{2n(p-2-q_{1,p-1,p}(t))} \cdot \frac{\varphi(t_1)R_1(t_1)R_{p-1}(t_{p-1})R_p(t_p)}{\binom{2p-q_{1,p-1,p}(x^*)-q_{1,p-1,p}(t)-4}{p-2-q_{1,p-1,p}(x^*)}} \\ \widehat{\mathcal{F}} &= \sum_{\substack{t \in \mathcal{T}\text{s.t.} \\ \Omega_{1,p-1,p}(t)' \subseteq \Omega_{1,p-1,p}(x^*)}} \frac{1}{2n(p-2-q_{1,p-1,p}(t))} \cdot \frac{\varphi(t_1)R_1(t_1)R_{p-1}(t_{p-1})R_p(t_p)}{\binom{2p-q_{1,p-1,p}(x^*)-q_{1,p-1,p}(t)-4}{p-2-q_{1,p-1,p}(x^*)}}} \\ \widehat{\mathcal{F}} &= \sum_{\substack{t \in \mathcal{T}\text{s.t.} \\ \Omega_{1,p-1,p}(t)' \subseteq \Omega_{1,p-1,p}(x^*)}}} \frac{1}{2n(p-2-q_{1,p-1,p}(t))} \cdot \frac{\varphi(t_1)R_1(t_1)R_{p-1}(t_{p-1})R_p(t_p)}{\binom{2p-q_{1,p-1,p}(x^*)-q_{1,p-1,p}(t)-4}{p-2-q_{1,p-1,p}(x^*)}}} \\ \widehat{\mathcal{F}} &= \sum_{\substack{t \in \mathcal{T}\text{s.t.} \\ \Omega_{1,p-1,p}(t)' \subseteq \Omega_{1,p-1,p}(x^*)}}} \frac{1}{2n(p-2-q_{1,p-1,p}(t)}} \\ \widehat{\mathcal{F}} &= \sum_{\substack{t \in \mathcal{T}\text{s.t.} \\$$

Putting the eight pieces together, we obtain:

$$\begin{split} \widehat{\phi_p}(x^*) &= \widehat{\mathcal{F}} - \widehat{\mathcal{G}} - \widehat{\mathcal{H}} + \widehat{\mathcal{I}} + \widehat{\mathcal{J}} - \widehat{\mathcal{K}} - \widehat{\mathcal{L}} + \widehat{\mathcal{M}} \\ &= \frac{1}{2n} \sum_{\substack{t \in \mathcal{T} \text{s.t.} \\ \Omega_{1,p-1,p}(t)' \subseteq \Omega_{1,p-1,p}(x^*)}} \frac{\frac{\varphi(x_1^*)R_1(x_1^*)}{p-2-q_{1,p-1,p}(x^*)} + \frac{\varphi(t_1)R_1(t_1)}{p-2-q_{1,p-1,p}(t)}}{\binom{2p-q_{1,p-1,p}(x^*)-q_{1,p-1,p}(t)-4}{p-2-q_{1,p-1,p}(x^*)}} \\ &\quad \cdot \Big(R_{p-1}(x_{p-1}^*)R_p(x_p^*) - R_{p-1}(x_{p-1}^*)R_p(t_p) - R_{p-1}(t_{p-1})R_p(x_p^*) + R_{p-1}(t_{p-1})R_p(t_p) \Big). \end{split}$$

To obtain the formula stated in the Theorem, notice that $q(x) = q_{1,p-1,p}(x) + R_1(x) + R_{p-1}(x) + R_p(x)$ and that the condition $\Omega_{1,p-1,p}(t)' \subseteq \Omega_{1,p-1,p}(x^*)$ in the summation may be replaced with the condition $R_j(t) = 1 \vee R_j(x_j^*) = 1 \,\forall j$: the only datapoints for which the two conditions differ are the points for which $R_j(t_j) = R_j(x_j^*) = 0$ for either j = 1, j = p - 1 or j = p. For such datapoints, the effect is null and thus does not affect the formula.